INFORMATION TO USERS

This manuscript has been reproduced from the microfilm master. UMI films the text directly from the original or copy submitted. Thus, some thesis and dissertation copies are in typewriter face, while others may be from any type of computer printer.

The quality of this reproduction is dependent upon the quality of the copy submitted. Broken or indistinct print, colored or poor quality illustrations and photographs, print bleedthrough, substandard margins, and improper alignment can adversely affect reproduction.

In the unlikely event that the author did not send UMI a complete manuscript and there are missing pages, these will be noted. Also, if unauthorized copyright material had to be removed, a note will indicate the deletion.

Oversize materials (e.g., maps, drawings, charts) are reproduced by sectioning the original, beginning at the upper left-hand corner and continuing from left to right in equal sections with small overlaps.

Photographs included in the original manuscript have been reproduced xerographically in this copy. Higher quality 6" x 9" black and white photographic prints are available for any photographs or illustrations appearing in this copy for an additional charge. Contact UMI directly to order.

ProQuest Information and Learning
300 North Zeeb Road, Ann Arbor, MI 48106-1346 USA
800-521-0600

Nanoscale Protein Analysis Utilizing Capillary Electrophoresis and Laser-Induced Fluorescence Detection

Michael D. Harvey

A Thesis

in

The Department

of

Chemistry and Biochemistry

Presented in Partial Fulfilment of the Requirements
For the Degree of Doctor of Philosophy at
Concordia University
Montréal, Québec, Canada

April 2001

ABSTRACT

Nanoscale Protein Analysis Utilizing Capillary Electrophoresis and Laser-Induced Fluorescence Detection

Michael D. Harvey
Concordia University, 2001

The trend towards high throughput applications and miniaturization necessitates approaches capable of microlitre volume sampling and low protein concentration detection. Furthermore, one of the major trends in high throughput screening is the growing replacement of technologies that depend on radioactivity to generate a signal with those that rely on fluorescence. This trend towards non-radioactive detection in general can be understood by some of the advantages inherent to these methods over radioactive modes. These include a significant reduction in safety concerns leading to a relaxation of strict laboratory procedures, elimination of expensive waste disposal, extended shelf-life of labeled reagents, and the possibility of acquiring multiplexed data through the spectral isolation of different wavelength signals. A variety of capillary electrophoretic (CE) approaches utilizing laser-induced fluorescence (LIF) have thus been developed, providing researchers with valuable tools in protein analysis.

Various covalent and non-covalent fluorescent derivatization approaches have been investigated, with emphasis on biochemical and/or clinical applications.

The non-covalent dye, NanoOrange, is used as a clinical diagnostic tool for early disease diagnosis, quantitating nanomolar concentrations of human serum albumin in solution, and obtaining fluorescence-based biofluid profiles. An alternate non-covalent labeling approach utilizing the fluorescent probe, Sypro Red, and capillary gel electrophoresis allows for rapid, sensitive analysis of protein sample purity as well as molecular weight determination. These two non-covalent approaches are complemented by the development of a fluorescent Insulin-Like Growth Factor-I (IGF-I) analog for use in bioanalytical applications.

Specific derivatization reaction conditions were developed to selectively label the N-terminus of the analog hence preserve biological activity. High-performance liquid chromatography and electrospray mass spectrometry were used to confirm the extent of labeling and modification site. Antibody recognition of this fluorescent analog was evaluated using CE-LIF, illustrating the clinical utility of this diagnostic reagent.

In addition to the above CE-LIF approaches, a fourth capillary electrophoretic tool is provided for the clinical chemist. Rapid analysis of biofluids is of significant importance in early disease diagnosis. As such, an extensive CE-based analysis of human seminal plasma is presented. Separation conditions, sample stability, and protein / non-protein zone identification issues are addressed. This study and the CE-LIF methodologies discussed above represent original approaches to nanoscale protein analysis.

This thesis is dedicated to my wife, Manon, my children, Alexia and Lucas,

and to my parents, Edmund and Elisabeth

Without your love and support this would not have been possible

ACKNOWLEDGEMENTS

I would like to thank my research supervisor, Dr. Peter R. Banks, for his enthusiasm, encouragement, and guidance. I wish to thank my research committee members, Dr. Claire Cupples and Dr. Marcus Lawrence, for the interest, guidance and support that they have shown throughout my studies.

I also wish to thank the following:

- Fellowships from David J. Azrieli, NSERC, FCAR, Tauba W. Landsberger, and Concordia University.
- The Department of Chemistry and Biochemistry.
- My labmates, Donald, Vincent, Dirk, Pieter for their support, and the many laughs and good times we shared together.
- Dr. Cameron D. Skinner for providing me with the opportunity to work in his laboratory.
- Vicky Bablekis, with whom it was truly a pleasure to work with.
- The faculty, staff and graduate students of this department, who have enriched my stay here at Concordia.
- Patricia Verret and Sylvana Novembre at the School of Graduate Awards.

TABLE OF CONTENTS

LIST OF FIGURES xiii

LIST OF TABLES xvii

LIST OF EQUATIONS xviii

LIST OF ABBREVIATIONS xix

CHAPTER 1

General Introduction to Protein Analysis by Capillary Electrophoresis 1

CAPILLARY ELECTROPHORESIS OVERVIEW 2

CAPILLARY ELECTROPHORETIC ANALYSIS OF PROTEINS 10

Capillary Zone Electrophoresis of Proteins 10

Protein Analysis in Simple Matrices 12

Complex Protein Analysis 13

Capillary Electrophoresis of Proteins Utilizing Polymer Matrices 14

Polymer Sieving Matrices in CE 15

Sodium Dodecyl Sulfate Capillary Gel Electrophoresis 20

OPTICAL DETECTION SCHEMES IN CAPILLARY ELECTROPHORESIS 22

Overview of Optical Detection in Capillary Electrophoresis 22

Laser-Induced Fluorescence Detection (LIFD) 25

Derivatization Approaches in Capillary Electrophoresis 26

BIOCHEMICAL & CLINICAL APPLICATIONS OF CE-LIFD 30

Protein Quantitation and Purity Assessment 30

CE-LIFD Immunoassays 31

CE Biofluid Profiling 32

CONCLUSIONS 33

OUTLINE OF THESIS 34

REFERENCES 36

CHAPTER 2

Capillary Electrophoretic Analysis of Human Seminal Plasma 41

ABSTRACT 42

INTRODUCTION 42

EXPERIMENTAL 45

RESULTS AND DISCUSSION 47

Buffer Concentration / pH / Separation Potential Study 47

Internal Standardization / Migration Time Reproducibility Study 53

Protease Inhibition, Temperature Stability, Freeze/Thaw Cycling 55

Non-Protein Zone Identification 59

Protein Zone Identification 59

CONCLUSIONS 62

FUTURE WORK 62

ACKNOWLEDGEMENTS 63

REFERENCES 63

CHAPTER 3

Utilization of the Non-Covalent Fluorescent Dye, NanoOrange, as a Potential Clinical Diagnostic Tool: Nanomolar Human Serum Albumin Quantitation 66

ABSTRACT 67

INTRODUCTION 68

EXPERIMENTAL 70

Apparatus 70

Reagents 72

Procedures 73

RESULTS AND DISCUSSION 75

NanoOrange Fluorescence Excitation and Emission Spectra 75

NanoOrange Buffer Species, Concentration, pH Study 77

Salt Concentration Study 86

NanoOrange Binding and Fluorescence Emission Kinetics 87

HSA Titration with NanoOrange 90

96-Well Microtitre Plate Assay for HSA 92

CE-LIF HSA Quantitation 92

CONCLUSIONS 97

ACKNOWLEDGEMENTS 98

REFERENCES 99

CHAPTER 4

Subnanomolar Detection Limit for Sodium Dodecyl Sulfate – Capillary Gel Electrophoresis Using a Fluorogenic, Noncovalent Dye 101

ABSTRACT 102

INTRODUCTION 102

MATERIALS AND METHODS 104

Instrumentation 104

Reagents 105

Sample Preparation 106

Gel Preparation 106

Capillary Gel Electrophoresis 107

RESULTS AND DISCUSSION 107

Gel-Filled Capillary Lifetime 107

Non-Covalent Fluorescent Labeling of Proteins 109

Denaturing, Non-reducing Gel Electrophoresis 109

Molecular Weight and Purity Assessment of Chorismate Mutase-Prephenate Dehydrogenase 112

Reproducibility of SDS-CGE Using Sypro Red 115

Detection limit of Sypro Red Protein Stain in SDS-CGE 117

CONCLUDING REMARKS 120

ACKNOWLEDGEMENTS 120

REFERENCES 121

CHAPTER 5

Site Specific Fluorescent Derivatization and LC/MS Characterization of Long R^3 IGF-I for Bioanalytical Applications 123

ABSTRACT 124

INTRODUCTION 124

EXPERIMENTAL SECTION 126

Chemicals 126

Instrumental Procedures 127

Preparation of Long R^3 IGF-I – Fluorescein Conjugate 128

CNBr Cleavage 129

Immunorecognition of Labeled Long R^3 IGF-I 129

RESULTS AND DISCUSSION 130

FITC Labeling of Long R^3 IGF-I 130

LC/MS Characterization of Single-Labeled Long R^3 IGF-I 131

Structural Characterization of Single- Labeled Long R^3 IGF-I by Chemical Cleavage and LC/MS 135

Monoclonal anti-IGF-I Binding to Single-Labeled Long R^3 IGF-I 140

CONCLUSIONS 144

ACKNOWLEDGEMENTS 144

REFERENCES 145

CHAPTER 6

CONCLUSIONS AND FUTURE WORK 146

GENERAL CONCLUSIONS 147

Limitations of these CE protein analysis tools 150

Future Work 152

REFERENCES 156

LIST OF FIGURES

Figure 1.1 Schematic illustration of a generic capillary electrophoresis system 4

Figure 1.2 Schematic representation of the electric double layer present at the capillary surface 8

Figure 1.3 Structures of three commonly used "linear" polymers in capillary gel electrophoresis 17

Figure 1.4a Capillary coating procedure for CGE: silanizing activation step 18

Figure 1.4b Capillary coating procedure for CGE: polymer derivatization 19

Figure 1.5 Separation mechanism differences between capillary zone electrophoresis and sodium dodecyl sulfate – capillary gel electrophoresis as expressed by their resultant mobility vectors 21

Figure 1.6 Generic design of CE-LIF on-column detection system 25

Figure 2.1 Effect of borate buffer concentration on the human seminal plasma profile 49

Figure 2.2 Effect of separation buffer pH on the human seminal plasma profile 51

Figure 2.3 Effect of varying separation potential on the human seminal plasma profile 52

Figure 2.4 Protease inhibition, temperature stability, and freeze/thaw cycling effects on human seminal plasma profiles.
Panel A. Effects of various storage temperatures on seminal plasma stability in the presence of PMSF 56
Panel B. Freeze-thaw cycling effects on human seminal plasma profiles in the presence of PMSF 58

Figure 2.5 Acetonitrile deproteinization of human seminal plasma 60

Figure 2.6 Human seminal plasma protein zone identification 61

Figure 3.1 Fluorescence excitation and emission spectra for 1x NanoOrange reagent +/- 10 μg/mL HSA in water at 25 °C 76

Figure 3.2 A comparison of the effects of acidic buffers on 1x NanoOrange fluorescence emission over time, in the presence of 15 μg/mL HSA.
Panel A 79
Panel B 80

Figure 3.3 A comparison of the effects of neutral and basic buffers on 1x NanoOrange fluorescence emission over time, in the presence of 15 μg/mL HSA.
Panel A: 83
Panel B: 84
Panel C: 85

Figure 3.4 Fluorescence emission decay curves for 1x NanoOrange in the presence of various HSA concentrations 89

Figure 3.5 Titration of 15 μg/mL HSA with NanoOrange concentrations ranging from 0 to 4x 91

Figure 3.6 CE-LIF calibration curves for HSA utilizing 2x NanoOrange in the run buffer 94

Figure 3.7 CE-LIF electropherogram of 60x diluted human serum utilizing 1x NanoOrange in the run buffer 96

Figure 4.1 Current stability as a function of buffer composition in SDS-CGE 108

Figure 4.2 Electropherogram of Sypro Red labeled standard proteins using 8% linear polyacrylamide gel and LIF detection 111

Figure 4.3 Plot of log (molecular mass) vs. average migration time of standards listed in Table 4.1, for molecular weight determination of CMPD 113

Figure 4.4 Electropherograms of Sypro Red labeled standard proteins and purified CMPD using 8% linear polyacrylamide gel and LIF detection 114

Figure 4.5 Electropherogram of 1.5 nM BSA labeled with Sypro Red using 8% linear polyacrylamide gel and LIF detection 118

Figure 5.1 TIC of LC separated Long R^3 IGF-I / FITC reaction products 132

Figure 5.2 Extracted ion mass spectra for FITC and its hydrolysis products 133

Figure 5.3 Convolved mass spectra of (A) Peak at 0.99-1.38 min of LC separated Long R^3 IGF-I / FITC reaction TIC 134

Figure 5.4 Amino acid sequence of Long R^3 IGF-I 136

Figure 5.5 Unlabeled Long R^3 IGF-I (No CNBr) 138

Figure 5.6 Unlabeled Long R^3 IGF-I CNBr digestion 139

Figure 5.7 Labeled Long R^3 IGF-I (No CNBr) 141

Figure 5.8 Single-labeled Long R^3 IGF-I CNBr digestion 142

Figure 5.9 CE-LIF electropherogram for the titration of purified single-labeled Long R^3 IGF-I with monoclonal anti-IGF-I 143

Figure 6.1 Undiluted human reflex tear fluid CE analysis using absorbance detection (no dye) and LIFD (NanoOrange in run buffer) 154

Figure 6.2 CE-LIFD analysis of on-column NanoOrange labeled human amniotic fluid 155

LIST OF TABLES

Table 2.1 Migration time reproducibility of various selected peaks in the seminal plasma profile 54

Table 4.1 Migration time reproducibility of Sypro Red SDS-CGE (8% Linear PAA) 116

Table 4.2 A Comparison of SDS-CGE LIF labeling approaches: lowest derivatizable protein concentrations reported 119

LIST OF EQUATIONS

Equation 1.1 Analyte electrophoretic velocity (v_{ep}) 5

Equation 1.2 Electrophoretic mobility (μ_{ep}) 5

Equation 1.3 Electroosmotic velocity (v_{eo}) 7

Equation 1.4 Electroosmotic mobility (μ_{eo}) 7

Equation 1.5 Net sample component velocity (V_{CZE}) 7

Equation 1.6 Analyte mobility in a capillary polyacrylamide matrix 9

Equation 1.7 Lambert-Beer Law 23

Equation 1.8 Fluorescence intensity (Φ_F) 24

LIST OF ABBREVIATIONS

CE	Capillary Electrophoresis
LIF	Laser-induced fluorescence
LIFD	Laser-induced fluorescence detection
IGF-I	Insulin-Like Growth Factor-I
HSA	Human serum albumin
SDS-CGE	Sodium dodecyl sulfate capillary gel electrophoresis
FITC	Fluorescein isothiocyanate
LC/MS	Liquid chromatography / mass spectrometry
CNBr	Cyanogen bromide
PMSF	Phenylmethylsulfonyl fluoride
CMPD	Chorismate mutase-prephenate dehydrogenase
BSA	Bovine serum albumin
HPLC	High-performance liquid chromatography
MS	Mass spectrometry
CZE	Capillary zone electrophoresis
CGE	Capillary gel electrophoresis
EOF	Electroosmotic flow
IHP	Inner Helmholtz plane
OHP	Outer Helmholtz plane
PAGE	Polyacrylamide slab gel electrophoresis
PAA	Polyacrylamide
PEO	Poly(ethylene oxide)
APS	Ammonium persulfate
TEMED	N,N,N',N'-Tetramethylethylenediamine
LOD	Limit of detection
NDA	Naphthalene-2,3-dicarboxaldehyde
CBQCA	3-(4-carboxybenzoyl)quinoline-2-carboxaldehyde
OPA	o-phthaldialdehyde
PSA	Prostate specific antigen
AT	α_1-antitrypsin
TF	Transferrin
NBD-Cl	4-chloro-7-nitrobenzofurazan
NBD-F	4-fluoro-7-nitrobenzofurazan
S/N	Signal to noise
FQ	3-(2-furoyl)quinoline-2-carboxaldehyde
TFA	Trifluoroacetic acid
EDTA	Ethylenediaminetetraacetic acid
DMF	N,N-Dimethylformamide
TIC	Total ion chromatogram
SPE	Solid-phase extraction
FP	Fluorescence polarization

CHAPTER 1

General Introduction to Protein Analysis by Capillary Electrophoresis

CAPILLARY ELECTROPHORESIS OVERVIEW

Capillary electrophoresis (CE) is a powerful analytical separation technique successfully utilized in a diverse set of bioanalytical applications including, amino acid, protein, nucleic acid, and drug analyses. CE has been compared to the "gold standard" separation technique of high-performance liquid chromatography (HPLC).[1] In terms of detection, configuration of CE with a mass spectrometer (MS) is significantly more difficult than for HPLC/MS. Furthermore, due to the inherently shorter pathlengths associated with CE, higher concentration sensitivity can be achieved using UV absorbance detection in HPLC. In terms of operating cost, CE holds many positive attributes, including inexpensive fused-silica capillaries, low solvent and reagent consumption, and greatly reduced organic solvent waste. Additional advantages of CE in comparison to HPLC include, generally shorter analysis times, nanoliter sample volume requirements, and the availability of multi-capillary configurations for high-throughput analyses. The development of CE-based protein analysis tools which exploit these attributes is thus of considerable interest.

The versatility of CE in protein analysis is due in part to its many modes of operation: capillary zone electrophoresis (CZE), micellar electrokinetic chromatography, capillary isotachophoresis, capillary isoelectric focusing, and capillary gel electrophoresis (CGE). Since the separation mechanisms in each of these modes are different, orthogonal and complementary information can be

obtained. The research presented herein has focused specifically on developing protein analysis tools that utilize CZE and CGE.

In brief, the mechanism of separation in CZE relies on differences in the free solution mobility of analytes, whereas in CGE separation is generally based on size. CZE is perhaps the simplist form of CE since the separation medium consists primarily of electrolyte. CGE is considerably more challenging given the need to (1) reproducibly introduce a polymer sieving medium into a capillary with an inner diameter of typically less than 50 microns, and (2) covalently modify the inner wall of the separation capillary. An overview of the electrophoretic process in each of these modes further accentuates the complementary information which can be acquired.

The theory of CZE and CGE is well documented in the literature.[2-4] A brief outline of CZE, including general instrument considerations, electroosmotic flow, and contributions to analyte mobility serves to delineate the differences between CZE and CGE. A generic representation of a CE instrument is illustrated in Figure 1.1. The basic components of a CE instrument include: a polyimide-coated capillary with an inner diameter typically less than 150 microns, an inlet and outlet buffer vial, a high voltage power supply (0 to 60 kV) connected to an anode and cathode, a detector, and data collection system. Sample injections are typically performed at the inlet of a buffer-filled capillary by a variety of methods: pressure, hydrodynamic, and electrokinetic injection. Immediately following injection, both ends of the capillary are immersed in buffer vials, and a separation potential

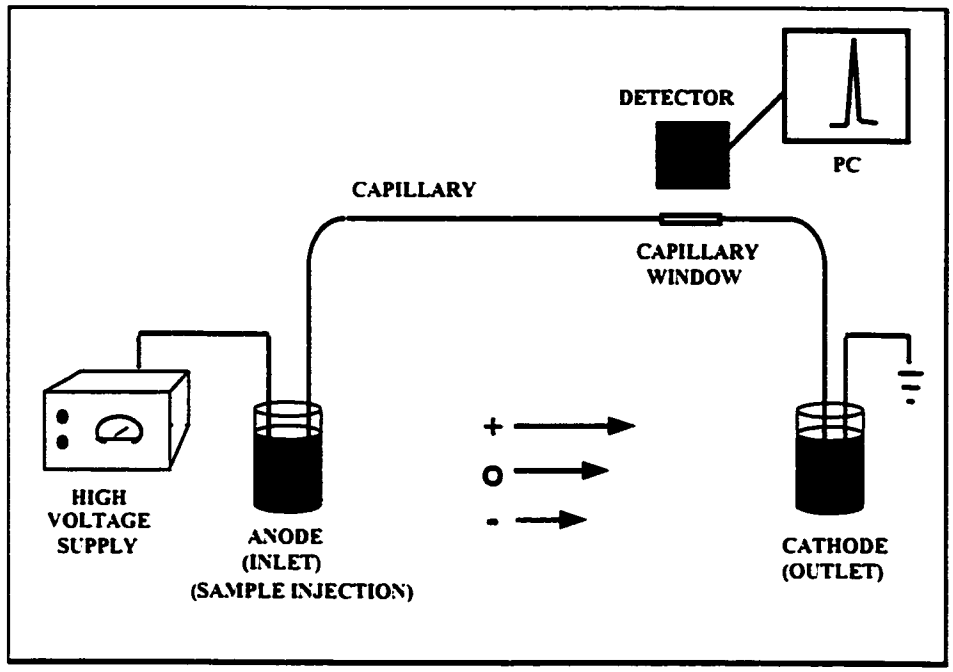

Figure 1.1 Schematic illustration of a generic capillary electrophoresis system.

applied, driving analytes towards a detector located near the outlet end of the capillary.

The separation of various analytes in CZE is based upon differences in analyte electrophoretic velocity (v_{ep}),

$$v_{ep} = \mu_{ep} E \qquad (1.1)$$

where μ_{ep} represents the electrophoretic mobility, and E the applied electric field. The electrophoretic mobility of a sample component is a physical constant, specific to each analyte in a particular electrolyte system. Assuming the component is spherical in shape, the electrophoretic mobility can be equated to:

$$\mu_{ep} = q / 6\pi\eta r \qquad (1.2)$$

where q is the analyte charge, η the buffer viscosity, and r the analyte's hydrodynamic radius. In the case of proteins, q is governed by the isoelectric point of the protein and the separation buffer pH used. In addition to electrophoretic migration there exists another force termed "electroosmotic flow", which drives the movement of all sample components towards the detector.

Electroosmotic flow (EOF) is a fundamental driving force in CZE. The basic principles of EOF have been examined extensively.[5-7] Capillaries commonly used in CZE are made of fused silica. Silicate glasses contain exposed silanol groups (Si-OH) on their surfaces. Ionization of these strongly acidic functional groups at pH greater than ~ 2 results in a net negative charge on the inner wall of the capillary which becomes more negative as the pH is increased. An idealized distance from the capillary wall to the middle of the negative charge associated with the deprotonated silanol groups is called the inner Helmholtz plane (IHP). The excess negative charge in the IHP attracts cations from the electrolyte solution, resulting in a compact, stagnant layer of positive charge. The distance from the middle of the negatively charged silanol groups to the midst of the positively charged adsorbed solution cations is referred to as the outer Helmholtz plane (OHP). A net excess positive charge extends into the electrolyte solution a short distance until a point is reached where charge balance is achieved, delineating the boundary of the diffuse layer. The combination of IHP, OHP, and diffuse layer is termed the electric double layer. A schematic of the electric double layer present at the capillary surface is presented in Figure 1.2.

A potential difference called the zeta (ξ) potential exists across the electric double layer. Application of an electric field results in movement of the diffuse layer, whereby excess cations are drawn towards the cathode (outlet). In aqueous buffer systems these cations are solvated and thus drag water molecules with them. Due to extensive hydrogen bonding between water molecules, there is a

uniform flow of buffer from the inlet end of the capillary to the outlet. This is referred to as electroosmosis. The velocity of the EOF (v_{eo}) is dependent upon the magnitude of the applied electric field, E, and the electroosmotic mobility, μ_{eo}, of the electrolyte.

$$v_{eo} = \mu_{eo} E \tag{1.3}$$

The electroosmotic mobility is dependent upon the zeta potential drop from the capillary wall to the boundary of the diffuse layer as well as the dielectric constant, ε, and viscosity, η, of the solution.

$$\mu_{eo} = \varepsilon\xi / 4\pi\eta \tag{1.4}$$

In CZE, the net migration velocity of sample components is thus the product of the applied electric field and the sum of the electroosmotic and electrophoretic mobilities.

$$V_{CZE} = (\mu_{eo} + \mu_{ep}) E \tag{1.5}$$

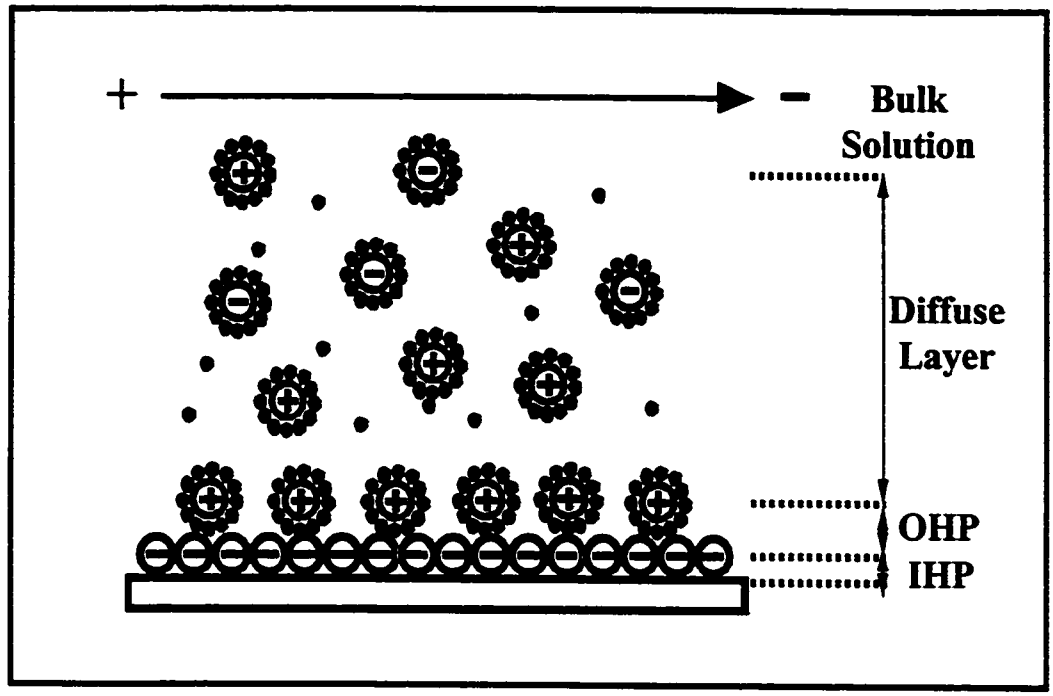

Figure 1.2 Schematic representation of the electric double layer present at the capillary surface. IHP = Inner Helmholtz Plane, OHP = Outer Helmholtz Plane, spheres surrounding cations and anions represent hydration. The direction of electroosmotic flow is that encountered in most cases (i.e. anode to cathode).

In basic conditions, μ_{eo} typically exceeds the μ_{ep} of anions present in a sample, such that all sample components will elute at the same end of the capillary.

The electrophoretic process in CGE differs significantly from that described above for CZE. In CGE the capillary is filled with either a crosslinked or linear polymer, creating a network of pores which separate macromolecules by a molecular sieving mechanism based on size. The capillary wall is typically modified to eliminate EOF hence preventing the polymer from extruding out of the capillary. Contrary to the process in CZE, the migration velocity of an analyte through a polymer-filled capillary therefore depends on its v_{ep} and on the pore structure of the polymer. In the case of polyacrylamide, the observed mobility of an analyte in the gel, μ, is a function of the analyte's mobility in the absence of polymer, μ_o, a retardation coefficient, k_R, and total concentration of total polymer in solution, % T.[2]

$$\log \mu = \log \mu_o - k_R (\% T) \qquad (1.6)$$

The theory of polymer solutions and CGE separation mechanism has been extensively reviewed in the literature.[8,9] It is clear from the above fundamental differences in separation mechanisms that one can obtain complementary information from these modes of CE in protein analysis.

CAPILLARY ELECTROPHORETIC ANALYSIS OF PROTEINS

Capillary Zone Electrophoresis of Proteins. The capillary electrophoretic analysis of proteins has been extensively reviewed in the literature.[10-13] Of interest are the numerous types of protein analysis which can be performed using this separation technique. These include enzyme assays, affinity interactions, chiral separations, protein folding, glycoform analysis, immunoassays, amino acid mutation analysis, purity, molecular weight and pI determination. CE thus serves as a viable alternative / complementary technique to more traditional protein analysis methods. CE-based protein analysis tools of the future must satisfy key requirements: rapidity, high-throughput analysis, the ability to detect low concentrations of protein, ease of automation, and cost-efficiency. The development of such methods further necessitates consideration of various parameters including capillary modification, buffer selection, protein characteristics, and mode of detection.

A central problem in CE protein analysis applications is interaction of the capillary wall with the analyte(s) of interest. As previously discussed, at pH values greater than ~ 2, the strongly acidic silanol groups on the inner surface of bare-fused silica capillaries become deprotonated, with increasing negative charge density at higher pH. Basic residues on the surface of proteins may consequently interact electrostatically with these sites, resulting in protein adsorption. In numerous instances this has been observed to have a negative effect upon

separation efficiency due to peak tailing and zone-broadening. Protein adsorption may also alter the magnitude of EOF during analysis or between runs, affecting migration time and peak area/height reproducibility. Common strategies to counteract this phenomenon include the use of buffer additives, capillary modification, and judicious buffer pH selection. It should be noted that to date there does not exist any one particular set of conditions proven effective for all protein analyses.

The research presented in Chapters 2 thru 5 has employed the last two of these strategies to varying extents. Various capillary coating chemistries have been thoroughly reviewed.[14-16] Coatings can be divided into two broad classes: covalent and dynamic. Covalent coatings involve attachment through a chemical bond, as opposed to dynamic coatings which interact non-covalently with the capillary wall (e.g. electrostatic, hydrophobic interactions). These broad categories can be further dissected into single-layer and multi layer coatings. In the latter, a bifunctional coating reagent is allowed to react with the capillary wall and serves as an anchor for the hydrophobic / electrostatic binding of a second bifunctional reagent. The ideal coating is reproducible, stable, and reduces all protein adsorption to insignificant levels. Though numerous types of coated capillaries are commercially available, these tend to be approximately 20 to 40-fold more expensive than bare-fused silica, and fail to perform satisfactorily for all protein applications. A complementary strategy to minimize protein adsorption is careful buffer selection.

Buffer selection is a key parameter in CE protein analysis due to its ability to influence protein structure, size, charge and capillary wall adsorption. The choice of buffering species, concentration, and pH is thus intimately linked to the properties of protein components in the sample of interest. In the case of neutral and acidic proteins (pI $\leq$ 7) the use of alkaline pH will promote electrostatic repulsion with the capillary wall. Similarly, basic protein (pI >7) adsorption can be minimized by operating under highly alkaline conditions (pH > 10). The use of highly acidic run buffers is another alternative since at pH < 3, most proteins are positively charged and silanol deprotonation is reduced.[13] This direction suffers from the extinguishing of electroosmosis leading to long migration times, however. Furthermore, applications requiring preservation of biological activity may suffer from such approaches. Despite these difficulties, CE has been successfully utilized in the analysis of proteins found in (a) simple matrices and (b) complex biological systems.

Protein Analysis in Simple Matrices. Numerous examples of CE-based analysis of proteins in simple matrices have been cited in the literature.[17] These include the study of recombinant protein variants whereby large quantitities of chromatographically purified proteins are present in a relatively simple buffer matrix. The high separation efficiency of CE allows one to detect the presence of closely related protein variants which may arise from single amino acid modifications such as deamidation, oxidation, glycosylation, and mutations. Over the last decade there has indeed been a dramatic increase in the number of CE

methods aimed at discriminating between protein variants: separation of desamido and didesamido forms of human growth hormone[18], incorrect disulfide bond formation in insulin-like growth factor-I[19], microheterogeneity of various glycoforms of recombinant human erythropoietin[20], analysis of charge heterogeneity of HIV-1 targeted soluble CD4 receptors[21], and protein phosphorylation.[22] The development of such methods has played an important role in the maturation of CE as a tool for the analysis of complex biological matrices.

Complex Protein Analysis. The ability of CE to serve as a useful tool in proteomics research has been demonstrated in applications such as tissue and biofluid profiling, single-cell analysis, and tryptic protein digest mapping.[23-26] The combination of high separation efficiency and nanolitre volume requirements renders CE particularly well-suited to such complex sample analyses. Capillaries in the low micron inner diameter range can be used effectively in the analysis of single, intact whole cells, the microenvironment surrounding a single cell, a cell's cytoplasmic contents, and the components within subcellular compartments such as vesicles. The success of such analyses is highly dependent on the use of detection schemes such as electrochemical, mass spectrometric, and laser-induced fluorescence detection. The development of CE-LIFD based protein methodologies may therefore be key to the movement of CE into the realm of proteomics. The extensive use of polymeric media in proteomic research further places a premium on the development of CGE-LIFD approaches.

Capillary Electrophoresis of Proteins Utilizing Polymer Matrices. The use of polyacrylamide slab gel electrophoresis (PAGE) for the separation of protein components according to molecular size has been an invaluable tool in the biochemical / clinical laboratory. The ability to perform these gel-based separations in a capillary has resulted in a significant reduction of analysis time. Protein separations by CGE can be typically achieved in fewer than 20 min, and are automatable.[27] Shorter analysis times are made possible by the highly efficient heat dissipation of fused-silica capillaries which allows for the application of significantly higher separation potentials (i.e. 20-30 kV). The use of CGE also obviates the need for lengthy staining/destaining steps by employing either absorbance or LIF on-column detection schemes. Furthermore, the advent of commercially available multi-capillary instrumentation has allowed for greater time savings with higher sample throughput. In CGE there are essentially two approaches to achieving protein separation by gel filtration.

Two types of sieving matrices have been utilized in CGE: cross-linked and linear polymers. In the case of cross-linked gels, a copolymerization reaction is initiated within the capillary, resulting in the formation of an extensive network of covalently cross-linked polymer chains. The pore size is controlled by varying the concentration of monomer at a fixed concentration of crosslinking agent. The most common example of a cross-linked gel is the radical copolymerization reaction of acrylamide and N,N'-methylenebisacrylamide, catalyzed by N,N,N',N'-tetramethylethylenediamine and ammonium peroxydisulfate.[28,29] Cross-linked gels

in a capillary format offer the advantage of increased mechanical strength and slightly improved resolution yet suffer from numerous disadvantages including gel shrinkage, bubble formation, and short lifespans.[30] Thus there has been significant interest in supplanting the use of cross-linked gels with linear polymer solutions in CGE.

A variety of non-cross-linked polymers have been successfully utilized in CGE. In the case of linear polymers, sieving is achieved above a critical concentration of polymer.[9] It is above this threshold concentration that the physical entanglement of polymer chains occurs, thus creating a network of pores. Perhaps the most commonly utilized CGE separation medium has been linear polyacrylamide.[27, 31-34] This sieving medium suffers however from low UV transparency from approximately 200 to 300 nm and is therefore ill-suited for UV-absorbance detection schemes. This has created a shift towards methods which utilize more suitable linear polymers with the following characteristics: lower viscosity, enhanced chemical stability, high hydrophilicity, low absorbance in the UV, and effective sieving ability. The key advantage of low viscosity linear polymers is the ability to rapidly flush and refill capillaries with fresh polymer solution between analyses.

Polymer Sieving Matrices in CE. Numerous linear polymers have been successfully utilized in protein CGE, including polyethylene oxide, dextran, and polyacrylamide.[35-37] The chemical structures of these polymers are illustrated in Figure 1.3. The predominant disadvantages of using low viscosity linear polymers

are decreased resolution and the requirement for a coated capillary. Coated capillaries are commercially available yet expensive, whereas in-house attempts to produce these capillaries are difficult to reproduce. A typical coating procedure has been previously described by Hjertén.[38] In order to fully appreciate the time investment and number of steps involved in such a procedure, the mono-molecular coating of a capillary with non-cross-linked polyacrylamide is illustrated in Figures 1.4 a, b. The advantage of this method is its simplicity relative to more stringent reaction schemes such as Grignard-based coating approaches. The result of such coatings is significant suppression of EOF such that the net analyte velocity remains proportional to molecular size and charge yet differs with respect to that observed in CZE. The fundamental difference between CGE and CZE is best illustrated by a vector diagram (Figure 1.5). The separation mechanism in CGE has been further modified in order to obtain protein molecular weight data, by both suppressing EOF and utilizing the denaturing surfactant, sodium dodecyl sulfate (SDS).

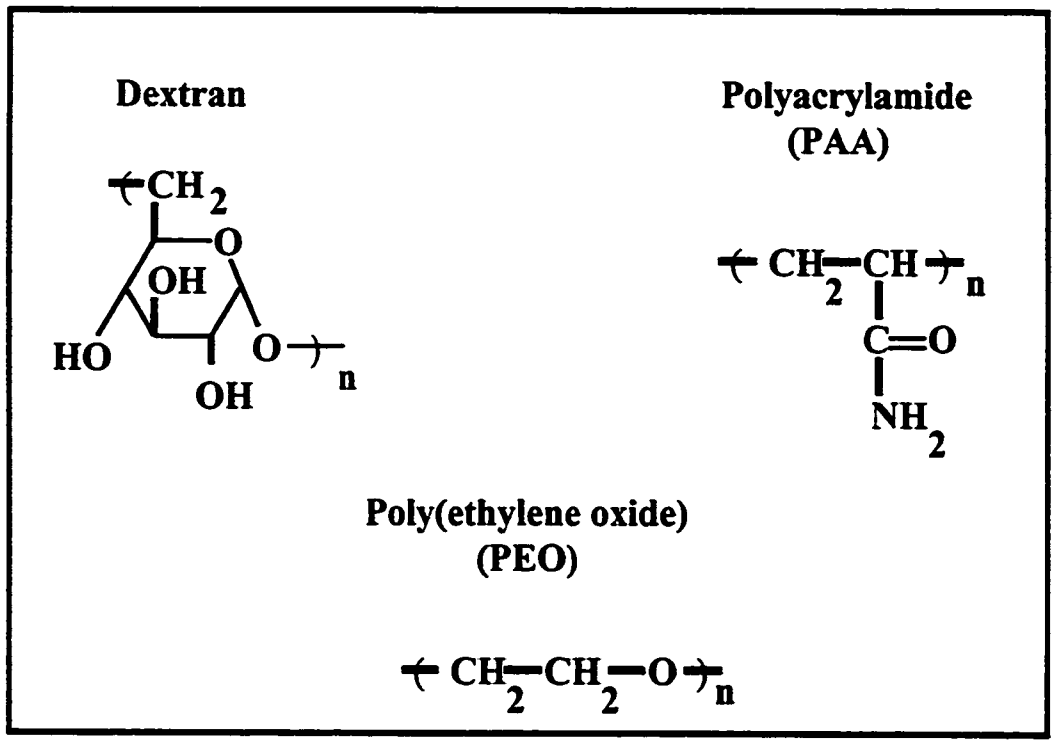

Figure 1.3 Structures of three commonly used "linear" polymers in capillary gel electrophoresis.

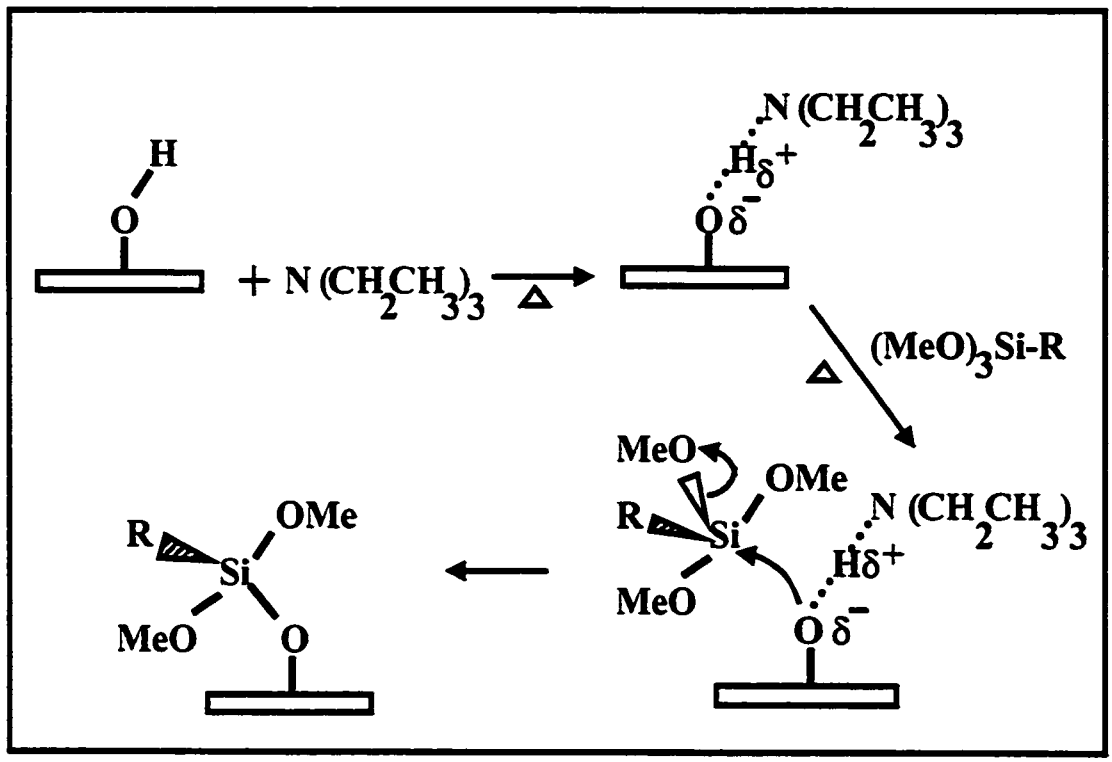

Figure 1.4a Capillary coating procedure for CGE: silanizing activation step.

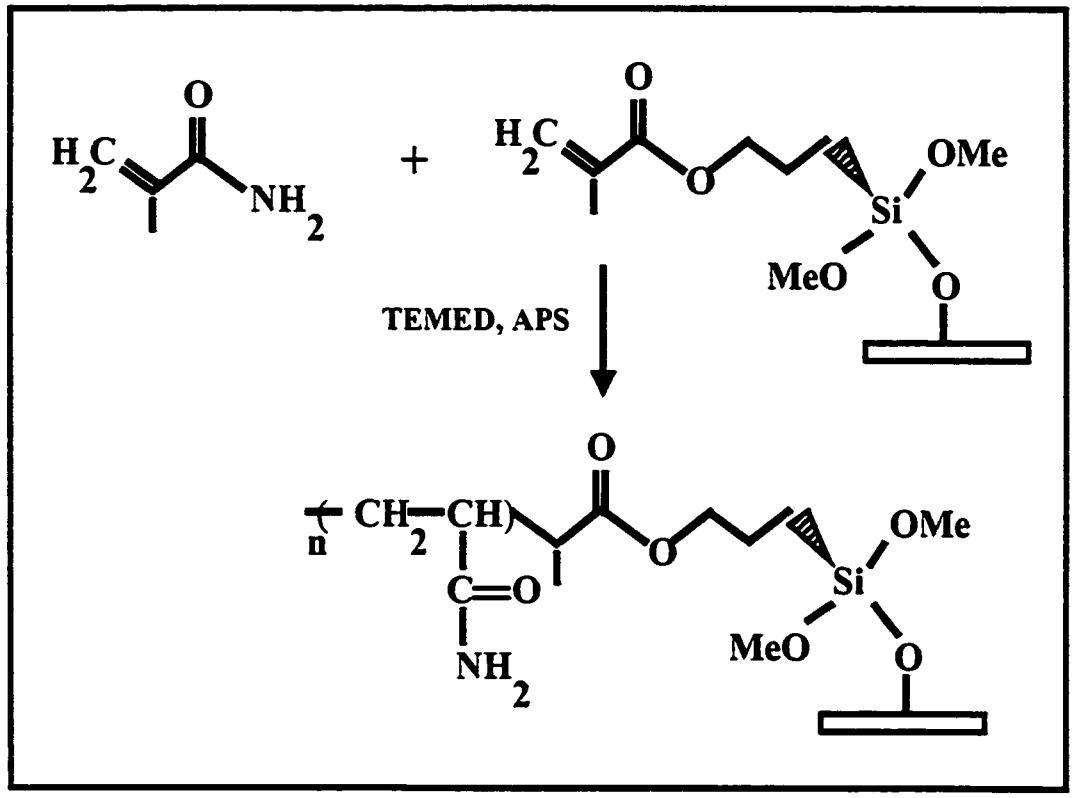

Figure 1.4b Capillary coating procedure for CGE: polymer derivatization.

Sodium Dodecyl Sulfate Capillary Gel Electrophoresis (SDS-CGE).

The use of slab gel SDS-PAGE is a widely accepted technique for the determination of protein purity and molecular weight. Composed of an anionic head group and long hydrophobic tail, SDS is well-suited for such determinations, generally binding with a constant surfactant to protein ratio of 1.4:1. Several models have been proposed for the structure and transport mechanism of these SDS-protein complexes.[39-41] In general, the constant binding ratio of SDS to protein imparts a uniform, highly negative charge density to protein species. In SDS-CGE, the magnitude of the electrophoretic vector is significantly increased due to the high negative charge of SDS-protein complexes. Differences in analyte electrophoretic velocity are consequently eliminated, and separation of proteins is according to molecular weight.

The advantages of SDS-CGE have been enumerated above. These merits have spurred the development of several commercially available SDS-CGE kits. The majority of commercial formulations currently require specially coated proprietary capillaries for satisfactory kit performance. Though this significantly increases the cost of performing SDS-CGE, successful separations of a wide variety of proteins have been achieved using commercial kits.[42, 43] Whether a commercial or in-house formulation is utilized, several limitations of SDS-CGE currently preclude its routine use in proteomics: reproducibility of capillary coatings, low resolution of protein components of low molecular mass

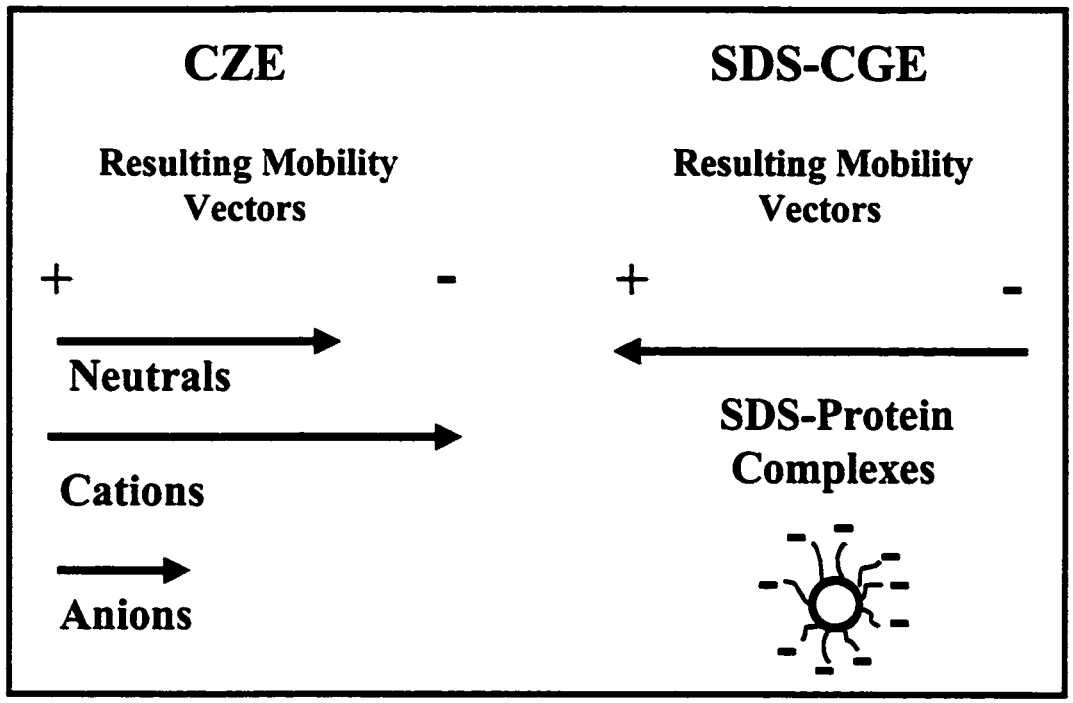

Figure 1.5 Separation mechanism differences between capillary zone electrophoresis and sodium dodecyl sulfate – capillary gel electrophoresis as expressed by their resultant mobility vectors.

(i.e. < 10 000 Da) due to requirements for higher polymer concentrations (i.e. higher viscosity), difficulties in recovering separated proteins, the complexity of performing two-dimensional CGE, and the need for optical detection schemes capable of detecting protein concentrations in the nanomolar range.

OPTICAL DETECTION SCHEMES IN CAPILLARY ELECTROPHORESIS

Overview of Optical Detection in Capillary Electrophoresis. Optical detection in CE can be categorized as either on-column or post-column. On-column detection requires prior removal of a short segment of a capillary's polyimide coating near the outlet. Analyte zones are detected as they pass through this detection "window". This format is most common and typically involves detection techniques such as UV-vis absorbance, fluorescence, refractive index and chemiluminescence. The advantages of using the capillary as a detection cell are simplicity and preservation of separation efficiency. Post-column detection is somewhat more complex, often requiring sheath-flow cells and elaborate optical component arrangements. The key advantage of this detection format is a significant reduction of scattering and background signal in fluorescence-based applications. This has been particularly successful in large-scale DNA sequencing by CGE.[44] Furthermore, the use of a mass spectrometer (MS) as a post-column detector in CE holds immense potential in the field of proteomics. Capable of

providing molecular weight and structural information, CE-MS has been successfully utilized in single-cell protein analysis.[45] However, similar to sheath-flow cuvette arrangements, interfacing the capillary to its post-column detector remains a considerable challenge. It is for this reason that the CE optical modes discussed below are most commonly used with on-column detection.

The primary optical detection schemes utilized in CE are UV-vis absorbance, fluorescence, chemiluminescence, indirect, and thermooptical detection. These have been described extensively in the literature.[1] The choice of a particular mode of detection is dependent upon several factors including the particular application, required detection limits, ease of use, and cost. The research presented in Chapters 2 thru 5 employs two of these approaches, absorbance and fluorescence detection.

Absorbance detection has been used extensively in CE due to its simplicity, low cost, and wide range of analytes that can be detected. The main disadvantage of this approach in CE is inherent in the Lambert-Beer Law,

$$\text{Log } I_o / I = A = \varepsilon b c \qquad (1.7)$$

where I_o is the source intensity upon the sample, I is the intensity of radiation through the analyte, ε is the molar extinction coefficient of the analyte, b is the optical pathlength, and c relates to the molar concentration of the analyte in the detection volume. It is clear from the above equation that the short optical pathlengths (i.e. typically 50 - 100 microns) utilized in CE will result in relatively poor concentration limits of detection and small linear dynamic ranges. Numerous

attempts have focused upon extending the absorbance pathlength yet these improve detection limits by at best one order of magnitude. There has thus been a growing trend towards fluorescence-based detection schemes in CE.

Fluorescence detection has been deemed the most "sensitive" detection mode in CE, whereby single molecule detection can been achieved.[46] Additional advantages of fluorescence detection include improved signal linearity and selectivity. In the case of dilute solutions, fluorescence intensity is directly proportional to the power of the excitation source:

$$\Phi_F = 2.3\ \phi_p\ \varepsilon\ b\ c\ P \qquad (1.8)$$

where Φ_F is the fluorescence radiant intensity in W, ϕ_p is the quantum yield of fluorescence, ε is the molar absorptivity at the excitation wavelength in L/(mol·cm), c is the analyte concentration in mol/L, b is the optical path length in cm, and P is the radiant power of the excitation source in W.[47] It is clear from the above equation that the greater the power of the incident light, the higher the fluorescence emission. Laser light is coherent, monochromatic, can be focused easily into a spot the size of the inner diameter of a CE separation capillary, and is of greater power than light from conventional incoherent excitation sources. This increased power compensates for the short path lengths encountered in CE. Laser-induced fluorescence (LIF) is thus the approach of choice in the development of CE-based applications requiring detection limits in the subnanomolar range.

Laser-Induced Fluorescence Detection (LIFD). CE-LIFD systems have been reported to produce concentration limits of detection (LODs) below 10^{-13} M.[48] A host of different fluorescence instrumental arrangements utilizing sheath-flow cuvettes, charge-coupled device cameras, and confocal microscopes have been reported in the literature.[3] A simplified on-column LIF detection system, as used in the various studies presented herein, is illustrated in Figure 1.6. Laser light is focused via a focusing objective onto a section of capillary where the polyimide

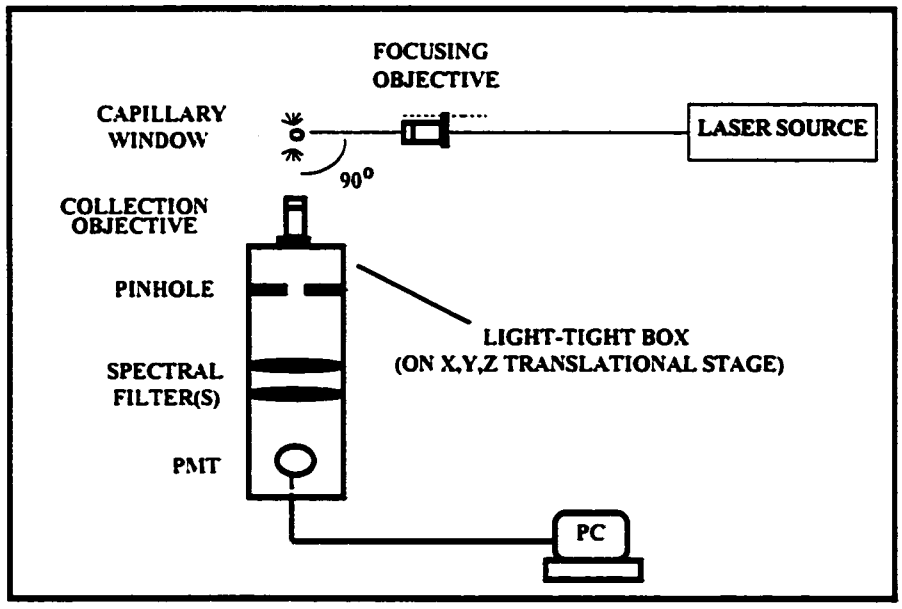

Figure 1.6 Generic design of CE-LIF on-column detection system.

coating has been removed. Emitted fluorescence is collected at right angles to the excitation source by a collection objective and passed through a pinhole so as to spatially filter scattered light. One or more wavelength selection filters are used to optically filter Raman and Rayleigh scatter, and allow only analyte fluorescence to reach the photomultiplier tube. Visible wavelength lasers such as He-Ne or Ar^+ ion lasers are well suited to this purpose since they have emission lines matching common fluorescent reagents and are relatively inexpensive. It should be noted however that most molecules are not naturally fluorescent and must therefore be derivatized with a fluorescent probe prior to analysis.

Derivatization Approaches in Capillary Electrophoresis. It is generally known that a significant number of proteins and peptides exhibit native fluorescence by virtue of their aromatic amino acid residues, and this has been successfully applied in CE body fluid profiling.[49] Tryptophan, phenylalanine and tyrosine fluoresce in the UV region yet only weakly, with quantum yields of 0.21 or less.[50] Fluorescence emission from these residues is dependent upon their local environment in the protein's tertiary structure.[51] Furthermore, it has been well-documented in the literature that the more fluorescent residues, tyrosine and tryptophan, are typically found in proteins at frequencies of 3.5% and 1.1%, respectively. For these reasons, native fluorescence detection is not considered a universal mode of detection in CE. The high cost of UV laser excitation further limits the use of this approach. The majority of CE-LIFD applications have thus focused on fluorescent derivatization and the use of visible wavelength lasers.

A variety of derivatization approaches have been utilized in CE-based protein analysis. The key difficulty encountered in derivatization is the production of a single desired product. The presence of numerous reactive moieties in the protein target often results in a host of derivatization products, complex electropherograms, poor peak quantitation and resolution.[52-55] Two opposite strategies have been utilized in an effort to address this issue. The first involves a "brute force" approach whereby one attempts to produce a fully tagged product by utilizing a large molar excess of derivatizing reagent relative to protein in conjunction with relatively harsh conditions (i.e. elevated temperature, high pH, longer reaction times, in the presence of denaturing agents).[56] A second approach involves the use of limited, stoichiometric amounts of labeling reagent, pH values which exploit p*Ka* differences between various functional groups, and milder reaction conditions.[57] This method is more conducive to the production of biologically active protein conjugates.

Both strategies may employ reagents which attach either covalently or non-covalently to their target. The most common derivatizing chemistries used in CE have been fluorescamine[58], fluorescein isothiocyanate[59, 60], NDA[61], CBQCA[62,63], and OPA.[64,65] Fluorescent labels may be classified furthermore, as either fluorogenic or non-fluorogenic. Fluorogenic tags are weakly fluorescent in the unbound form, with a significant increase in fluorescence emission upon conjugation, whereas non-fluorogenic labels emit "significantly" both in their bound and unbound states. The use of fluorogenic labeling reagents is desirable

since it obviates the need to separate unreacted reagent from reaction products, hence reducing electropherogram complexity and facilitating analyte quantitation. Derivatization reactions can also be categorized according to whether they are performed prior to, during, or immediately following the CE separation.

The majority of conjugation reactions in CE are performed pre-column. In the pre-column format, derivatization is completed prior to sample injection into the capillary. Advantages of this approach include: the ability to employ reaction conditions which are not compatible with the CE system, the absence of restrictions relating to reaction kinetics, the ease with which multi-step reactions can be performed, the availability of numerous labeling reagents, and simplified instrumental setup.[66] Disadvantages of pre-column conjugation include: formation of side products and derivatives of additional sample components, the need for conjugate stability, and analytes are not separated in their unmodified form.

In post-column labeling procedures, separated analyte zones are allowed to mix briefly with derivatizing reagent immediately prior to detection. In this mode, the drawbacks of pre-column labeling listed above are circumvented. Disadvantages include a limited selection of reaction conditions, a requirement for rapid reaction kinetics, the need for additional instrumentation such as a sheath-flow cuvette or capillary connectors which can lead to peak broadening as analyte zones traverse the "reactor", and reduced selection of suitable labeling reagents (i.e. fluorogenic).[66] The least common approach is on-column labeling.

On-column derivatization utilizes the capillary as a reaction chamber. Typically, a sample is injected prior to or immediately following injection of a plug of derivatizing reagent. The order of injection is determined by the relative electrophoretic mobilities of the dye and sample components. Sample components are labeled as they migrate through or are overtaken by the plug of derivatizing reagent. In the case of fluorogenic labeling reagents, the capillary may be completely filled with run buffer containing the dye prior to sample injection.[67] The main advantages of on-column labeling include: minimal sample dilution, reduced reagent consumption, and relatively simple instrumentation. A key requirement is that the reaction be rapid and quantitative. The use of these various derivatization schemes in the development of novel CE-LIFD protein analysis applications is, in turn, of significant interest in the analytical, biochemical, and clinical laboratory. Of particular interest are CE-LIFD protein applications falling into three key categories: general protein quantitation and purity assessment, immunoassays, and biofluid profiling.

BIOCHEMICAL & CLINICAL APPLICATIONS OF CZE-LIFD

Protein Quantitation and Purity Assessment. The ability to quantitate low concentrations of proteins both in solution and within a polymer matrix, in a time efficient and cost effective fashion, has been the focus of many studies. Protein quantitation in solution is usually achieved by several absorbance-based colorimetric methods. These include the Bradford, bicinchoninic acid, and Lowry assays and variations thereof.[68-70] The major problem with colorimetric methods is their inability to quantitate proteins in the sub-microgram per milliliter concentration range. For this reason, attention has shifted towards the development of various fluorometric methods. Recent advances in fluorophore chemistry such as NanoOrange and 3-(4-carboxybenzoyl)-quinoline-2-carboxaldehyde (CBQCA) have permitted protein quantitation in the range of 10 ng/mL to 10 μg/mL.[71] The ability to perform these assays in a CZE-LIFD format has been recently demonstrated.[67] In comparison to conventional microtitre plate methods where total protein is measured, CE allows for the separation of various sample components prior to detection, thus permitting the quantitation of each species in the mixture.

Complementary to solution phase CZE-LIFD protein quantitation has been the development of CGE-LIFD methodologies. These have occurred primarily in the area of SDS-CGE for molecular weight and purity determination. Visualization of separated proteins in slab gel SDS-PAGE is typically achieved by

staining with Coomassie Brilliant Blue or silver stain dyes. Unfortunately, Coomassie Brilliant Blue provides semiquantitative results with limits of detection considered insufficient for accurate purity determinations. The goal of many SDS-CGE-LIFD methods is to match the 10 ng/mL concentration detection limits of silver staining in a fraction of the time required to perform SDS-PAGE. Several groups have attempted to reach this goal utilizing both covalent and non-covalent fluorogenic dyes such as fluorescamine, naphthalene-2,3-dicarboxaldehyde, 4-fluoro-7-nitrobenzofurazan, and Sypro Red.[72-74] In addition to molecular weight and protein purity determinations, CE-LIFD has been successfully employed in specific analyte quantitation using immunorecognition.

CE-LIFD Immunoassays. The high selectivity arising from specific antibody/analyte interactions is a powerful means of quantitating trace levels of particular antigens within a complex matrix. CE-LIFD immunoassays possess a clear advantage over traditional immunoassay approaches: rapid, high resolution separations of multiple analytes, with few if any wash steps. The majority of CE immunoassays have utilized fluorescent derivatization, providing detection limits in the subnanomolar range, and selective detection (i.e. all non-labeled components of the sample mixture are not detected). These assays can be categorized as either noncompetitive or competitive.

In the noncompetitive format, an excess of fluorescently labeled antibody is incubated with the sample solution and allowed to form a complex with its specific antigen. Electropherograms in noncompetitive immunoassays typically

contain two zones, corresponding to the antibody-antigen complex and excess antibody tracer. The amount of antigen present in the initial sample can be determined by quantitating either of the two zones. A major difficulty with noncompetitive approaches is the development of a uniform antibody derivatization procedure.

Fluorescent conjugation of the target analyte is a common alternative to noncompetitive assays. In competitive CE-LIFD immunoassays, a fixed concentration of fluorescently labeled antigen standard is incubated with a sample containing the unlabeled analyte, followed by the addition of a limited amount of antibody. The rapid, effective separation of bound and free labeled antigen using CE, produces two zones which each provide quantitative information on the initial amount of analyte in the sample. This format has been highly successful in the determination of insulin and other proteins.[25, 75] In addition to the specific detection and quantitation of proteins by competitive immunoassays, CE has been particularly useful in biofluid profiling.

CE Biofluid Profiling. Biofluid profiling has traditionally been performed by cellulose acetate or agarose gel electrophoresis. However, advantages such as on-line detection, complete automation, reduced analysis time and capillary array instrumentation has made CE an attractive alternative. Contrary to the above two key applications of CE-LIFD, relatively few CE-LIFD biofluid profiling applications have been developed.[76] The main advantage of utilizing LIFD in biofluid profiling is the ability to detect proteins at concentrations up to three

orders of magnitude lower than with UV absorbance. This is of obvious benefit for early disease diagnosis. To date, CE has been successfully utilized in disease diagnosis by providing rapid serum, urine, cerebrospinal fluid, saliva, amniotic, and tearfluid profiles. For example, the diagnosis of Bence-Jones proteinuria, a serious disorder, is made possible by the detection of Bence-Jones protein in a urinary profile.[77, 78] Similarly, the presence of oligoclonal bands in CE profiles of cerebrospinal fluid is a rapid screening tool for multiple sclerosis.[79] The development of simple, fluorescence-based biofluid profiling methods capable of providing insights into disease etiology and early detection is thus an area of continued interest.

CONCLUSIONS

The trend towards high-throughput and miniaturization has placed a premium on rapid nanoscale techniques. Among these techniques is CE, a powerful, automated analytical separation technique capable of providing high resolution and rapid nanolitre sample analysis at a reduced cost. The CE user is nonetheless faced with the non-trivial task of obtaining physiologically relevant detection limits while avoiding sample matrix interference. Advances in fluorescent dye chemistry have enabled the development of various non-CE-based protein analysis tools capable of quantitating proteins in the subnanomolar concentration range. These fluorescence-based methods are indeed becoming increasingly popular with respect to radioactive approaches, due in part to the

inherent disposal and regulatory issues surrounding radioisotope use. The development of CE-LIFD protein analysis tools which exploit advances in fluorescence while matching the throughput of traditional microplate, HPLC, and slab-gel methodologies is a prerequisite to the acceptance of CE in the field of proteomics.

The research presented herein is focused primarily on achieving this goal, as well as implementing fluorescent dyes which have never been utilized in a CE format, developing novel CE biofluid analysis methodology, and producing a novel fluorescent protein conjugate for bioanalytical applications.

OUTLINE OF THESIS

The studies presented in Chapters 2 thru 5 provide a detailed account of the development of novel CE protein analysis tools in four key areas: biofluid profiling, protein quantitation, molecular weight and purity assessment, and immunorecognition. Chapter 2 describes the CZE analysis of seminal plasma, a biofluid which has received virtually no attention using this analytical technique. This absorbance-based study is complemented by the development of a CE-LIFD approach (Chapter 3) for the solution-phase quantitation of protein in complex matrices such as seminal plasma. The main advantage of this approach is its simplicity both in terms of instrumentation and derivatization. The above solution-phase protein analysis tools were subsequently complemented by a SDS-CGE LIFD approach providing information on the purity and molecular weight of

nanomolar levels of protein (Chapter 4). To date, relatively few polymer-based SDS-CGE methods have been able to match the detection limits reported in this work.

Whereas the above methods provide a rapid means of analyzing complex samples, the ability to selectively detect and quantitate a particular analyte within complex matrices such as seminal plasma and serum requires the use of immunorecognition. Current CE methodology for the selective quantitation of the clinically relevant analyte, insulin-like growth factor I (IGF-I) suffers from suboptimal detection limits and matrix interferences. Various dynamic capillary coating procedures are required to achieve these detection limits. Unfortunately, the stability of such coatings is such that relatively frequent capillary reconditioning is required. In an effort to improve detection limits of IGF-I while obviating the need for such coatings, site specific fluorescent derivatization, LC/MS characterization, and CE-LIFD evaluation of a potent IGF-I analogue, Long R3 IGF-I was performed (Chapter 5).

Chapter 6 is a summary of the results presented in Chapters 2 thru 5, and presents suggestions for future work. The experiments presented in Chapters 2, 4, and 5 were designed and performed by Michael D. Harvey. Preliminary experiments pertaining to SDS-CGE stability were performed by Dirk Bandilla. The work described in Chapter 3 was designed, analyzed and processed by Michael D. Harvey. Microplate studies were performed by Vicky Bablekis under my direction. CE-LIFD experiments including biofluid profiles were conducted by

Michael D. Harvey. Initial drafts of manuscripts in Chapters 2 thru 5 were written by Michael D. Harvey, and were coedited with Dr. Peter R. Banks (Chapters 2, 3, 4, 5) and Dr. Cameron D. Skinner (Chapter 3).

REFERENCES

(1) Kitagishi, K. in *Handbook of Capillary Electrophoresis Applications*; Shintani, H., Polonsky, J. Eds.; Chapman & Hall: London, 1997; p. 137.

(2) Baker, D.R. in *Capillary Electrophoresis*; John Wiley & Sons: New York, 1995; p. 1, 76.

(3) Oda, R.P., Landers, J.P. in *Handbook of Capillary Electrophoresis (Second Edition)*; Landers, J.P. Ed.; CRC Press: Boca Raton, 1997; 2, 397.

(4) Heiger, D.N. in *High Performance Capillary Electrophoresis – An Introduction (Second Edition)*; Hewlett-Packard Company: Paris, 1992; p.12.

(5) Hunter, R.J. in *Colloid Science: Principles and Applications*; Academic Press: New York, 1981, Chapter 2.

(6) Lukacs, K.D., Jorgenson, J.W.; *J. High Res. Chromatog.* **1985**, 8, 407.

(7) Bruin, G.J.M., Chang, J.P., Kuhlman, R.H., Zegers, K., Kraak, J.C., Poppe, H.; *J. Chromatog.* **1989**, 471, 429.

(8) Bae, Y.C., Soane, D.; *J. Chromatog. A* **1993**, 652, 17.

(9) Heller, C.; *J. Chromatog. A* **1995**, 698, 19.

(10) Deyl, Z., Struzinsky, R.; *J. Chromatogr.* **1991**, 569, 63.

(11) Schöneich, C., Kwok, S.K., Wilson, G.S., Rabel, S.R., Stobaugh, J.F., Williams, T.D., Vander Velde, D.G.; *Anal. Chem.* **1993**, 65, 67R.

(12) Schöneich, C., Hühmer, A.F.R., Rabel, S.R., Stobaugh, J.F., Jois, S.D.S., Larive, C.K., Siahaan, T.J., Squier, T.C., Bigelow, D.J., Williams, T.D.; Anal. Chem. **1995**, 67, 155R.

(13) Wehr, T., Rodriguez-Diaz, R., Liu, Cheng-Ming in Advances in Chromatography; Brown, P.R., Grushka, E. Eds.; Marcel Dekker: New York, 1997, Volume 37, p. 237.

(14) Wehr, T.; *LC-GC*, **1993**, 11, 14.

(15) Turner, K.A.; *LC-GC*, **1991**, 9, 350.

(16) Mazzeo, J.R., Krull, I.S.; *Biochromatography*, **1991**, 10, 638.

(17) Teshima, G., Wu, S.; *Methods in Enzymology* **1996**, 271, 264.

(18) Nielson, R.G., Sittampalam, G.S., Rickard, E.C.; *Anal. Biochem.* **1989**, 177, 20.

(19) Ludi, H., Gassman, E., Grossenbacher, H., Marki, W.; *Anal. Chim. Acta* **1988**, 213, 215.

(20) Tran, A.D., Park, S., Lisi, P.J.; *J. Chromatog.* **1991**, 542, 459.

(21) Wu, S.L., Teshima, G., Cacia, J., Hancock, W.S.; *J. Chromatog.* **1990**, 516, 115.

(22) Fadden, P., Haystead, T.A.J.; *Anal. Biochem.* **1995**, 225, 81.

(23) Phillips, T.M., Kimmel, P.L.; *J. Chromatogr.* **1994**, 656, 259.

(24) Molteni, S., Frischnecht, H., Thormann, W.; *Electrophoresis* **1994**, 15, 22.

(25) Schultz, N.M., Huang, L., Kennedy, R.T.; *Anal. Chem.* **1995**, 67, 924.

(26) Rush, R.S., Derby, P.L., Strickland, T.W., Rohde, M.F.; *Anal. Chem.* **1993**, 65, 1834.

(27) Regnier, F.E., Wu, D.; *J. Chromatogr.* **1992**, 608, 349.

(28) Chrambach, A., Rodbard, D.; *Science* **1971**, 172, 440.

(29) Wu, D., Regnier, F.E.; *Anal. Chem.* **1993**, 65, 2029.

(30) Chiari, M., Righetti, P.G.; *Electrophoresis* **1995**, 16, 1815.

(31) Cohen, A.S., Karger, B.L.; *J. Chromatogr.* **1987**, 397, 409.

(32) Widhalm, A., Schwer, C., Blaas, D., Kenndler, E.; *J. Chromatogr.* **1991**, 549, 446.

(33) Werner, W.E., Demorest, D.M., Stevens, J., Wiktorowicz, J.E.; *Anal. Biochem.* **1993**, 212, 253.

(34) Yin, H.F., Lux, J.A., Schomburg, G.; *J. High Resolut. Chromatogr.* **1990**, 13, 624.

(35) Guttman, A., Shieh, P., Lindahl, J., Cooke, N.; *J. Chromatogr.* **1994**, 676, 227.

(36) Ganzler, K., Greve, K.S., Cohen, A.S., Karger, B.L., Guttman, A., Cooke, N.C.; *Anal. Chem.* **1992**, 64, 2665.

(37) Hunt, G., Nashabeh, W.; *Anal. Chem.* **1999**, 71, 2390.

(38) Hjertén, S.; *J. Chromatogr.* **1985**, 347, 191.

(39) Guo, X-H., Chen, S-H.; *Chemical Physics* **1990**, 149, 129.

(40) Samsó, M., Daban, J-R., Hansen, S., Jones, G.R.; *Eur. J. Biochem.* **1995**, 232, 818.

(41) Coello, A., Meijide, F., Mougán, M.A., Núñez, E.R., Tato, J.V.; *J. Chem. Educ.* **1995**, 72, 73.

(42) Guttman, A., Nolan, J.; *Anal. Biochem.* **1994**, 221, 285.

(43) Guttman, A., Nolan, J.A., Cooke, N.; *J. Chromatog.* **1993**, 632, 171.

(44) Takahashi, S., Murakami, K., Anazawa, T., Kambara, H.; *Anal. Chem.* **1994**, 66, 1021.

(45) Hofstadler, S.A., Swanek, F.D., Gale, D.C., Ewing, A.G., Smith, R.D.; *Anal. Chem.* **1995**, 67, 1477.

(46) Lee, Y.-H., Maus, R.G., Smith, B.W., Winefordner, J.D.; *Anal. Chem.* **1994**, 66, 4142.

(47) Van Den Beld, C.M.B., Lingeman, H. in *Luminescence Techniques in Chemical and Biochemical Analysis*. Marcel Dekker Inc.: New York, 1991.

(48) Timperman, A.T., Khatib, K., Sweedler, J.V.; *Anal. Chem.* **1995**, 67, 139.

(49) Paquette, D.M., Sing, R., Banks, P.R., Waldron, K.C.; *J. Chromatogr. B* **1998**, 714, 47.

(50) Teale, F.W.J., Weber, G.; *J. Biochem.* **1957**, 65, 476.

(51) Timperman, A.T., Oldenburg, K.E., Sweedler, J.V.; *Anal. Chem.* **1995**, 67, 3421.

(52) Krull, I.S., Strong, R., Sosic, Z., Cho, B.-Y., Beale, S., Cohen, S.; *J. Chromatogr. B* **1997**, 699, 173.

(53) Szulc, M.E., Swett, P., Krull, I.S.; *Biomed. Chromatogr.* **1997**, 11, 207.

(54) Banks, P.R.; *Trends in Anal. Chem.* **1998**, 17, 612.

(55) Banks, P.R., Paquette, D.M.; *J. Chromatogr. A* **1995**, 693, 145.

(56) Li, G., Yu, J., Krull, I.S., Cohen, S.; *J. Liquid Chromatogr.* **1995**, 18, 3889.

(57) Hentz, N.G., Richardson, J.M., Sportsman, J.R., Daijo, J., Sittampalam, G.S.; *Anal. Chem.* **1997**, 69, 4994.

(58) Shippy, S., Jankowski, J.A., Sweedler, J.V.; *Analytica Chimica Acta* **1995**, 307, 163.

(59) Sweedler, J.V., Shear, J.B., Fishman, H.A., Zare, R.N., Scheller, R.H.; *Anal. Chem.* **1991**, 63, 496.

(60) Wu, S., Dovichi, N.J.; *J. Chromatogr.* **1989**, 480, 141.

(61) Ueda, T., Mitchell, R., Kitamura, F., Metcalf, T., Kuwana, T., Nakamoto, A.; *J. Chromatogr.* **1992**, 593, 265.

(62) Liu, J., Shirota, O., Wiesler, D., Novotny, M.; *PNAS* **1991**, 88, 2302.

(63) Liu, J.P., Hsieh, Y.Z., Wiesler, D., Novotny, M.; *Anal. Chem.* **1991**, 63, 408.

(64) Nickerson, B., Jorgenson, J.W.; *J. Chromatogr.* **1989**, 480, 157.

(65) Pentoney, S., Huang, X., Burgi, D., Zare, R.N.; *Anal. Chem.* **1988**, 60, 2625.

(66) Bardelmeijer, H.A., Lingeman, H., de Ruiter, C., Underberg, W.J.M.; *J. Chromatogr. A* **1998**, 807, 3.

(67) Harvey, M.D., Bablekis, V., Skinner, C.D.; *J. Chromatogr. B* (accepted).

(68) Bradford, M.M. *Anal. Biochem.* **1976**, 72, 248.

(69) Smith, P.K., Krohn, R.I., Hermanson, G.T., Mallia, A.K., Gartner, F.H., Provenzano, M.D., Fujimoto, E.K., Goeke, N.M., Olson, B.J., Klenk, D.C. *Anal. Biochem.* **1985**, 150, 76.

(70) Lowry, O. *et al.*, *J. Biol. Chem.* **1951**, 193, 265.

(71) Haugland, R.P. (Ed.) in *Handbook of Fluorescent Probes and Research Chemicals (Sixth Edition)*; Molecular Probes: Portland, 1996; 180.

(72) Gump, E.L., Monnig, C.A.; *J. Chromatogr. A* **1995**, 715, 167.

(73) Wise, E.T., Navjot, S., Hogan, B.L.; *J. Chromatogr. A* **1996**, 746, 109.

(74) Harvey, M.D., Bandilla, D., Banks, P.R.; *Electrophoresis* **1998**, 19, 2169.

(75) Schultz, N.M., Kennedy, R.T.; *Anal. Chem.* **1993**, 65, 3161.

(76) Varnell, R.J., Maitchouk, D.Y., Beuerman, R.W., Salvatore, M.F., Carlton, J.E., Haag, A.M.; *J. Cap. Elec.* **1997**, 4, 1.

(77) Friedberg, M.A., Shihabi, Z.K.; *Electrophoresis* **1997**, 18, 1836.

(78) Jenkins, M.A.; *Electrophoresis* **1997**, 18, 1842.

(79) Shihabi, Z.K.; *Ann. Clin. Lab. Sci.* **1991**, 21, 346.

CHAPTER 2

Capillary Electrophoretic Analysis of Human Seminal Plasma

M.D. Harvey and P.R. Banks, Submitted Journal of Chromatography B:

Biomedical Sciences and Applications

Reprinted with permission from Elsevier Science

ABSTRACT

Human seminal plasma is a complex mixture of protein and non-protein components which provide an indication of prostatic, semeniferous tubule and Cowper gland function. The ability to rapidly screen seminal plasma samples for changes in the quantity of key seminal plasma components such as prostate specific antigen, human serum albumin, α_1-antitrypsin, and transferrin, is of significant interest to the clinical chemist. This paper investigates the suitability of capillary electrophoresis with UV absorbance detection as a separation technique for the analysis of human seminal plasma. Specific issues concerning the clinical chemist are addressed: identification of optimal separation conditions to minimize analysis time, migration time reproducibility, internal standardization, utilization of protease inhibitors, freeze/thaw cycling, biofluid temperature stability, and protein/non-protein zone identification.

INTRODUCTION

The profiling of biofluids has received increasing attention in the clinical laboratory. This has been fueled in part by advances in various analytical separation techniques. Perhaps one of the most powerful of these techniques is two-dimensional slab gel electrophoresis, whereby the various components of a biofluid are separated according to their molecular weights and isoelectric points.

A typical two-dimensional gel can separate hundreds of proteins, allowing one to compare the profiles obtained in various disease states to those of normal individuals.[1-4] Further insights into the pathogenesis of disease can be obtained by observing an increase or decrease in the levels of particular proteins in the profile. Though highly informative, two-dimensional slab gels are semi-automated and extremely time-consuming. The need for high throughput in early disease diagnosis has no doubt required an alternate approach in biofluid profiling.

Capillary electrophoresis has been proven to be a highly effectual analytical separation technique for biofluid profiling, including serum[5,6], cerebrospinal fluid[7], urine[8,9], and tear fluid analyses.[10] The advantages of this approach are well documented: low microlitre sample volume requirement, nanolitre sample consumption, separations on the order of minutes. Furthermore, absorbance detection can be performed on-column, obviating the need for lengthy staining and destaining steps. Contrary to two-dimensional gels, many small non-protein components can thus be visualized by this approach. It is generally accepted that the resolution obtained by two-dimensional gels cannot be readily attained by one-dimensional capillary electrophoresis. Nonetheless, various well-characterized zones in a capillary electrophoretic biofluid profile can be extremely useful in early disease diagnosis.[11-13] The advent of commercially available multi-capillary, automated instrumentation capable of sampling from 96-well microtitre plates has further promoted capillary electrophoresis as a high throughput tool for disease diagnosis.[14-17]

Despite efforts to characterize a multitude of human biofluids by capillary electrophoresis, there have been relatively few reports on the analysis of human seminal plasma.[18] This fluid has however received considerable attention due to its ability to indicate the function of various organs. Two-dimensional slab gel analysis has revealed a significant number of protein components. At least five major components have been identified by Western blotting and include prostate specific antigen (PSA), prostatic acid phosphatase, transferrin, serum albumin (HSA), and α_1-antitrypsin (AT).[19] It has been proposed that prostatic, Sertoli cell / semeniferous tubule, and Cowper's gland function can be assessed by the various levels of these proteins.[20-23] In addition, several non-protein species have been implicated in fertility.[24-26] As a result, it was the goal of this study to characterize human seminal plasma by capillary electrophoresis.

Several important considerations must be addressed in the capillary electrophoretic analysis of biofluids. These include buffer selection (buffer species, concentration, pH), protein adsorption, separation potential, migration time reproducibility, internal standardization, utilization of protease inhibitors, freeze/thaw cycling, biofluid temperature stability over time, and capillary conditioning between runs. It is also of value to determine zones corresponding to protein/non-protein components. Additional characterization involves the identification of these various zones so as to allow the clinical chemist to rapidly spot abnormal levels of a particular component. Capillary electrophoretic analysis of human seminal plasma has thus been performed, with particular attention to the

above considerations. To our knowledge, this is the first time that such an analysis of human seminal plasma has been performed by capillary electrophoresis.

EXPERIMENTAL

Boric acid, sodium tetraborate, sodium hydroxide, phenylmethylsulfonylfluoride (PMSF), human serum albumin (HSA), transferrin (TF), and α_1-antitrypsin (AT) and Orange G marker were all purchased from Sigma (Mississauga, Ont., Canada). All buffers were prepared using nanopure water (18.3 MΩ cm^{-1}) (Barnstead). HPLC grade acetonitrile used in protein precipitation was purchased from Fisher (Fairlawn, NJ). Prostate specific antigen (PSA) was purified in-house according to the method of Sensabaugh.[27] All seminal plasma samples (n=3) were handled in accordance with protocols outlined by the World Health Organization. It is recommended that in the handling of any biofluid, caution be exercised due to the potential for disease transmission.

Seminal plasma samples were collected directly into sterile 15-mL Fisher tubes. To study the effect of using protease inhibitors, 3 mL of freshly obtained seminal plasma was centrifuged at +4 °C for 12 min at 25 000 rpm using a Beckman Ti45 rotor to spin down cellular material and debris. The supernatant was divided into two 1 mL aliquots. One of these aliquots was treated with 40 µL of 12.5 mM PMSF. Both treated and untreated seminal plasma was further divided into 45 µL aliquots, and frozen at -20 °C. An aliquot of each was also

immediately run on the CE instrument to compare profiles in the presence and absence of protease inhibitor. Samples were stored on ice between runs except in freeze/thaw analyses, in which case an aliquot stored at -20 °C was thawed, sample injected into the capillary, and then refrozen at -20 °C. Acetonitrile deproteinization was performed by thawing a fresh 100 µL aliquot of seminal plasma, adding 150 µL of 100 % acetonitrile, and centrifuging at 14 000 rpm for 2 min. The supernatant was transferred to another tube, the remaining protein pellet washed with 5 x 100 µL of acetonitrile, centrifuging for 1 min at 14 000 rpm centrifugation between washes. After the last centrifugation step, the pellet was resuspended in 100 µL of 0.1 M Borax-NaOH, pH 9.99 buffer. Protein zone identification experiments consisted of spiking aliquots of freshly thawed undiluted seminal plasma with 10 µL increments of the following standard protein solutions prepared in run buffer: 2.5 mg/mL HSA, 2.5 mg/mL TF, 2 mg/mL PSA, and 10 mg/mL AT.

Capillary electrophoresis was performed using an in-house built system previously described.[28] Separations were conducted in bare-fused silica capillaries (Polymicro Technologies, AZ) with the following dimensions: 356 µm O.D., 50 µm I.D., 60 cm total length, 45 cm effective length. Samples were introduced via hydrodynamic injection at 4 cm for 10 sec. The capillary tip was rinsed in run buffer following injection then placed into the inlet vial. Separations were performed using normal polarity, 5, 10, 15, 20 kV for the separation potential

study, 20 kV for the pH study and 15 kV for all remaining analyses, using a Spellman (Plainview, NY) model CZE1000R high-voltage power supply. Capillary conditioning, consisting of a 1 min flush with 0.1 M NaOH, 1 min flush with 1% SDS, and 1 min purge with run buffer, was performed manually between runs using a 1 cc syringe fitted with a glass adapter. In the interest of safety, all separations were performed with the inlet vial / anode in a plexiglass box. Absorbance was monitored at 200 nm using an ATI Unicam (Mississauga, Ont.) 4225 model UV-VIS absorbance detector equipped with a deuterium lamp. Data was acquired at 10 Hz using a National Instruments (Austin, TX) NB-MIO-16X-H (16 bit resolution) data acquisition board and stored as binary files on a PowerMac PC 7100 (Apple, Cupertino, CA) using an application developed in LabView (National Instruments). All data was analyzed using Igor Pro software (WaveMetrics, Lake Oswego, OR).

RESULTS AND DISCUSSION

Buffer Concentration/pH/Separation Potential Study

Capillary electrophoretic biofluid analysis is often performed using a high pH borate buffer system. Borate buffers are generally ideal in capillary electrophoresis due to their low current generation and low UV absorbance. An important consideration in bare-fused silica capillary biofluid separations is protein adsorption to the capillary wall. Performing separations at high pH can

effectively reduce this adsorption phenomenon by protonating the negatively charged silica groups on the wall's surface. The use of high buffer concentrations may be advantageous in minimizing sample matrix / run buffer salt concentration differences which can have an effect on peak shape and resolution. In an attempt to determine the optimal separation conditions for the rapid analysis of human seminal plasma, three parameters were investigated in sequence: borate buffer concentration, separation pH, and separation potential.

Borate concentrations of 25 mM, 50 mM, 75 mM, and 100 mM were analyzed using a separation potential of 15 kV. As indicated in Figure 2.1, there are noticeable differences in the electrophoretic profiles obtained at these various concentrations. At concentrations of 25, 50, and 75 mM, seminal plasma components are much less well resolved with a general broadening of the profile. Optimal resolution in the shortest amount of time is achieved at a buffer concentration of 100 mM. Borate concentrations greater than 100 mM were not investigated due to the potential for increased zone broadening caused by joule heating. The use of buffer concentrations lower than 100 mM may be suboptimal due to increased differences in ionic strength between the run buffer and sample as previously described. A buffer concentration of 100 mM was thus selected for the subsequent pH study.

Whereas all of the above buffer concentrations were analyzed at pH 9.96, it was necessary to further optimize the separation pH. Borate buffers of pH 8.0, 8.5, 9.0, 9.5, and 10.0 were analyzed using a separation potential of 20 kV.

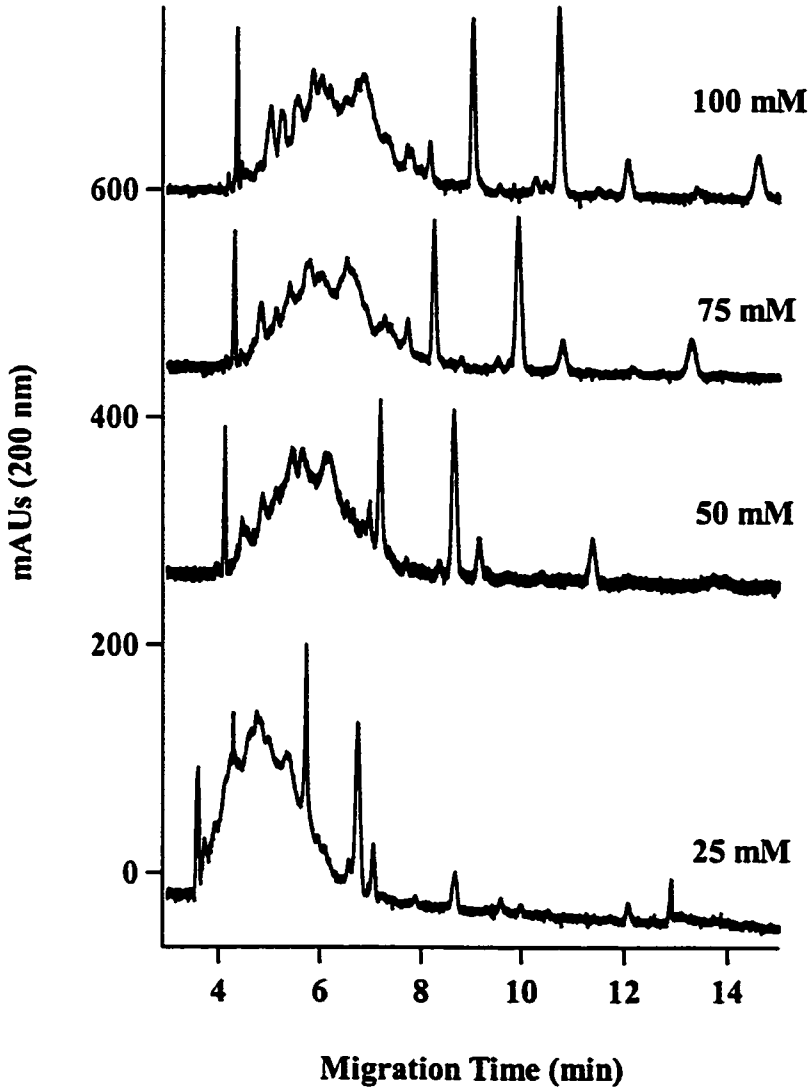

Figure 2.1 Effect of borate buffer concentration on the human seminal plasma profile.

As demonstrated in Figure 2.2, the use of pH values above 9.5 served to increase electroosmotic flow, resulting in faster analysis times (up to 1.2 times shorter) but diminished resolution. In this case, the various components were not afforded enough time to adequately separate into their respective zones prior to reaching the detector. Performing separations below pH 9.5 resulted in lower electroosmotic flow, and increased analysis times (up to 1.5 times longer). There was thus a compromise between resolution, analysis time, and sample adsorption to the capillary wall. Utilizing 100 mM Borate, pH 9.5 resulted in optimal resolution in the least amount of time. This buffer pH is consistent with that chosen in similar studies with other biofluids and is deemed effective in reducing sample adsorption to the capillary wall.

In addition to buffer pH and concentration, the applied separation potential can have an effect on the quality of the electrophoretic seminal plasma profile. In selecting an appropriate separation voltage, it is necessary to allow enough time for components to separate sufficiently for effective zone analysis. However, in order for capillary electrophoresis to be feasible as a tool in high throughput seminal plasma analysis, sufficiently low analysis times must be respected. The effect of varying the separation potential on resolution and analysis time is exhibited in Figure 2.3. It is evident from Figure 2.3 that the optimal separation potential for this buffer system is 15 kV. The use of higher potentials results in diminished analyte resolution due to joule heating effects, whereas lower voltages result in extended analysis times.

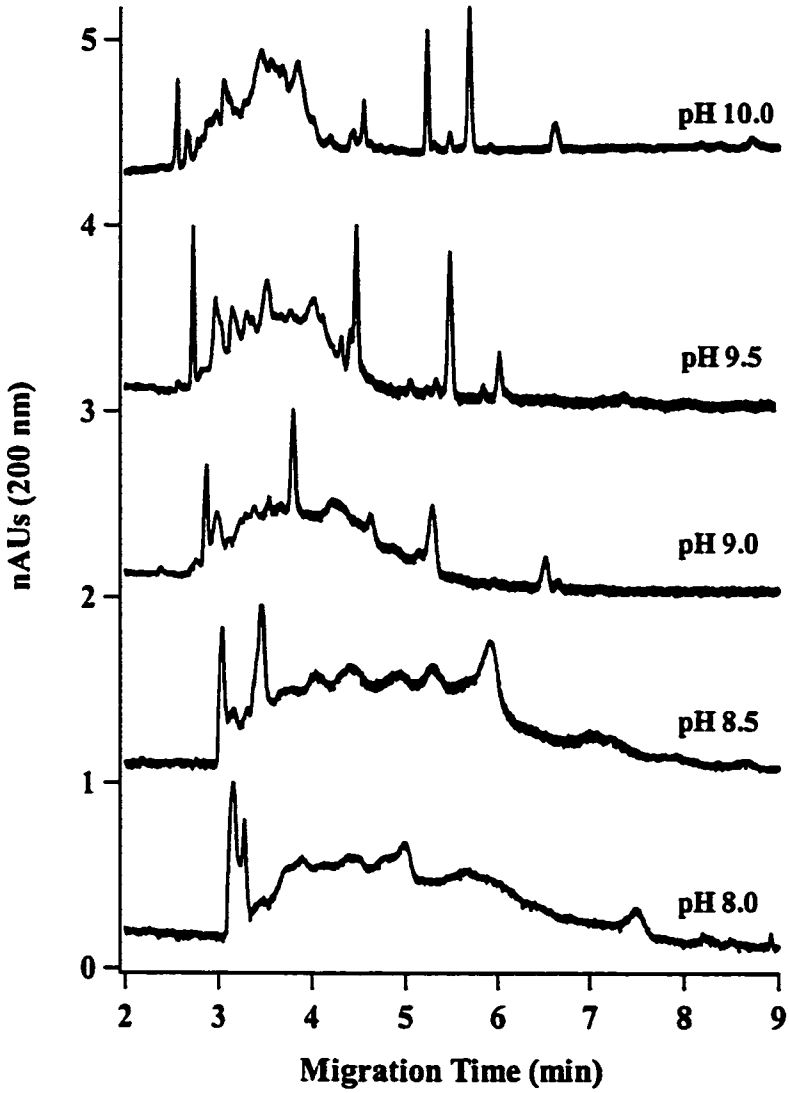

Figure 2.2 Effect of separation buffer pH on the human seminal plasma profile.

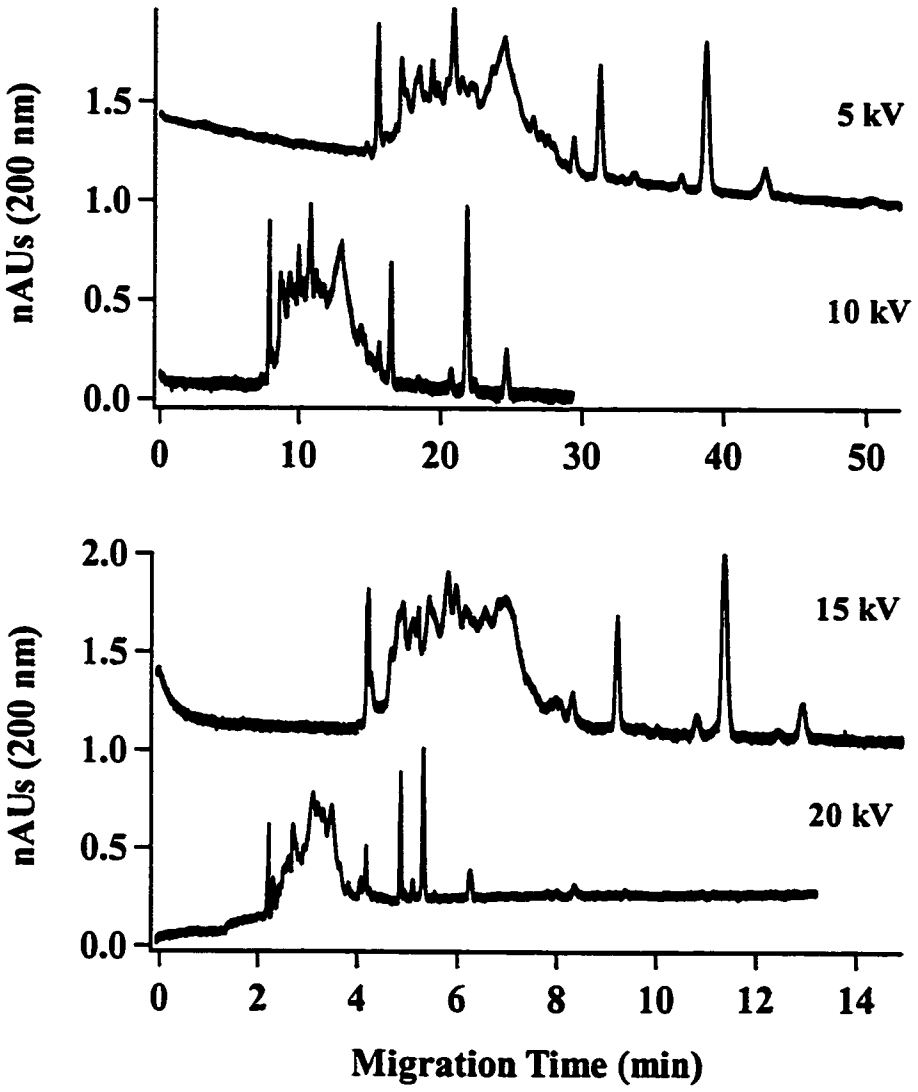

Figure 2.3 Effect of varying separation potential on the human seminal plasma profile.

The above buffer concentration, pH, and separation potential studies have thus identified optimal separation conditions (100 mM Borate, pH 9.5 run buffer, 15 kV separation voltage) for the analysis of human seminal plasma within 15 minutes.

Internal Standardization / Migration Time Reproducibility Study

The use of an internal standard in biofluid analysis is particularly important in the correct assignment of zones for disease diagnosis according to migration times, and for analyte quantitation. Selection of a suitable commercially available internal standard, that neither interacted nor co-migrated with endogenous seminal plasma components was required. Possessing good absorbance characteristics and routinely used in sodium dodecyl sulfate capillary gel electrophoresis applications, Orange G marker satisfied these requirements. A migration time reproducibility study was thus performed in the presence of Orange G marker. Migration time reproducibility data for various peaks selected throughout the seminal plasma profile are presented in Table 2.1. It is clear from Table 2.1 that excellent migration time reproducibilities can be achieved, facilitating zone assignments in disease diagnosis. It was noted that migration time reproducibility is significantly improved upon capillary conditioning between runs, as this served to remove any adsorbed analytes from the capillary surface (data not shown).

	Migration Time (min)											
Peak	1	2	3	4	5	6	7	8	9	AVG	SD	% RSD
1	4.36	4.53	4.60	4.36	4.36	4.36	4.39	4.43	4.50	4.43	0.09	2.0
2	5.86	6.07	6.21	5.82	5.86	5.82	5.93	5.96	6.04	5.95	0.13	2.2
3	6.84	7.09	7.20	6.84	6.88	6.84	6.95	6.98	7.09	6.97	0.13	1.9
4	8.16	8.50	8.61	8.05	8.12	8.05	8.20	8.31	8.46	8.27	0.21	2.5
5	9.04	9.48	9.59	8.78	8.86	8.86	9.00	9.19	9.37	9.13	0.29	3.2
6	10.73	11.14	11.26	10.55	10.66	10.58	10.73	10.92	11.14	10.86	0.27	2.4

Table 2.1 Migration time reproducibility of various selected peaks in the seminal plasma profile. Migration times for n=9 consecutive runs, utilizing Orange G marker for profile alignment. Average (AVG), standard deviation (SD) and percent relative standard deviation (% RSD) for six zones are listed.

Protease Inhibition, Temperature Stability, Freeze/Thaw Cycling

In addition to migration time reproducibility and the selection of an appropriate internal standard it was necessary to examine protease activity inherent to seminal plasma. Seminal plasma is known to contain various proteases and has been traditionally treated with the serine protease inhibitor, PMSF, prior to analysis. To investigate the impact of PMSF addition on the capillary electrophoretic seminal plasma profile, fresh samples were analyzed approximately one hour after addition of serine protease inhibitor. Use of PMSF had little impact on the resulting profile, with the appearance of the same number of peaks. There did not appear to be any significant proteolysis of earlier migrating components of seminal plasma. Furthermore, analysis of the same samples stored at +4 °C for 18 hours did not indicate any further profile changes (data not shown).

The temperature stability of seminal plasma can be readily analyzed by capillary electrophoresis. It was necessary to determine if the profile changes with time under two typical biofluid storage conditions, +4 °C and -20 °C. The stability of seminal plasma under these conditions is shown in Figure 2.4 (panel A). There was no noticeable difference between samples run immediately following cell removal and those stored at -20 °C. The seminal plasma profile did however change significantly over time when stored at +4 °C. An increase in the number of peaks was noted within approximately one hour at this temperature, and was consistent with the profiles obtained with samples used in the buffer study (stored at +4 °C). Following the appearance of these peaks, the electrophoretic

Panel A

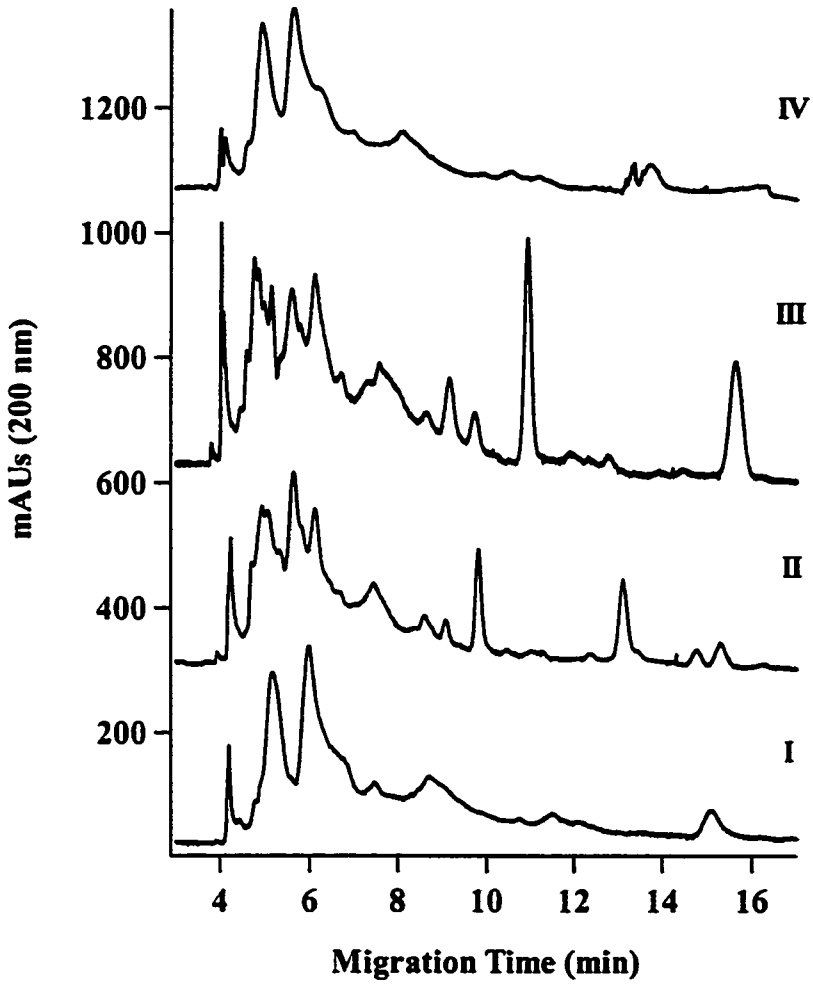

Figure 2.4 Protease inhibition, temperature stability, and freeze/thaw cycling effects on human seminal plasma profiles. Panel A. Effects of various storage temperatures on seminal plasma stability in the presence of PMSF. I. Immediate run; II. After 18 hours at +4 °C; III. After 48 hours at +4 °C; IV. Stored at -20 °C.

profile remained stable for at least 48 hours. Since PMSF was present in these samples, the changes observed are not believed to be due to the action of serine proteases. They may however be attributed to non-serine proteases towards which PMSF would be ineffective. Two-dimensional gel analyses of seminal plasma have relied for the most part on the use of PMSF for countering protease activity. The seminal plasma stability study performed herein suggests that a cocktail of protease inhibitors may be warranted. Nonetheless, in order to mimic the sample pretreatment utilized in two-dimensional gel analysis, only PMSF was investigated in this study. Non-enzymatic sample degradation is considered less likely given the rapid rate of appearance of these additional peaks at storage conditions of +4 °C.

In addition to temperature stability, a freeze/thaw study was performed. It is generally recommended that biofluid samples not be subjected to repeated freeze/thaw cycles in order to preserve the integrity of protein components. In order to address this issue with human seminal plasma, samples were subjected to repeated freeze/thaw cycles, and analyzed by capillary electrophoresis. As shown in Figure 2.4 (panel B), there did not appear to be any effect of repeated freeze/thaw cycles on the seminal plasma profile. At least six freeze/thaw cycles could be performed with no change in the profile. Since capillary electrophoresis consumes nL amounts of sample, this allows the clinical chemist to perform rapid screens of seminal plasma with a minimal amount of material, while preserving samples for later immunologic analysis if required.

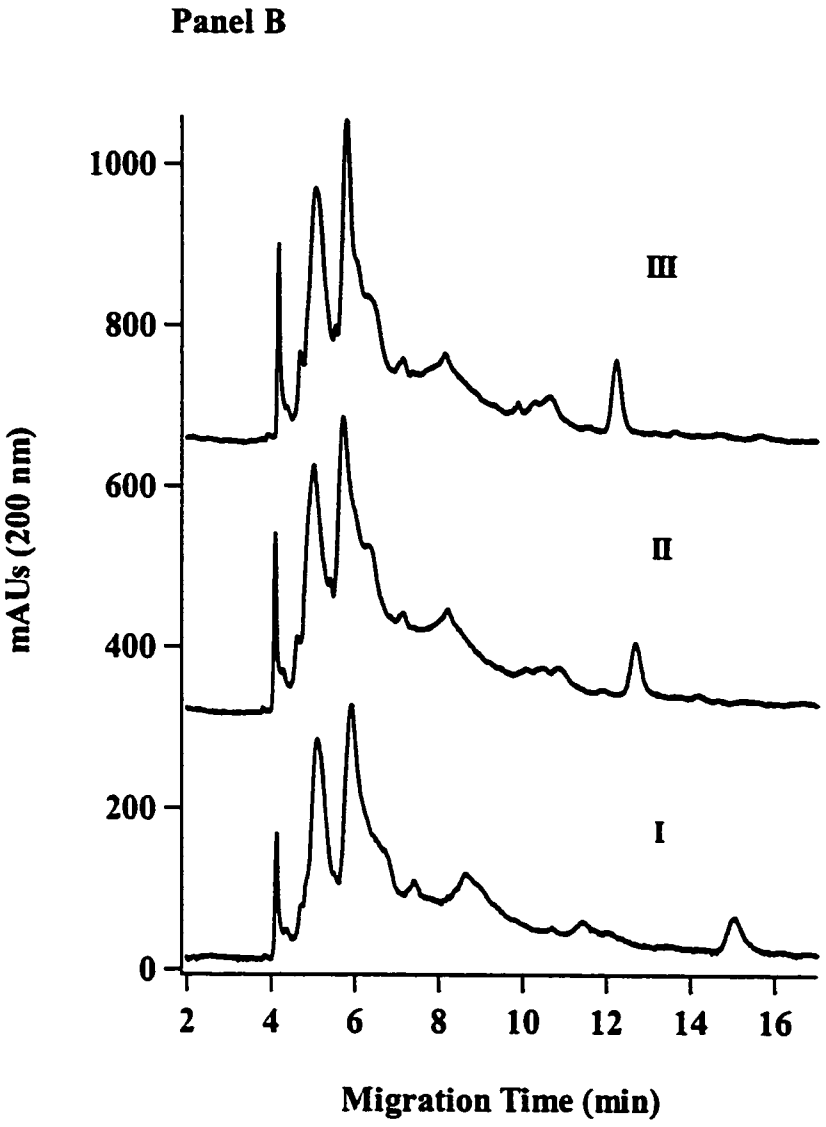

Figure 2.4 Protease inhibition, temperature stability, and freeze/thaw cycling effects on human seminal plasma profiles. Panel B. Freeze-thaw cycling effects on human seminal plasma profiles in the presence of PMSF. I. Fresh sample; II. After one freeze-thaw cycle. III. After six freeze-thaw cycles. Electrophoretic conditions for panels A & B corresponded to optimal conditions previously described. Electropherograms offset vertically for clarity.

Non-Protein Zone Identification

In order to further characterize human seminal plasma into its protein / non-protein zones, acetonitrile protein precipitation was performed. A 60% acetonitrile sample treatment is often used in drug analysis to precipitate proteins from the sample, followed by analysis of the supernatant by CE. This has proven effective in various capillary electrophoretic drug studies.[29, 30] Figure 2.5 indicates that five non-protein zones not observed in the resuspended protein pellet can be identified at migration times of approximately 4, 8, 9, 11, and 12 min. These species may be attributed to various peptides or polyamine species known to be in seminal plasma yet remain to be identified. It should be noted that the supernatant still contained some protein components yet these were in much lower amounts relative to the non-protein zones, indicating incomplete protein precipitation. The results indicate that for those wishing to analyze drugs in seminal plasma, complete removal of proteins may require more rigorous conditions. Various zones from 5 to 8 min of the electrophoretic profile were further characterized by protein standard spiking experiments.

Protein Zone Identification

Two-dimensional slab-gel analysis of human seminal plasma followed by Western blotting has indicated the presence of at least four major proteins in the presence of PMSF. In order to localize these proteins into general zones in the capillary electrophoretic seminal plasma profile, spiking experiments with the standard proteins were performed. As illustrated in Figure 2.6, TF, PSA, HSA, and

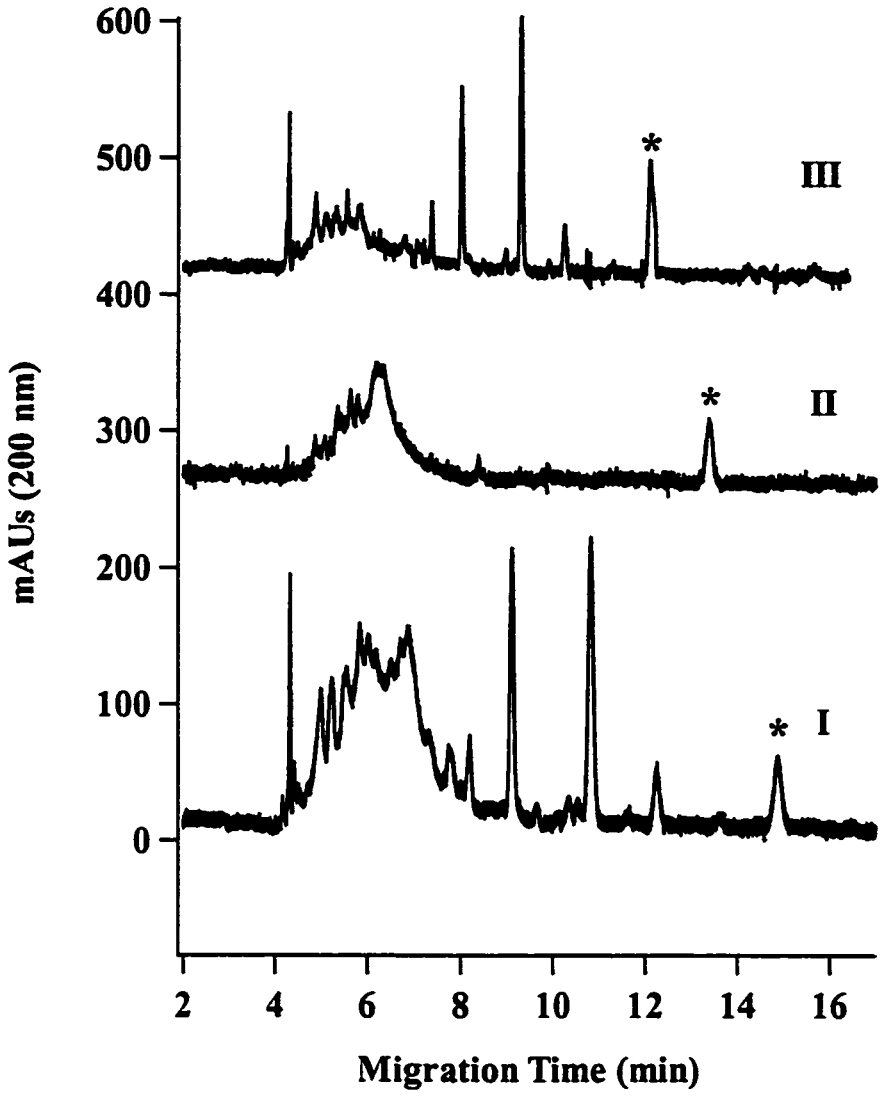

Figure 2.5 Acetonitrile deproteinization of human seminal plasma. I. Seminal plasma not treated with acetonitrile; II. Resuspended protein pellet following seminal plasma deproteinization; III. Supernatant from acetonitrile-treated seminal plasma. Orange G marker represented by an asterisk. Electrophoretic conditions corresponded to optimal conditions previously described. Electropherograms offset vertically for clarity.

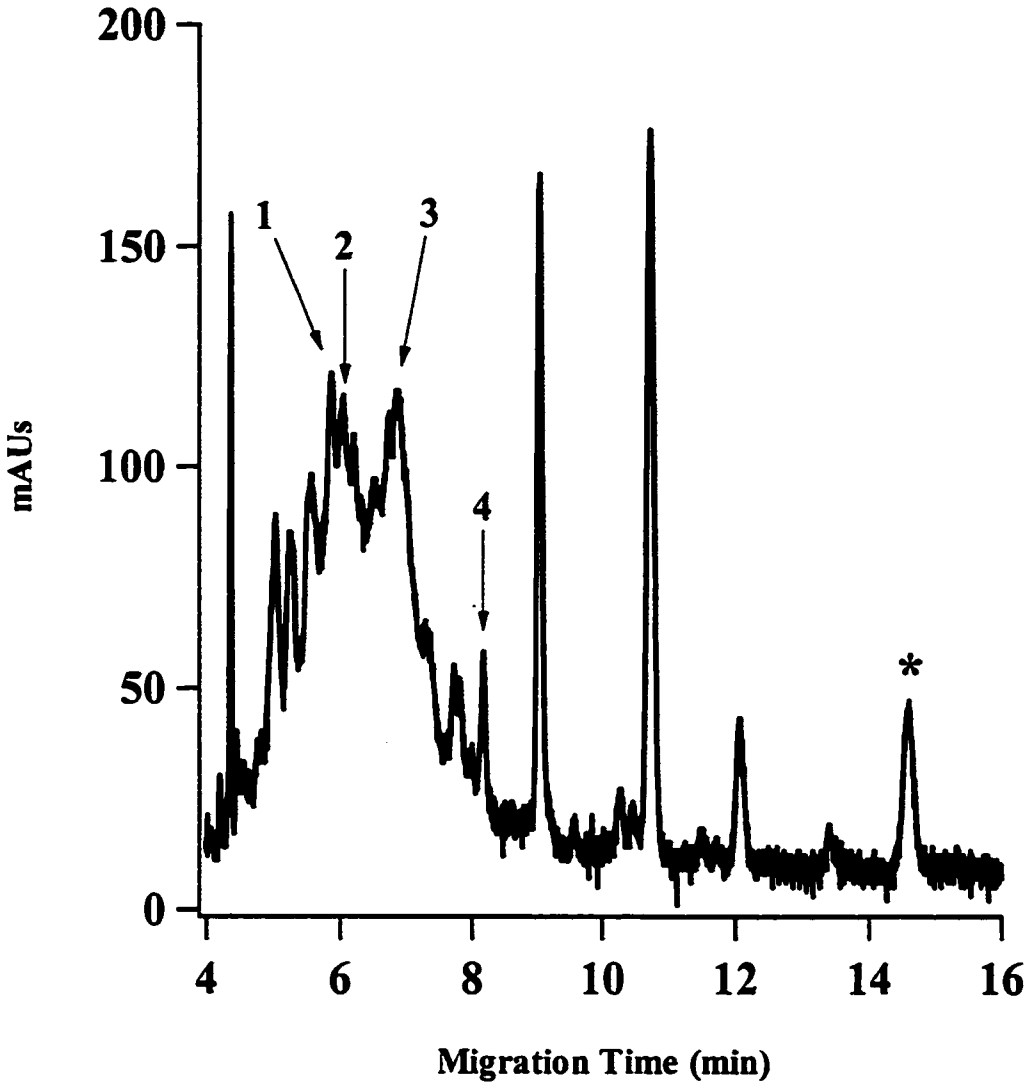

Figure 2.6 Human seminal plasma protein zone identification. Zones identified by standard spiking experiments corresponding to: 1. PSA; 2. transferrin; 3. α_1-antitrypsin; 4. HSA. Similar electrophoretic conditions as previously described. Orange G marker represented by an asterisk.

AT zones can be readily identified. It should be noted that these spiking experiments indicate the zones in which the particular proteins can be found. Due to the complexity of the biofluid (i.e. numerous protein components) it is possible that these zones contain additional minor proteins which can contribute to peak height/area. Nonetheless, the proteins identified are major components in seminal plasma and can be screened rapidly for organ function. A particular disease state would thus be manifested by a qualitative increase or decrease in a particular zone.

CONCLUSIONS

Capillary electrophoretic analysis of human seminal plasma has been performed, addressing various issues confronting the clinical chemist. A seminal plasma profile can be obtained from low microlitre sample volumes in under 15 minutes using optimized run buffer and separation conditions. To our knowledge, this is the first time that seminal plasma zones corresponding to the clinically relevant proteins PSA, HSA, transferrin, and α_1-antitrypsin, as well as non-protein zones have been identified using CE.

FUTURE WORK

Future directions of this research include profiling various disease states by capillary electrophoretic analysis of human seminal plasma. These include benign prostatic hyperplasia and semeniferous tubule malfunction. Other areas of research involve the quantitation of various major proteins in human seminal plasma by

capillary electrophoresis. This includes development of a CE-based Insulin-like Growth Factor I immunoassay.

ACKNOWLEDGEMENTS

The authors wish to acknowledge the financial support of the Natural Sciences and Engineering Research Council (NSERC) and David J. Azrieli.

REFERENCES

(1) Wiltfang J, Otto M, Baxter HC, Bodemer M, Steinacker P, Bahn E, Zerr I, Kornhuber J, Kretzschmar HA, Poser S, Ruther E, Aitken A. *J Neurochem* **1999**, 73, 2485.

(2) Sanchez-Campillo M, Bini L, Comanducci M, Raggiaschi R, Marzocchi B, Pallini V, Ratti G. *Electrophoresis* **1999**, 20, 2269.

(3) Jungblut PR, Zimny-Arndt U, Zeindl-Eberhart E, Stulik J, Koupilova K, Pleissner KP, Otto A, Muller EC, Sokolowska-Kohler W, Grabher G, Stoffler G. *Electrophoresis* **1999**, 20, 2100.

(4) Lopez MF *J Chromatogr B Biomed Sci Appl* **1999**, 722, 191.

(5) Jenkins MA, Ratnaike S. *J Biochem Biophys Methods* **1999**, 41, 31.

(6) Miura T, Funato T, Yabuki S, Sasaki T, Kaku M. *Clin Chim Acta* **2000** 299: 87.

(7) Sanders E, Katzmann JA, Clark R, Oda RP, Shihabi Z, Landers JP *Clin Chem Lab Med* **1999**, 37, 37.

(8) Paquette DM, Sing R, Banks PR, Waldron KC *J Chromatogr B Biomed Sci Appl* **1998**, 714, 47.

(9) Jenkins MA *Electrophoresis* **1997**, 18, 1842.

(10) Varnell RJ, Maitchouk DY, Beuerman RW, Salvatore MF, Carlton JE, Haag AM *J Capillary Electrophor* **1997**, 4, 1.

(11) Giordano BC, Muza M, Trout A, Landers JP *J Chromatogr B Biomed Sci Appl* **2000**, 742, 79.

(12) Clark R, Katzmann JA, Kyle RA, Fleisher M, Landers JP *Electrophoresis* **1998**, 19, 2479.

(13) Voelter W, Schutz J, Tsitsiloni OE, Weiler A, Grubler G, Paulus G, Stoeva S, Lehmann R. *J Chromatogr A* **1998**, 807, 135.

(14) Liu MS, Rampal S, Hsiang D, Chen FT *Mol Biotechnol* **2000**, 15, 21.

(15) Petrini C, Alessio MG, Scapellato L, Brambilla S, Franzini C. *Clin Chem Lab Med* **1999**, 37, 975.

(16) Bossuyt X, Schiettekatte G, Bogaerts A, Blanckaert N. *Clin Chem* **1998**, 44, 749.

(17) Bienvenu J, Graziani MS, Arpin F, Bernon H, Blessum C, Marchetti C, Righetti G, Somenzini M, Verga G, Aguzzi F. *Clin Chem* **1998**, 44, 599.

(18) Tie J, Tsukamoto S, Oshida S. *Nippon Hoigaku Zasshi* **1993**, 47, 295.

(19) Edwards JJ, Tollaksen SL, Anderson NG *Clin Chem* **1981**, 27, 1335.

(20) Irisawa C, Nakada T, Kubota Y, Sasagawa I, Adachi Y, Yaguchi H. *Arch Androl* **1993**, 30, 13.

(21) Cek M, Curgul S, Ertas M, Sozer T, Alpacar Z. *Urol Int* **1992**, 49, 218.

(22) Pedron P, Traxer O, Haab F, Farres MT, Tligui M, Thibault P, Gattegno B. *Prog Urol* **1997**, 7, 563.

(23) Oesterling, JE *J. Urol.* **1991**, 145, 907.

(24) Patel SM, Skandhan KP, Mehta YB *Acta Eur Fertil* **1988**,19, 329.

(25) Kavanagh, JP *J. Reprod. Fert.* **1985**, 75, 35.

(26) Zaneveld LJD, Jeyendran, RS Biochemical Analysis of Seminal Plasma and Spermatozoa, in *CRC Handbook of the Laboratory Diagnosis and Treatment of Infertility*, Brooks AK, Webster BW, Eds., CRC Press, Boca Raton, **1990**, 79-96.

(27) Sensabaugh GE, Blake ET. *J Urol* **1990**, 144, 1523.

(28) Banks PR, Paquette DM *J Chromatogr A* **1995**, 693, 145.

(29) Shihabi ZK, Hinsdale ME *J Chromatogr B Biomed Appl* **1996**, 683, 115.

(30) Shihabi ZK, Constantinescu MS *Clin Chem* **1992**, 38, 2117.

CHAPTER 3

Utilization of the Non-Covalent Fluorescent Dye, NanoOrange, as a Potential Clinical Diagnostic Tool: Nanomolar Human Serum Albumin Quantitation

Reprinted from Journal of Chromatography B: Biomedical Sciences and Applications, Vol 754(2), Harvey M.D., Bablekis V., Banks P.R., Skinner C.D., 345-356, Copyright 2001, with permission from Elsevier Science

ABSTRACT

The commercially available dye, NanoOrange, has been investigated as a potential tool for clinical diagnostics due to its low cost, ease of use, and ability to detect nanomolar concentrations of protein. Virtually non-fluorescent in dilute aqueous solutions, NanoOrange fluorescence is enhanced by at least an order of magnitude upon non-covalent interaction with proteins. These features, coupled with the requirement for high throughput assays in the clinical laboratory has prompted the development of two orthogonal NanoOrange approaches. Human Serum Albumin (HSA) was used as a model protein for the development of both 96-well microplate, and capillary electrophoresis laser-induced fluorescence (CE-LIF) assay formats. Dye performance in five commonly used buffers of various concentrations and pH indicated considerable flexibility in assay buffer selection, with optimal performance at pH 9.0. A salt concentration study indicated that increasing NaCl concentration generally decreases fluorescence emission and can be minimized by pre-diluting biological samples to a final salt concentration of 20-80 mM. Titration of protein with NanoOrange resulted in optimal HSA/NanoOrange complex formation utilizing 1x and 2x NanoOrange in the 96-well microplate, and CE-LIF approaches, respectively. A NanoOrange binding model based on rapid signal enhancement and zero order fluorescence emission kinetics is proposed. The utilization of NanoOrange in CE-LIF based human

serum analysis results in a signal to background ratio improvement of up to two orders of magnitude.

INTRODUCTION

The trend towards rapid analyses in the clinical laboratory has fueled the development of commercially available high throughput analytical instrumentation. Capillary electrophoresis (CE) has gained increased acceptance as a powerful tool in clinical diagnostics, with the advent of commercially available eight capillary instrumentation capable of sampling from 96-well microplates.[1-4] This acceptance has also been dependent on advances in optical detection techniques such as laser-induced fluorescence, which have allowed for capillary electrophoretic protein analysis in the subnanomolar range.[5-8] This in turn has required the development of rapid, effective fluorescent derivatization approaches.

Covalent and non-covalent fluorescent labeling strategies have been utilized in numerous clinical CE analyses.[9-12] Covalent labeling reagents such as fluorescein isothiocyanate, tetramethylrhodamine succinimidyl ester, and CBQCA target specific functional groups such as primary amines. The extent of conjugation is thus dependent on the number and accessibility of the respective reactive functional groups.[13] In contrast, non-covalent fluorescent probes have received increased attention in CE, particularly with respect to DNA analysis.[14,15] Non-covalent probes such as Sypro Red and Indocyanine green have been utilized

effectively in subnanomolar protein analysis in a capillary format.[16,17] These dyes are believed to bind rapidly with their protein targets via electrostatic and/or hydrophobic interactions, and often do not require the same degree of reaction condition stringency typically required in covalent labeling approaches. The ideal non-covalent probe is simple to use, binds rapidly to its target, is fluorogenic, sensitive, and economical.

These features are satisfied by the relatively new commercially available dye NanoOrange. The unique chemistry of this dye is currently applied to the accurate detection of proteins in solution at concentrations between 10 ng/mL and 10 μg/mL.[18] Highly soluble and virtually non-fluorescent in aqueous solutions, NanoOrange fluorescence is dramatically increased upon protein binding. Bound dye is efficiently excited with the 488 nm line of a relatively inexpensive air-cooled Ar^+ laser, and possesses a large Stokes' shift with maximum emission at about 580 nm. Furthermore, NanoOrange can be readily used in currently available high-throughput instrumentation such as fluorescence microplate readers.

The numerous attributes of NanoOrange can be effectively used with those of CE to provide the clinical chemist with a valuable tool in clinical diagnosis: low protein concentration detection, nanolitre sample consumption and short analysis times. The suitability of NanoOrange in clinical diagnostics is demonstrated here in the quantitation of human serum albumin (HSA). HSA is a clinically relevant protein used in the diagnosis of various disease states such as microalbuminuria,

and has proven useful in drug binding studies.[19-22] Rapid 96-well fluorescence microplate and CE-LIF based assays for HSA are thus presented. NanoOrange performance in five commonly used buffers of various concentrations and pH is evaluated. Salt concentration effects, binding/fluorescence emission kinetics, and the "stoichiometry" of HSA/NanoOrange complex formation are examined. The use of NanoOrange in biofluid profiling is demonstrated. To our knowledge this is the first time NanoOrange has been used in a CE-LIF format for the quantitation of nanomolar concentrations of a clinically relevant protein, and in biofluid profiling.

EXPERIMENTAL SECTION.

Apparatus. Microtitre plate assays were performed using Costar 96-well black flat bottom microplates (Corning, Acton, MA, USA) and a "Victor^2" fluorescence plate reader (EG&G Wallac, Ackron, OH, USA). All measurements were performed using a continuous lamp source energy of 9000 units and a 485 nm / 535 nm filter set for excitation and emission, respectively. Fluorescence emission was measured in the normal aperture mode for 1.0 s at a measurement depth of 8 mm. Orbital shaking settings consisted of normal speed selection with an orbital diameter of 1.00 mm.

Capillary electrophoresis with laser-induced fluorescence was performed using a Crystal 310 Series CE system (ATI-Unicam, Mississauga, Canada)

equipped with a 48 position Peltier-cooled autosampler. Analyte detection was achieved using an in-house built system.[16] Briefly, the photomultiplier tube current was monitored via a current to voltage converter at 10 Hz using a National Instruments (Austin, TX, USA) NB-MIO-16-H (16 bit resolution) data acquisition board. All instrument settings were controlled by a LabView (National Instruments) application through the I/O port of the NB-MIO board. The 488 nm line from a 2 mW air-cooled Ar^+ laser (Ion Laser Technologies, Salt Lake City, UT, USA) was focused onto the capillary window using a 6.3 X focusing objective (Melles Griot, Irvine, CA, USA) with a numerical aperture of 0.2. System alignment was performed using a three-axis gimble mount (Newport, Irvine, CA, USA). Fluorescence emission was collected at right angles to the excitation beam using a 16 X microscope objective with a numerical aperture of 0.32 and working distance of 3.7 mm (Melles Griot), spatially filtered through a 800 μm pinhole, then spectrally filtered sequentially by a longpass 515EFLP and 580DF30 bandpass filter (Omega Optical, Brattleboro, VT, USA). The photons produced by the fluorophore were detected using a multi-alkali photocathode photomultiplier tube (R1477, Hamamatsu, Middlesex, NJ, USA) powered by a HC123-01, Hamamatsu high voltage power supply with an output range of -300 to -1100 volts. Unless otherwise indicated, the photomultiplier tube was operated at -700 V. The photocurrent was passed through a current-to-voltage converter and lowpass filter (10 MΩ resistor, 0.1 μF capacitor) and digitized at 10 Hz using the data acquisition system previously described. The collection objective and

photomultiplier tube were fixed to a light-proof box containing the pinhole and filters. The data obtained was graphically illustrated using Igor Pro (Wavemetrics, Lake Oswego, OR, USA). CE experiments with absorbance detection were performed using previously described instrumentation.[13]

Fluorescence excitation and emission spectra were obtained using an SLM-Aminco-Bowman spectrofluorimeter (Spectronic Unicam, Rochester, NY, USA). All measurements were performed at 25 °C with a continuous 150 W Xenon lamp, scan rate of 2 nm/s, and photomultiplier tube setting of 700 V. Excitation spectra from 350 nm to 550 nm were obtained using an emission monochromator setting of 580 nm bandpass of 4 nm, whereas emission spectra from 500 nm to 700 nm were obtained with an excitation monochromator setting of 488 nm bandpass of 4 nm.

Reagents. All buffer reagents as well as HSA were purchased from Sigma (Mississauga, Canada). NanoOrange dye (supplied as a 500x proprietary concentrate) was obtained as part of a NanoOrange Quantitation Kit (Molecular Probes, Eugene, OR, USA). CE-LIF separations were performed using 186 μm O.D., 50 μm I.D., 60 cm total length, 45 cm effective length bare-fused silica capillaries (Polymicro Technologies, Phoenix, AZ, USA). Nanopure water with a conductivity of 18.3 $M\Omega\text{-}cm^{-1}$ (Barnstead, Boston, MA, USA) was used for all buffer and dye solution preparations.

Procedures.

Buffer concentration and pH studies, were performed in 96-well microtitre plate wells by adding reagents in the following order: buffer, water, HSA and 10x NanoOrange. The HSA (1 mg/mL) and NanoOrange stock solutions (10x) were prepared fresh daily using nanopure water. NanoOrange was purchased initially as a 500x concentrate which was diluted 50-fold in water immediately prior to use in the above studies. Each well of the microtitre plate contained 130 μL of buffer, 20 μL of water, 20 μL of 10x NanoOrange, and 30 μL of 1 mg/mL HSA, for a total assay volume of 200 μL. All assays consisted of simultaneously loading eight wells with identical samples using a multichannel pipettor. Measurements were performed immediately following HSA addition and at 1 min intervals for five minutes with orbital shaking between readings.

NanoOrange fluorescence with varying HSA concentration studies utilized a similar approach to the above. In brief, HSA concentrations of 0, 10, 15, 20, and 25 μg/mL were examined at 1 min time intervals over a 30 min period, using an optimized assay buffer consisting of 15 mM borate (pH 9.0).

Effect of salt concentration, on fluorescence emission was monitored by preparing 15 mM borate (pH 9.0) solutions containing 20 μg/mL HSA, and 0 to

100 mM NaCl. Fluorescence emission was measured immediately and after 1 min of orbital shaking.

Optimization of NanoOrange Concentration. Titration of HSA with NanoOrange was performed so as to take into account the time dependency of fluorescence emission. A stock solution of 10x NanoOrange was prepared in 15 mM borate (pH 9.0). Various volumes of this stock were added to wells containing 15 mM borate (pH 9.0) and 15 μg/mL HSA to obtain the desired final dye concentrations. The total volume of all wells was 200 μL. The fluorescence emission at a particular dye concentration was measured after 1 min of orbital shaking, followed by preparation and measurement of the next dye concentration.

96-Well Microplate HSA Calibration Curve. A microtitre plate calibration curve for HSA was constructed as follows. Various HSA concentrations ranging from 1.67 μM to 1.67 nM were prepared by performing serial dilutions of a 1 mg/mL HSA stock in 15 mM borate (pH 9.0). Eight wells were filled with 180 μL of a particular HSA concentration, followed by addition of 20 μL of 10x NanoOrange. Measurements were performed as described above.

CE-LIF NanoOrange HSA analysis. CE-LIF analyses were performed using the following procedure. Human serum albumin samples were injected at 100 mbar for 0.1 min, followed by a 0.01 min capillary tip / electrode rinse in buffer.

Electrophoretic separations were performed by applying a potential of 30 kV (i.e. 500 V/cm). The capillary was conditioned with 0.1 M NaOH (1 bar for 30 s) followed by NanoOrange run buffer (1 bar for 60 s) between runs. The NanoOrange run buffer was prepared fresh by performing a 250-fold dilution of 500x dye stock in 15 mM borate (pH 9.0). It was deemed necessary to adequately filter the borate buffer using a Millipore Millex-LCR hydrophilic PTFE 0.45 μm syringe filter to avoid particulate scatter during the CE run. It should be noted that NanoOrange should be added to the filtered buffer but not prior to filtration, since dye retention by both nylon and hydrophilic PTFE membranes was observed.

CE-LIF calibration curves for HSA were constructed using similar HSA concentrations as for the microplate approach, but in this case NanoOrange was not added to the HSA solutions prior to analysis. HSA solutions were directly injected into the capillary and labeled on-column by incorporating NanoOrange in the run buffer. All HSA solutions were kept on ice between analyses.

RESULTS AND DISCUSSION

NanoOrange Fluorescence Excitation and Emission Spectra. The spectral characteristics of NanoOrange in the absence and presence of HSA were examined in order to determine the spectral filtering requirements of the assay. Figure 3.1 illustrates the excitation and emission spectra obtained upon HSA binding. In the

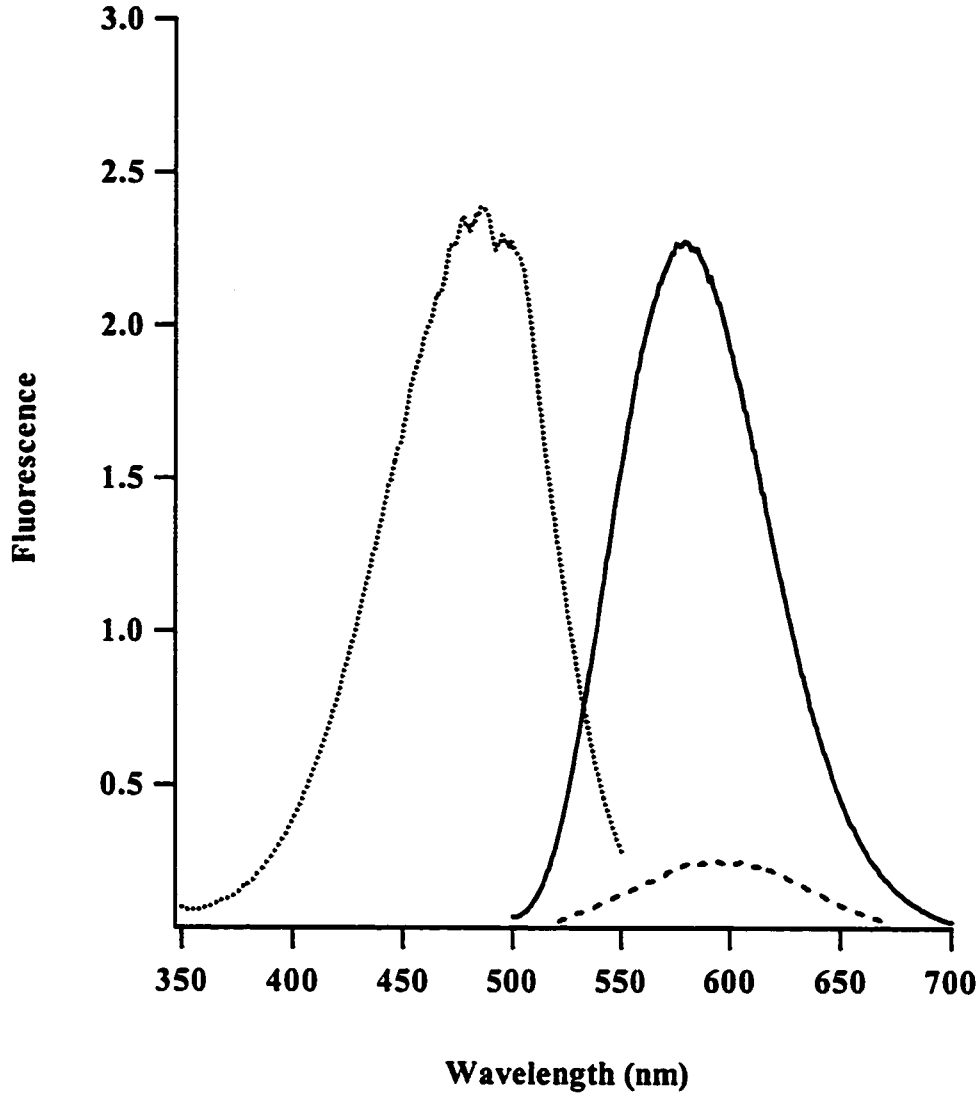

Figure 3.1 Fluorescence excitation and emission spectra for 1x NanoOrange reagent +/- 10 μg/mL HSA in water at 25 °C. Excitation spectrum (.....), emission spectrum in the absence of HSA (----), and emission spectrum in the presence of HSA (—).

presence of HSA, $\lambda_{em,\,max}$ is blue-shifted by 24 nm from 604 nm to 580 nm. This shift was not accompanied by a corresponding shift in $\lambda_{ex,\,max}$ (data not shown). The large Stokes' shift, of approximately 100 nm, allows for efficient spectral discrimination between excitation light and fluorescence emission. Furthermore, a significant enhancement in fluorescence emission (i.e. 10-fold) is produced in the presence of 10 μg/mL HSA. NanoOrange's large emission band allows one the flexibility to utilize commonly used filters (eg: fluorescein or tetramethylrhodamine-based emission filters), while still obtaining nanomolar protein detection limits.

NanoOrange Buffer Species, Concentration, pH Study. Five different buffers were chosen to cover a variety of useful pH ranges which are typically encountered in bioanalysis. The goal of this study was to characterize the effect of varying buffer species, concentration and pH on NanoOrange fluorescence emission upon protein binding.

The following buffers were chosen for study: Tris-HCl, acetate, citrate, phosphate, and borate. Recognized for its utility as a disease marker in various biofluid analyses, HSA was chosen as a model protein for this buffer study.

Two buffer systems were selected for evaluating the performance of NanoOrange under acidic conditions. Acetate has a useful pH range of about 3.5 to 5.5 which closely matches that of another commonly used buffer, citrate, which

has a useful pH range of 3.0 to 5.0. A comparison of the effects of acetate and citrate on NanoOrange fluorescence emission is illustrated in Figure 3.2. At low concentrations of both citrate (panel B) and acetate (i.e. 6.5 mM, 15 mM) (panel A), a trend of increased fluorescence emission with increasing pH was observed. This may be attributed to more favourable dye binding conditions as target residues of HSA and/or various NanoOrange functional groups are ionized. Due to the proprietary nature of this dye, no structural information on NanoOrange is presently available for confirmation of the latter. Increasing the buffer concentration to 32.5 mM disrupted this trend. Fluorescence emission decreased to a level equivalent to that observed for the middle of the useful pH range. Furthermore, a significant decrease in inter-well signal reproducibility (from 10 to 30%) was noted for these acidic buffers when the buffer concentration was increased from 6.5 mM to 32.5 mM. These effects are believed to be due in part, to a destabilizing effect on dye binding, caused by increasing salt concentration. In both buffer systems the counter ion was Na^+. This was examined in more detail in the salt concentration study described below. For both acetate and citrate buffers there was a gradual decrease in fluorescence emission ranging from 10 to 30% over a five minute incubation period. Since this trend was observed for all buffer systems examined, a proposed NanoOrange binding model is discussed in the binding kinetics section below.

Panel A

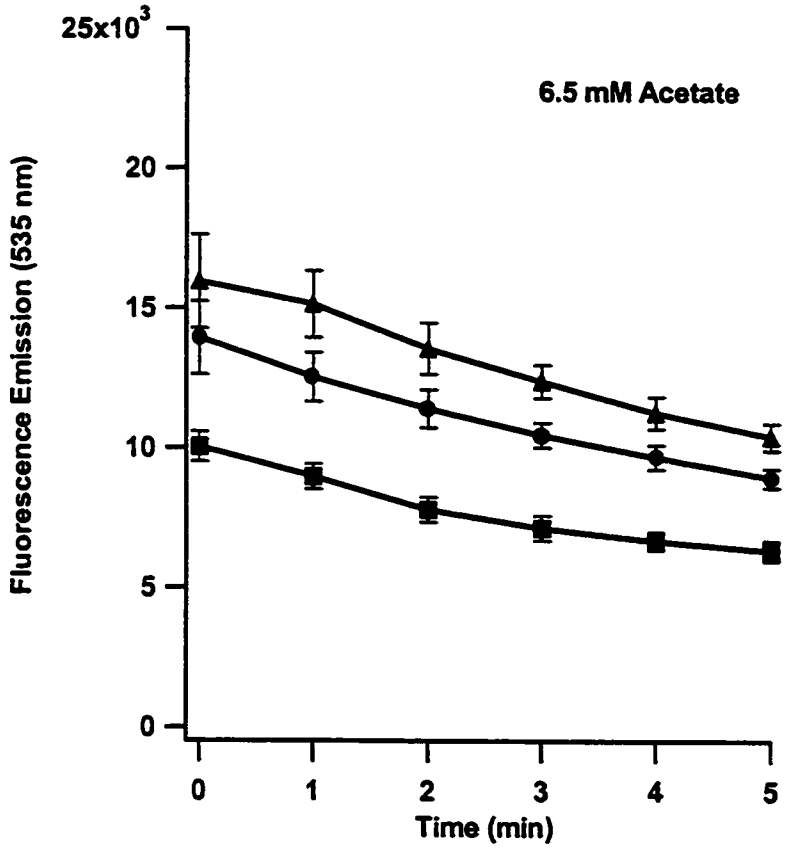

Figure 3.2 A comparison of the effects of acidic buffers on 1x NanoOrange fluorescence emission over time, in the presence of 15 μg/mL HSA. Panel A: 6.5 mM acetate at pH 3.5 (■), pH 4.5 (●), pH 5.5 (▲).

Panel B

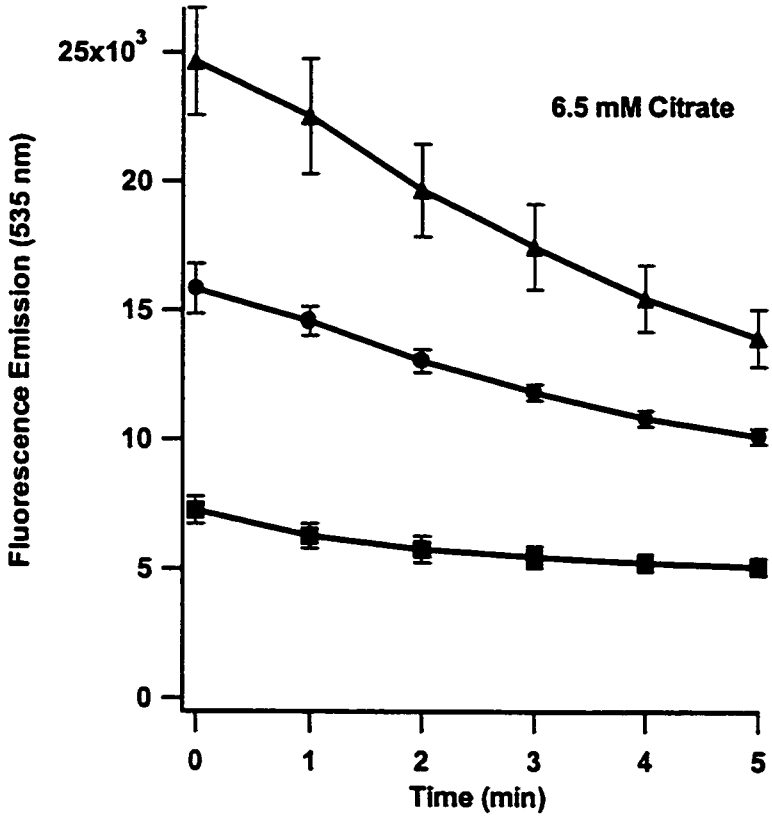

Figure 3.2 A comparison of the effects of acidic buffers on 1x NanoOrange fluorescence emission over time, in the presence of 15 µg/mL HSA. Panel B: 6.5 mM citrate at pH 3.0 (■), pH 4.0 (●), pH 5.0 (▲). Similar results to those shown were obtained for 15 mM, 32.5 mM acetate and citrate (data not shown). Error bars represent +/- 1 SD for eight replicate measurements.

In order to examine NanoOrange performance under neutral and basic conditions, three buffers with overlapping pH ranges were selected: phosphate (pH 6.0-8.0) (panel C), Tris-HCl (pH 7.0-9.0) (panel A), and borate (pH 7.0-9.0) (panel B). A comparison of the effects of phosphate, Tris-HCl, and borate concentrations on NanoOrange fluorescence emission is illustrated in Figure 3.3. In the case of phosphate, significant deviations from the trends established by the other buffers were observed. At 6.5 mM phosphate, increased stability in fluorescence emission over time resulted in higher emission intensity at pH 6.0 than at pH 7.0 or 8.0. Though such signal stability is highly desirable, the low fluorescence emission observed at pH 6.0 was considered suboptimal for achieving nanomolar HSA detection limits. Increasing the phosphate concentration to 15 mM (pH 6.0) resulted in a four to five-fold enhancement in signal intensity with a corresponding loss in fluorescence stability (10% min^{-1}). Interestingly, further augmenting the concentration to 32.5 mM decreased the fluorescence emission at pH 7.0 and 8.0 by 30-40%, while maintaining signal intensity at pH 6.0. In terms of the binding model proposed below, it appears that at pH 6.0, and low phosphate concentration (i.e. 6.5 mM), relatively few NanoOrange molecules can stack onto the HSA surface. This may be due to repulsive effects between dye molecules. The inability to stack onto the surface of HSA thus manifests itself in reduced signal intensity and increased stability. Increasing the phosphate ion concentration is thought to enhance fluorescence emission by shielding the proposed ionized groups on NanoOrange, hence promoting dye stacking. However, since Na^+ is

correspondingly increased in concentration, one cannot arbitrarily increase phosphate concentrations with the hopes of boosting signal intensity.

Tris-HCl did not manifest all of the same trends as for phosphate (Figure 3.3). Similar to the acidic buffer study, Tris-HCl exhibited a trend of increased fluorescence emission with increasing pH for all concentrations tested. In comparison to the phosphate study, increasing Tris-HCl concentration had a similar effect, augmenting emission intensity by 2 to 3.5-fold. In this case, Cl^- ions may be playing a similar role to phosphate ions in providing a charge shielding effect.

In comparison to Tris-HCl and phosphate, 6.5 mM borate provided higher fluorescence emission at the pH values examined, and exhibited the same trend between pH and signal intensity as Tris-HCl. Once again, emission was enhanced approximately 50% by increasing buffer concentration to 15 mM. Use of 32.5 mM borate did not result in significantly improved fluorescence emission.

Thus, there is a certain degree of flexibility in buffer selection for use with NanoOrange. In general, acidic buffers such as citrate and acetate are not recommended due to inferior fluorescence emission. Phosphate, Tris-HCl and borate are all acceptable choices, with a preference for concentrations in the 15 to 32.5 mM concentration range. Of the five buffers examined, 30 mM Tris-HCl (pH 9.0), 15 mM phosphate (pH 9.0), 15 mM borate (pH 9.0) and 32.5 mM borate (pH 9.0) were the best candidates for use in a HSA assay. The pH optimum of these various buffers (i.e. pH 9.0) was well suited to a CE-based HSA assay since

Panel A

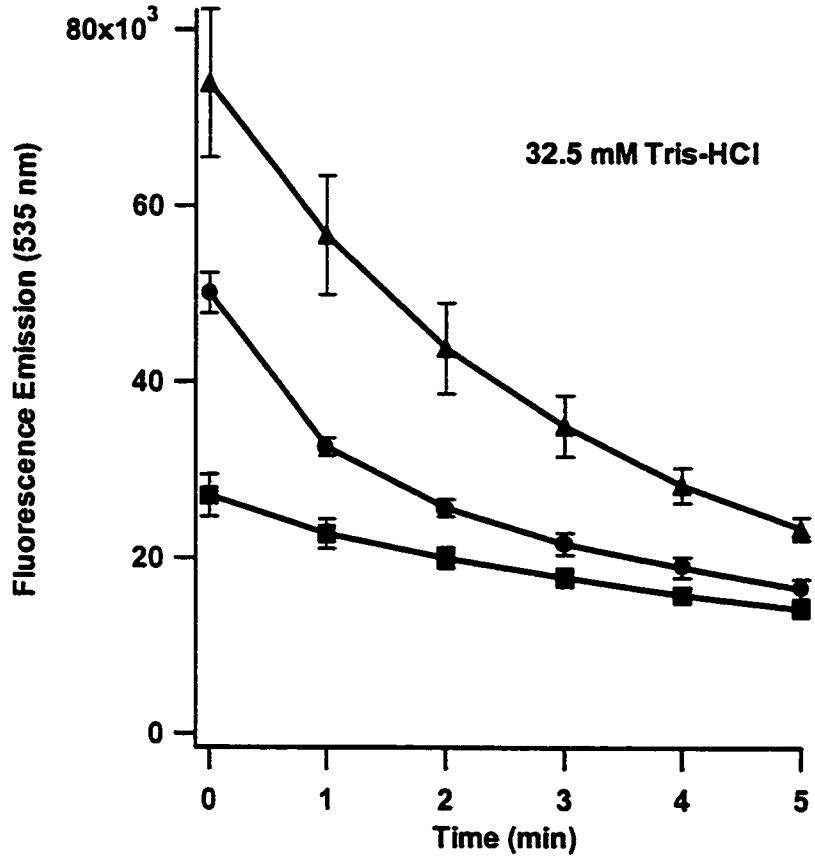

Figure 3.3 A comparison of the effects of neutral and basic buffers on 1x NanoOrange fluorescence emission over time, in the presence of 15 µg/mL HSA. Panel A: 32.5 mM Tris-HCl at pH 7.0 (■), pH 8.0 (●), pH 9.0 (▲). Error bars represent +/- 1 SD for eight replicate measurements.

Panel B

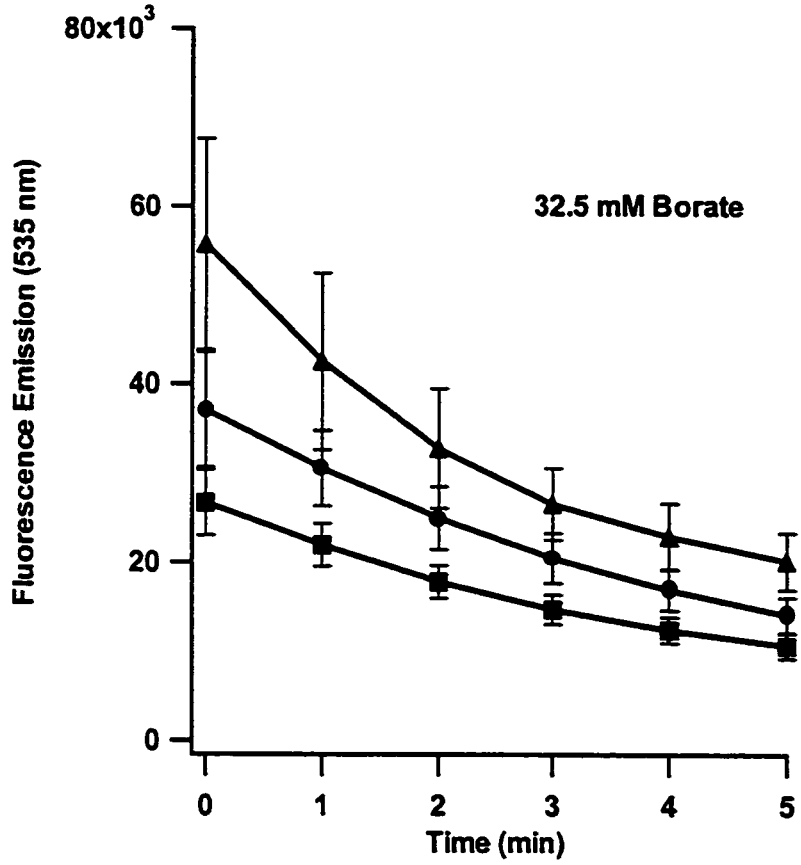

Figure 3.3 A comparison of the effects of neutral and basic buffers on 1x NanoOrange fluorescence emission over time, in the presence of 15 μg/mL HSA. Panel B: 32.5 mM borate at pH 7.0 (■), pH 8.0 (●), pH 9.0 (▲). Error bars represent +/- 1 SD for eight replicate measurements.

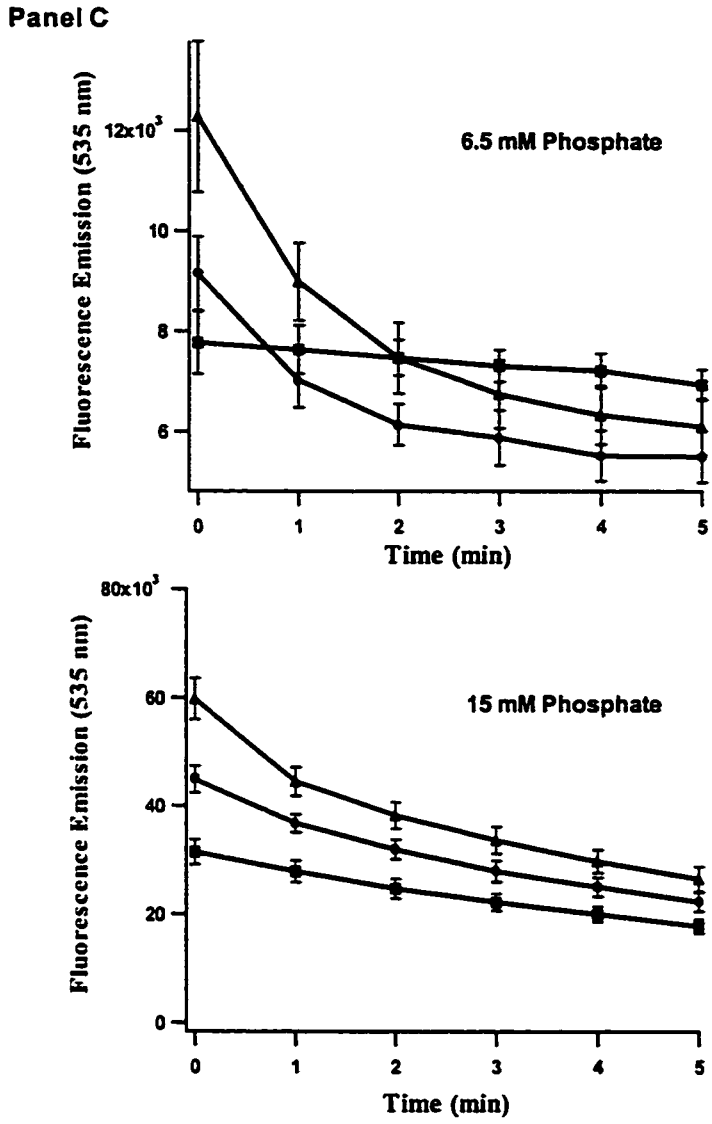

Figure 3.3 A comparison of the effects of neutral and basic buffers on 1x NanoOrange fluorescence emission over time, in the presence of 15 µg/mL HSA. Panel C: 6.5 mM phosphate, 15 mM phosphate, at pH 6.0 (■), pH 7.0 (●), pH 8.0 (▲). Similar results to those shown were obtained for 6.5 mM, 15 mM Tris-HCl and borate (data not shown). Error bars represent +/- 1 SD for eight replicate measurements.

protein adsorption to the capillary wall is significantly reduced at high pH.[23] The buffer selected for further studies consisted of 15 mM borate (pH 9.0). Borate has been successfully used in CE-based biofluid analysis and the well-documented effectiveness of this buffer system was considered more important than a ca. 1.5-fold increase in fluorescence emission one would obtain using Tris-HCl. Use of borate was favored over phosphate due to current generation / Joule heating issues which could require a lower separation potential hence longer analysis times. Fluorescence emission was only marginally higher at 32.5 mM borate (pH 9.0) than 15 mM borate (pH 9.0) hence in an effort to minimize current generation during the separation, the latter was selected.

Salt Concentration Study. Since biofluids often contain relatively high salt concentrations (i.e. 400 mM), a study was performed to ascertain the impact of increasing salt concentration on NanoOrange fluorescence emission. Utilizing 15 mM borate (pH 9.0), NaCl concentrations ranging from 0 to 100 mM were added to the assay buffer. Increasing the concentration of NaCl had a detrimental effect on fluorescence emission. After as little as one minute of incubation, NanoOrange fluorescence intensity decreased by approximately 13% in the absence of NaCl as opposed to a relatively consistent decrease of 25% in the presence of NaCl. Furthermore, after 1 min of incubation, a plateau region from 20 to 80 mM NaCl was observed, over which fluorescence emission declined marginally by 5%. Two significant drops of 30% and 20% were observed on either side of this plateau as

the NaCl concentration was increased from 0-20 mM and 80-100 mM, respectively. The data suggests that in the presence of NaCl, optimal fluorescence emission is attained by prediluting biofluid samples so as to diminish salt concentration to a level ranging from 20 to 80 mM. Combined with the effects of increasing buffer concentration on fluorescence emission, it appears as though NanoOrange fluorescence is related to several factors which include counter-anion stabilization and Na^+ destabilization. By analogy, recent crystallographic and energetic analyses of binding of selected anions to the yellow variants of Green Fluorescent Protein has indicated anion binding effects on fluorescence emission.[24]

NanoOrange Binding and Fluorescence Emission Kinetics. The fluorescence stability of non-covalent dyes under aqueous conditions is often a key parameter for successful protein labeling. Indeed, dye stability was an issue in a previous CE-LIF based HSA assay which utilized the tricarbocyanine dye Indocyanine Green.[17] NanoOrange-protein complexes are stable for at least six hours when diluted in a detergent-based 1x quantitation diluent (provided in the NanoOrange quantitation kit). However, the present study utilized a modification of this protocol which does not utilize detergent. An examination of NanoOrange fluorescence emission versus time revealed that fluorescence enhancement upon binding is rapid. Maximal fluorescence emission essentially occurs in the time required to add HSA to a microtitre plate and place it in the instrument. The

fluorescence emission of NanoOrange / HSA complexes decreases over time. The fluorescence decay curves (see Figure 3.4) for various HSA concentrations indicate that fluorescence emission follows zero order kinetics with respect to protein concentration. In the absence of HSA, unbound NanoOrange fluorescence emission is relatively stable.

In order to explain this rapid decay in fluorescence emission, a NanoOrange binding model is proposed. NanoOrange molecules are believed to rapidly bind to the surface of HSA, producing maximal fluorescence emission. These dye molecules in turn serve as "nucleation" sites for further dye binding. This slower process of NanoOrange accumulation results in fluorescence self-quenching. The self-quenching capability of dye molecules in close proximity to one another is in fact used extensively in fluorescence-based phospholipase detection methods.[25] In the manufacturer's NanoOrange labeling method, heating in the presence of a detergent solution for 10 min is followed by a 20 min cooling period prior to analysis. The above quenching effect, as shown in Figure 3.4, may not be observed in the manufacturer's method, since after 30 minutes fluorescence intensity is such that HSA concentrations as low as 10 ng/mL can still be detected.

This has implications in the design of a NanoOrange HSA assay, with highest sensitivity obtained at short incubation times (i.e. 1 min). Contrary to many detection schemes which require several minutes to several hours of incubation for maximal signal generation, the use of NanoOrange has a

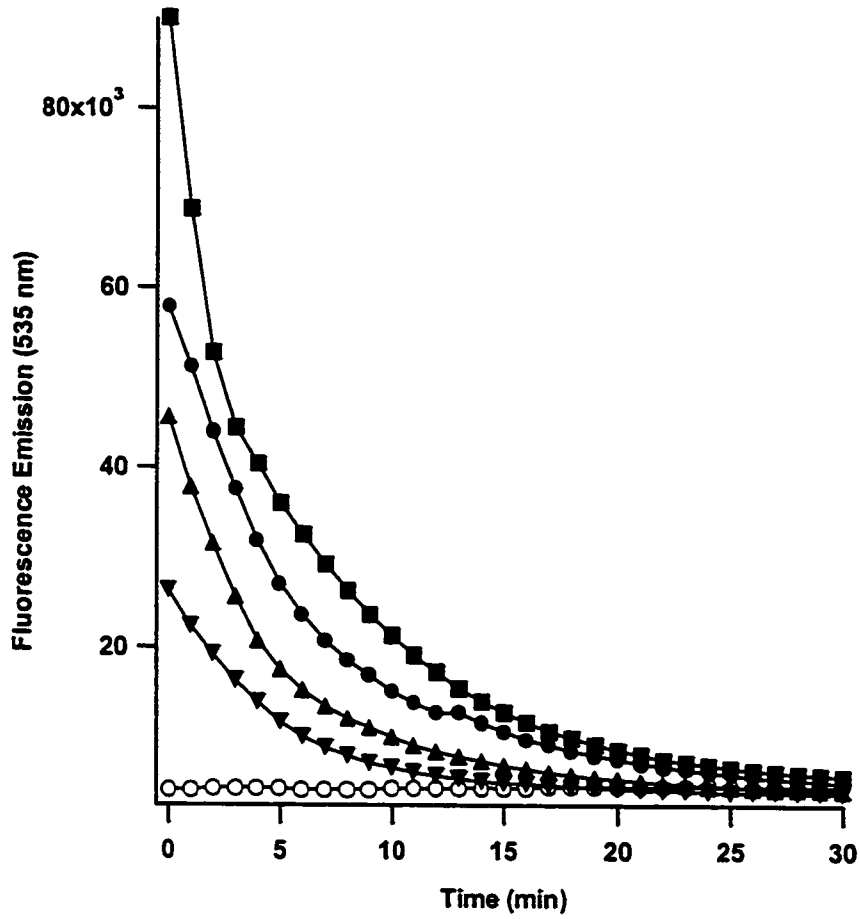

Figure 3.4 Fluorescence emission decay curves for 1x NanoOrange in the presence of various HSA concentrations in 15 mM borate (pH 9.0): 25 μg/mL (■), 20 μg/mL (●), 15 μg/mL (▲), 10 μg/mL (▼), 0 μg/mL HSA (O). SD for all data points (eight replicate measurements) = +/- 10%.

requirement for analysis within only a few minutes of protein addition. The high-throughput nature of this assay is thus highly attractive.

HSA Titration with NanoOrange. The development of cost-effective assays capable of detecting nanomolar protein concentrations is of significant value to the clinical laboratory. It was thus necessary to determine the optimal amount of NanoOrange to include in the assay buffer. A titration of 15 μg/mL HSA with NanoOrange concentrations ranging from 0 - 4x was performed (Figure 3.5). A saturable binding curve was obtained, there appears to be no advantage to using more than 1x NanoOrange. Use of 1.5 to 2x NanoOrange did not produce a change in the signal to background ratio. However, dye concentrations of 2.5x and higher resulted in decreased fluorescence emission. Quenching and the inner filter effect are believed to play an increasingly important role at these elevated concentrations, resulting in reduced signal intensity. It should be noted that the conventional detergent-based NanoOrange protocol also recommends the use of 1x NanoOrange. Since NanoOrange is provided as a 500x concentrate, it is not possible to express binding stoichiometry in terms of a mole fraction. It is likely however that many different complexes are formed from the addition of dye to HSA, especially in light of the binding model proposed above. A 1x NanoOrange concentration was thus used for the microplate assay described below.

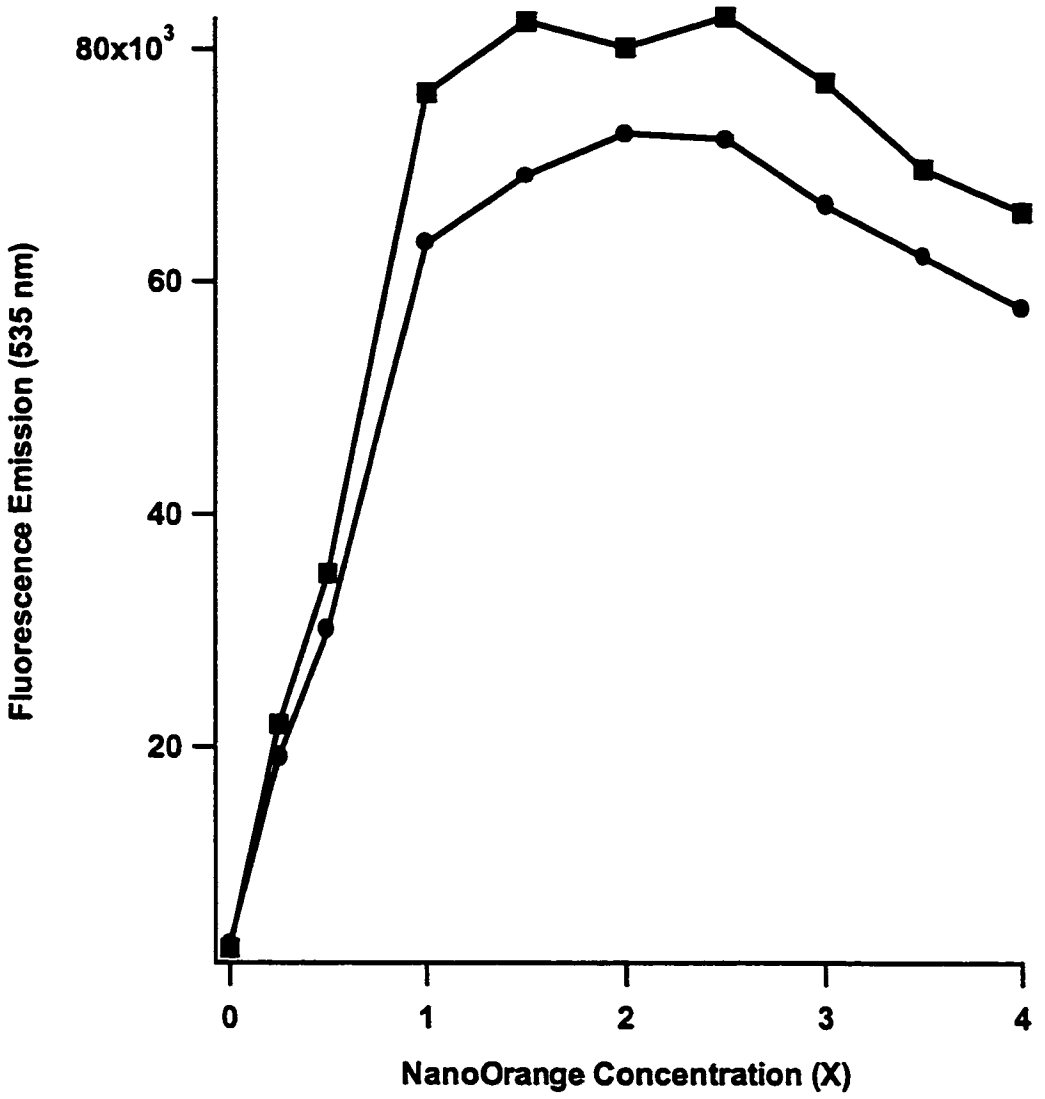

Figure 3.5 Titration of 15 µg/mL HSA with NanoOrange concentrations ranging from 0 to 4x. Measurements performed in 15 mM borate (pH 9.0) at t=0 min (■) and t=1 min (●). SD for all data points (eight replicate measurements) = +/- 10%.

96-Well Microtitre Plate Assay for HSA. A 96-well microtitre plate assay was developed for the sensitive detection of HSA. A HSA calibration curve was constructed (n=8) (data not shown). This curve consisted of two distinct linear regions: 91 nM to 1.47 μM, and 1.47 nM to 46 nM HSA. The assay may thus be performed for HSA concentrations which span three orders of magnitude by selecting the appropriate linear portion from the calibration curve. The calibration curve resembles that observed in the presence of detergent.[18] A signal to background noise ratio of nine was obtained for 1.47 nM HSA. It should be noted that a 535 nm emission filter was utilized in this assay, an emission filter centered at 580 nm would be expected to produce lower detection limits. The intra-assay precision for this microplate assay ranged from 10.5 to 7.8 % for 1.47 nM and 1.47 μM HSA, respectively. The use of black microplates is highly recommended due to the high background obtained with clear bottom plates. Due to the fluorescence emission decay rate previously discussed, it is beneficial to utilize a multichannel pipettor or suitable rapid automated well dispensing unit.

CE-LIF HSA Quantitation. A CE-LIF based assay which utilizes NanoOrange as an on-column labeling reagent was developed. A small sample plug is injected into the capillary, analytes are separated and labeled with NanoOrange as they migrate electrophoretically through a run buffer containing the fluorogenic dye, followed by on-column detection. This ability to derivatize analytes on-column confers several notable advantages. Contrary to off-column

derivatization schemes in which labeled samples are consumed/dedicated to a particular analysis, the NanoOrange CE-LIF assay described below ensures sample vials never come into contact with dye. Furthermore, automated sample injection systems typically require 10 μL sample volumes for injection. These features are particularly useful in cases where a limited amount of sample is available, or cost restrictions result in reduced sample accessibility. Since only nanolitre sample volumes are injected onto the capillary, one can essentially preserve the initial sample for later use in performing other analyses such as mass spectrometry and ELISA.

CE-LIF calibration curves for HSA (n=3) were determined as shown in Figure 3.6. Individual curves exhibited relative linearity (R=0.99) from 3.2 nM to 0.82 μM. However, a gradual decrease in assay sensitivity over time was observed. The time required to construct each curve was approximately one hour, such that the third curve was obtained at least three hours following initial preparation of the NanoOrange run buffer. At HSA concentrations below 0.4 μM, calibration curves constructed within the first two hours of run buffer preparation possess very similar sensitivities. Longer time periods (i.e. 3 hours) tended to be associated with significantly lower calibration curve sensitivity. This was attributed to increased dye instability in aqueous conditions. The lifetime of NanoOrange thus appeared to be reduced ca. 3-fold when not diluted in the standard detergent solution provided in the kit. As such, periodic calibration

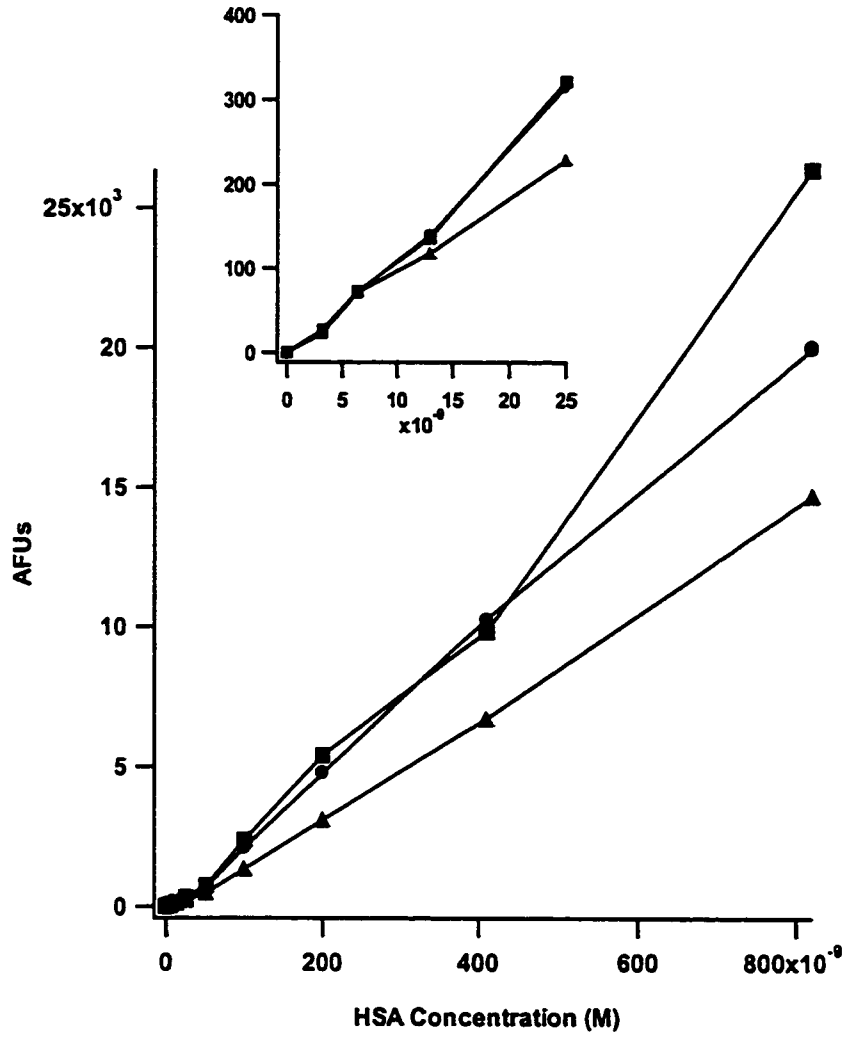

Figure 3.6 CE-LIF calibration curves for HSA utilizing 2x NanoOrange in the run buffer. Conditions: 60 cm, 186 μm o.d., 50 μm i.d., bare-fused silica capillary; 15 mM borate, (pH 9.0) / 2x NanoOrange run buffer, 0.6 bar • s injection, 500 V/cm separation potential; LIF detection (arbitrary fluorescence units - AFUs representing peak height). Calibration curves at t=1 (■), t=2 (●), and t=3 hours (▲) after buffer preparation. Inset shows linear portion (R=0.99) for HSA concentrations in the nanomolar range.

and /or standardization would be required, the internal standardization method may also be particularly effective in this case.

A key feature of the assay is the ability to efficiently label HSA as it migrates through the capillary. Contrary to the microplate scenario, the HSA sample plug is initially devoid of NanoOrange, and is flanked on both sides with run buffer containing NanoOrange. Labeling efficiency thus depended on the analyte's ability to migrate into the adjacent NanoOrange zone, or the dye's ability to overtake the sample plug within a short period of time. This electrophoretic mixing process, as opposed to microplate orbital shaking, resulted in different optimal dye concentrations.

It was determined that incorporation of 2x NanoOrange in the run buffer enhanced the signal to noise ratio by approximately a factor of two (results not shown). A signal to noise ratio of 5.6 was obtained for 3.2 nM HSA. It is important to note that this corresponds to actually labeling 3.2 nM HSA and not simply labeling at high protein concentration followed by serial dilutions typical of other labeling methods. For comparative purposes, an instrumental limit of detection of 0.1 nM was obtained for fluorescein alone (no HSA) using the same experimental parameters, replacing the 580DF30 filter with a 535DF55 filter. In the interest of developing a low cost assay, concentrations of greater than 2x were not examined, though these could feasibly result in improved detection limits. According to the proposed NanoOrange binding model, dye/protein complexation is followed by self-quenching over time. In the present assay format,

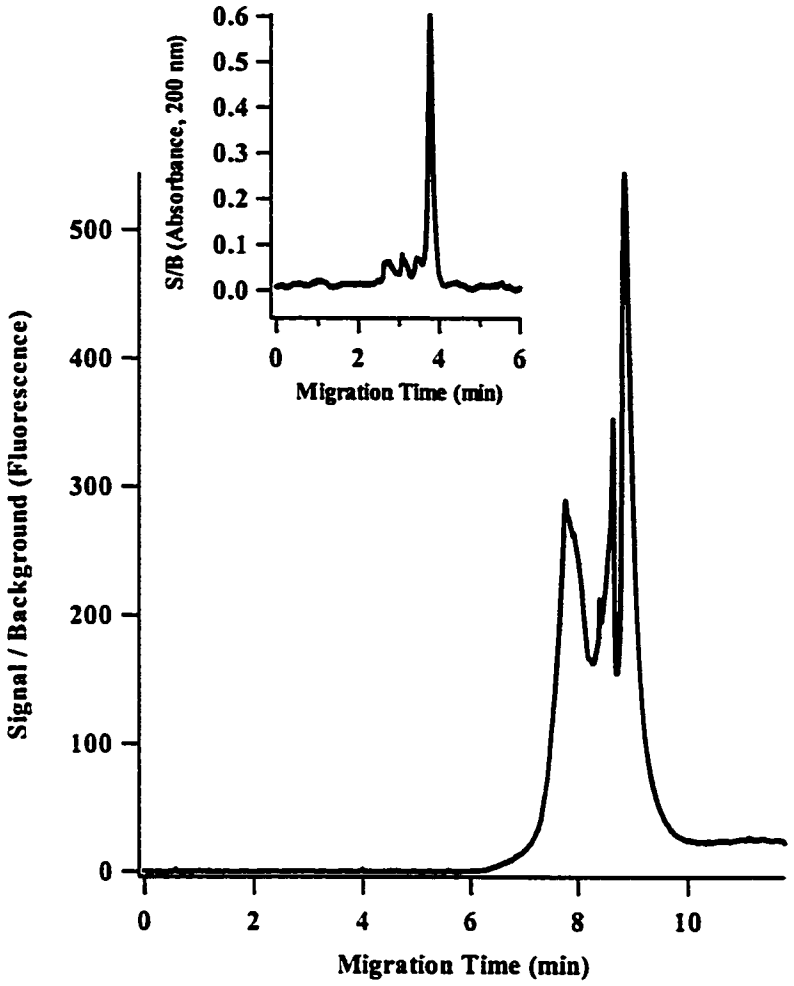

Figure 3.7 CE-LIF electropherogram of 60x diluted human serum utilizing 1x NanoOrange in the run buffer. Conditions: 60 cm total length, 45 cm effective length, 186 μm o.d., 50 μm i.d., bare-fused silica capillary; 20 mM borate, (pH 9.25) / 1x NanoOrange run buffer, 0.6 bar • s injection, 250 V/cm separation potential; spectral filters = 515 EFLP / 535df55, PMT= - 0.900 kV. Inset illustrates human serum profile obtained using a 60 cm total length, 45 cm effective length, 350 μm o.d., 50 μm i.d., bare-fused silica capillary; 20 mM borate, (pH 9.25) run buffer, 5 cm / 60 s hydrodynamic injection, 417 V/cm separation potential and absorbance detection.

HSA/NanoOrange complex migration times of approximately three minutes are attained. Improved detection limits can therefore be expected with shorter analysis times (i.e. shorter effective capillary lengths).

The advantages of utilizing NanoOrange in biofluid analysis are illustrated in Figure 3.7. On-column labeling of human serum with NanoOrange enhances the signal to background ratio of all components by up to two orders of magnitude. This essentially allows one to detect lower concentrations of biofluid protein components than in absorbance detection schemes. Furthermore, the profile obtained using NanoOrange and LIF shows similarities to that observed in the absence of dye with absorbance detection. Systematic improvements in resolution were observed by lowering the electric field in the case of NanoOrange labeling to 250 V/cm, as shown in Figure 3.7. Significant improvements were not observed at electric fields below 250V/cm (data not shown). Addition of NanoOrange to the serum significantly enhanced the signal observed for some zones but may have also altered the electrophoretic mobilities making direct comparisons to the absorbance literature problematic. Positive identification of the sample zones has not yet been accomplished, and will be the focus of future work.

CONCLUSIONS

The numerous attributes of NanoOrange have been effectively coupled with those of CE to provide the clinical chemist with a valuable tool in clinical diagnosis: low protein concentration detection, nanolitre sample consumption and

short analysis times. To our knowledge, this is the first time that the non-covalent fluorogenic dye, NanoOrange, has been used for the on-column labeling of a clinically significant protein in CZE-LIF, as well as for biofluid analysis.

The above approach incorporated NanoOrange in the run buffer to achieve dye-protein complex formation. In order to further reduce assay cost, a plug-plug on-column labeling strategy is currently being investigated. In this format, a plug of analyte is injected, followed by a nL plug of dye (or vice versa depending on their relative electrophoretic mobilities). We are currently examining the use of NanoOrange in a microchip format, as well as a CE-LIF based clinical biofluid analysis tool. Additional protocols are being evaluated in order to expand the scope of NanoOrange as a universal labeling reagent.

ACKNOWLEDGMENTS

The authors are grateful to the Concordia University Centre for Structural and Functional Genomics for use of the Victor^2 fluorescence plate reader. The authors wish to acknowledge financial support provided by the Natural Sciences and Engineering Research Council of Canada (NSERC), Fonds pour la Formation de Chercheurs et l'Aide à la Recherche (FCAR), and David J. Azrieli.

REFERENCES

(1) Kelly, M.T., Fabre, H., Perrett, D. *Electrophoresis* **2000**, 21, 699.

(2) Liu, M.S., Rampal, S., Hsiang, D., Chen, F.T. *Mol. Biotechnol.* **2000**, 15, 21.

(3) Petrini, C., Alessio, M.G., Scapellato, L., Brambilla, S., Franzini, C. *Clin. Chem. Lab. Med.* **1999**, 37, 975.

(4) Bossuyt, X., Schiettekatte, G., Bogaerts, A., Blanckaert, N. *Clin. Chem.* **1998**, 44, 749.

(5) Lee, I.H., Pinto, D., Arriaga, E.A., Zhang, Z., Dovichi, N.J. *Anal. Chem.* **1998**, 70, 4546.

(6) Schmerr, M.J., Jenny, A.L., Bulgin, M.S., Miller, J.M., Hamir, A.N., Cutlip, R.C., Goodwin, K.R. *J. Chromatogr. A.* **1999**, 853, 207.

(7) Hunt, G., Nashabeh, W. *Anal. Chem.* **1999**, 71, 2390.

(8) Yeung, E.S. *J. Chromatogr. A.* **1999**, 830, 243.

(9) Caslavska, J., Allemann, D., Thormann, W. *J. Chromatogr. A.* **1999**, 838, 197.

(10) German, I., Kennedy, R.T. *J. Chromatogr. B. Biomed. Sci. Appl.* **2000**, 742, 353.

(11) McWhorter, S., Soper, S.A. *Electrophoresis* **2000**, 21, 1267.

(12) Walz, T., Geisel, J., Bodis, M., Knapp, J.P., Herrmann, W. *Electrophoresis* **2000**, 21, 375.

(13) Banks, P.R., Paquette, D.M. *J. Chromatogr. A.* **1995**, 693, 145.

(14) Reyderman, L., Stavchansky, S. *Anal. Chem.* **1997**, 69, 3218.

(15) Marino, M.A., Devaney, M., Davis, P.A., Girard, J.E. *J. Chromatogr. B. Biomed. Sci. Appl.* **1999**, 732, 365.

(16) Harvey, M.D., Bandilla, D., Banks, P.R. *Electrophoresis* **1998**, 19, 2169.

(17) Moody, E.D., Viskari, P.J., Colyer, C.L. *J. Chromatogr. B. Biomed. Sci. Appl.* **1999**, 729, 55.

(18) Haugland, R.P. (Ed), *Handbook of Fluorescent Probes and Research Chemicals*, 6th ed.; Molecular Probes: Eugene (OR), 1996.

(19) Pedersen, L.M., Sorensen, P.G. *Acta. Oncol.* **2000**, 39, 145.

(20) Jensen, J.S., Feldt-Rasmussen, B., Strandgaard, S., Schroll, M., Borch-Johnsen, K. *Hypertension* **2000**, 35, 898.

(21) Purcell, M., Neault, J.F., Tajmir-Riahi, H.A. *Biochim. Biophys. Acta.* **2000**, 1478, 61.

(22) Frostell-Karlsson, A., Remaeus, A., Roos, H., Andersson, K., Borg, P., Hamalainen, M., Karlsson, R. *J. Med. Chem.* **2000**, 43, 1986.

(23) Landers, J.P. (Ed), *Handbook of Capillary Electrophoresis,* 2nd ed.; CRC Press: Boca Raton, 1996.

(24) Wachter, R.M., Yarbrough, D., Kallio, K., Remington, S.J. *J. Mol. Biol.* **2000**, 301, 157.

(25) Meshulam, T., Herscovitz, H., Casavant, D., Bernardo, J., Roman, R., Haugland, R.P., Strohmeier, G.S., Diamond, R.D., Simons, E.R. *J. Biol. Chem.* **1992**, 267, 21465.

CHAPTER 4

Sub-Nanomolar Detection Limit for Sodium Dodecyl Sulfate – Capillary Gel Electrophoresis Using a Fluorogenic, Non-covalent Dye

Harvey, M.D., Bandilla, D., Banks, P.R. *Electrophoresis* **1998**, 19, 2169

Reprinted with permission from Wiley-VCH

ABSTRACT

Picomolar limits of detection are obtained using the non-covalent, fluorogenic dye Sypro Red. The size separation of four commonly used SDS-CGE molecular weight markers with 8% linear polyacrylamide (PAA) as the sieving matrix is used to construct a calibration curve for molecular weight determinations. An SDS-CGE purity and molecular weight determination of purified Chorismate Mutase-Prephenate Dehydrogenase from *Escherichia coli* is shown to be comparable in accuracy with slab gel SDS-PAGE. A migration time precision study indicates excellent reproducibility. Sypro Red labeling of SDS-BSA complexes at nanomolar protein concentrations suggests assay detection limits surpassing those of silver staining. This detectability exceeds that achieved in previous SDS-CGE laser-induced fluorescence studies. This approach is expected to be easily adapted for use with commercial polymer formulations and automated instrumentation.

INTRODUCTION

The translation of SDS-PAGE to a capillary format (SDS-CGE) was begun about a decade ago by Cohen and Karger.[1] Size separation of model proteins was demonstrated using 75 μm i.d. capillaries and UV absorbance detection. In the early '90s, a number of groups were experimenting with linear polyacrylamide instead of cross-linked gels. It was found that linear polyacrylamide was simpler to use[2], circumvented gel shrinkage problems[3] and possessed significantly greater lifetimes.[2-4] Yet, in each of these publications UV absorbance detection was used. Polyacrylamide is a medium that significantly absorbs UV radiation where the detection of protein is at an optimal level with regard to signal to noise ratio. Thus, wavelengths of 230 nm or above are typically used, which limits the detection limit of the technique.

A number of groups have investigated the use of different, non-absorbing polymers as sieving matrices in an effort to improve detection limits[4-6], while others have looked to other detection schemes involving derivatization of the protein analytes. Efforts in this direction have been used in capillary zone electrophoresis (CZE) for the improvement of detection limits. A number of publications attest to the ability to detect sub-micromolar concentrations of analyte.[5-7] When dealing with large analytes, such as proteins with multiple functional groups, however, derivatization with common amine reactive probes is a problem. In the case of the most common amine reactive fluorescent probe, fluorescein isothiocyanate, incorporation into the protein typically replaces the positive charge of lysine residues (pKa ~ 10.5) with a doubly charged anion.[8] The resulting distribution of products from the derivatization reaction is only partially separated by CZE leading to quantitatively useless results.[9]

This multiple-labeling problem is less evident in SDS-CGE due to the incorporation of the anionic detergent onto the protein to form a highly charged complex. Most proteins incorporate a constant amount of 1.4 g of SDS for every 1 g of protein. Thus for carbonic anhydrase, a protein with a molecular weight of 29 kDa, there are over 150 SDS molecules incorporated into each protein molecule. The amount of charge associated with this incorporation overwhelms any inherent charge associated with the protein and also any heterogeneity in charge to size ratio in an individual protein population brought about by derivatization. Gump and Monnig examined the use of the probes NDA, OPA and fluorescamine for the enhancement of UV absorbance detection and also for fluorescent detection.[10] Wang and Beale extended the use of derivatization in SDS-CGE with the amine reactive fluorescent probe, fluorescein isothiocyanate in an investigation of gel step gradients in a capillary.[11] Hogan's group has recently demonstrated SDS-CGE protein separations with a detection capability that exceeds that of

Coomassie blue staining. Their methodology relies on pre-column derivatization of proteins with fluorogenic amine reactive probes NBD-F or NBD-Cl.[12] Each of these methods are amine reactive, thus detection limits can be a function of the number of primary amine groups available for derivatization. Consequently, there is protein to protein variability in detection limits.

Recently, Sypro Orange and Sypro Red, two new types of fluorescent dye have been developed for the staining of proteins following SDS-PAGE.[13] These dyes are not amine reactive, rather they interact with the SDS-protein complex, thus it is believed that the Sypro dyes should provide more reliable qualitative and quantitative results for general protein detection compared to their amine reactive counterparts. Furthermore, the detection limit of these dyes in a slab gel format surpasses that of Coomassie Blue staining (2.5 μg/mL), and rivals silver staining (25 ng/mL).[12,13]

This work investigates the use of Sypro Red as a protein stain for SDS-CGE. Sypro Red has an absorbance λ_{max} of 580 nm which can be efficiently excited by a Green HeNe laser operating at 543.5 nm for laser-induced fluorescence detection. The aim of this work is to achieve silver stain limits of detection (~ ng/mL) for proteins separated by SDS-CGE.

MATERIALS AND METHODS

Instrumentation. Experiments were performed using an in-house built CE-LIF instrument similar to that previously described.[14] The capillary current was monitored via a current to voltage converter at 10 Hz using a National Instruments (Texas, USA) NB-MIO-16-H (16 bit resolution) data acquisition board. All voltages were controlled by LabView applications through the I/O port of the NB-MIO board. Bare fused-silica capillaries of 186 μm o.d., 50 μm i.d.

(Polymicro Technologies, Phoenix, AZ) were used. The injection end of the capillary was placed in a safety interlock-equipped plexiglass box built in-house.

A 1.5 mW green helium-neon laser (Melles Griot, Irvine, California) with a wavelength output of 543.5 nm was used as the excitation source. A 6.3 x microscope objective (Melles Griot) with a numerical aperture of 0.2 was used to focus the laser beam on the capillary. System alignment was performed using a five-axis gimbal mount (Newport, Irvine, California). Fluorescence emission was collected at right angles to the excitation beam using a 16x microscope objective with a numerical aperture of 0.32 and a working distance of 3.7 mm, and spatially filtered by an iris diaphragm (Newport) and a 635DF55 bandpass filter (Omega Optical, Brattleboro, VT) to remove scattered light. The photons produced by the fluorophore were detected using a multi-alkali photocathode photomultiplier tube (R1477, Hamamatsu, Middlesex, NJ) powered by a HC123-01, Hamamatsu high voltage power supply with an output range of -300 to -1100 volts. Unless otherwise indicated, the photomultiplier was operated at 800 volts.

The photocurrent was passed through a current to voltage converter and low-pass filter (10 Mega Ohm resistor, 0.1 mF capacitor) and digitized at 10 Hz using the data acquisition system previously described. The collection objective and photomultiplier tube were fixed to a light proof box containing the iris and filters. The data obtained was graphically illustrated using Igor Pro (Wavemetrics, Oregon, USA).

Reagents. Sodium tetraborate (borax), boric acid, and sodium dodecyl sulfate (SDS) were all of SigmaUltra grade (Sigma, St. Louis, MO). All buffers and sample solutions were prepared using HPLC-grade water (Nanopure, Barnstead, Boston, MA). Buffer solutions were filtered with a 0.22 μm filter (Fisher Scientific, Fair Lawn, NJ) and subsequently with a 0.2 μm (25 mm) nylon

syringe filter (Nalgene, Rochester, NY). Acrylamide, ammonium persulfate, and N,N,N',N'-tetramethylethylenediamine (TEMED) were of the highest purity provided by Sigma. Carbonic anhydrase (29 kDa), ovalbumin (43 kDa), bovine serum albumin (66 kDa), and conalbumin (78 kDa) were purchased from Sigma, dissolved in water, and stored at 4 ^{0}C. Sypro Red protein gel stain was obtained from Molecular Probes (Eugene, OR) and stored in the dark at 4 ^{0}C. Chorismate mutase-prephenate dehydrogenase (CMPD) was purified from *E. Coli*.

Sample Preparation. A 999 μL solution that contained carbonic anhydrase, ovalbumin, BSA, and conalbumin (all at 50 μg/mL) was prepared in a 1.5 mL microfuge tube by adding 10 μL of each 5 mg/mL protein stock solution to 929 μL of water and 30 μL of 2% SDS (w/v) in 0.1 M Tris-0.25 M Borate, pH 8.10. The ratio of SDS:Protein (w/w) was 3:1 for all experiments. Individual protein samples for the purpose of peak identification and determination of detection limits, were prepared in a similar fashion. Samples were heated at 100 ^{0}C for 6.5 min in a water bath and allowed to cool in an ice bath for 5 min prior to the addition of 1 μL of 5000x Sypro Red concentrate. Samples were vortexed and allowed to sit in an ice bath in the dark for 15 min prior to sampling.

Gel Preparation. Linear polyacrylamide (8%) was prepared by dissolving 0.8 g of acrylamide in 9.898 mL of 0.1 M Tris-0.25 M Borate, pH 8.10 + 0.05% SDS (w/v) and 100 μL of 10% ammonium persulfate (w/v in water). The solution was filtered, and vacuum degassed for 30 minutes prior to the addition of 2 μL TEMED. Capillaries were treated with 0.1 M NaOH for 30 min followed by washing with HPLC-grade water and purged for 5 min with helium gas. A detector window was prepared 15 cm from one end by burning the polyimide coating. Immediately following TEMED addition and gentle mixing, the

polymerizing solution was introduced into the capillary via vacuum for 20 minutes. On-column polymerization was allowed to proceed for a minimum of one hour at room temperature on a flat surface before applying voltage. Approximately 1 cm of capillary was trimmed from both ends following installation of the capillary in the in-house instrument. The capillary was equilibrated with the same 8% polyacrylamide solution as used for filling by applying a 50 V/cm electric field for 30 min.

Capillary Gel Electrophoresis. Samples were injected at the cathodic end for 5 seconds at 50 V/cm unless indicated otherwise. Separations were performed by applying +10 kV to the anodic end of the capillary. Samples were kept in the dark and on ice between runs.

RESULTS AND DISCUSSION

Gel-Filled Capillary Lifetime. The lifetime of capillaries filled with 8% linear PAA was on the order of four to six hours with the continuous application of voltage. This is comparable to lifetimes reported in other studies.[3,12] Of critical importance to the lifetime of polymer filled capillaries is the presence of polymer in the run buffer. The absence of polymer in the run buffer leads to spatial and temporal depletion of ions at the gel-liquid interface,[15] a slow steady decline in current, and eventual gel breakdown (Figure 4.1). Bubble formation was consistently localized to the first few centimeters of the cathodic end of the capillary. Incorporation of the same percentage of polymer in the run buffer produces a highly stable current and extended capillary lifetime. The viscosity of linear PAA increases exponentially with concentration[3] and it was deemed

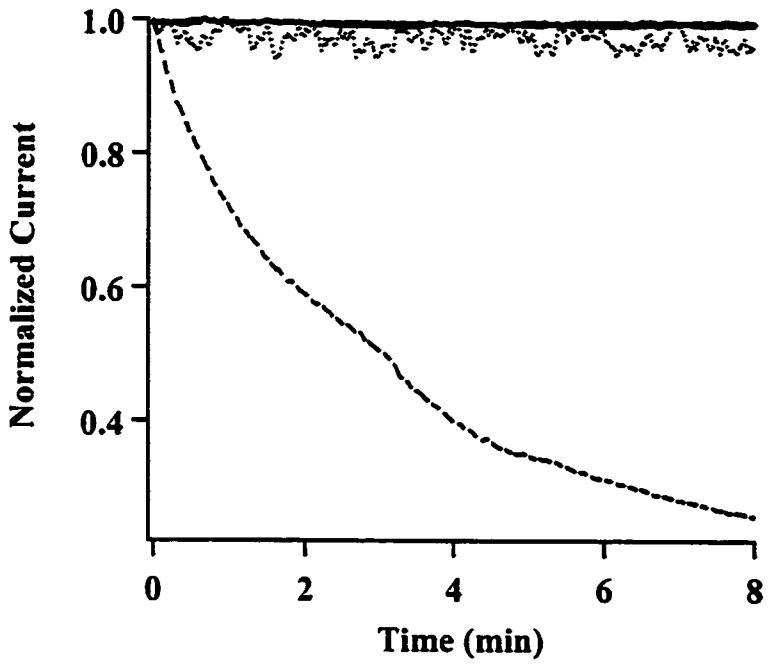

Figure 4.1 Current stability as a function of buffer composition in SDS-CGE. Untreated capillary, no polymer in run buffer (....); Polymer-filled capillary, No polymer in run buffer (---); Polymer-filled capillary, Polymer in run buffer (—).

unnecessary to coat capillaries when working with 8% linear PAA. The high viscosity of an 8% linear PAA solution precluded its removal from the capillary upon bubble formation, however. Adaptation of the methodology to less viscous polymers such as dextran would allow for replacement of the gel formulation between runs thus significantly increasing capillary lifetime.

Non-Covalent Fluorescent Labeling of Proteins. The detection limit and specificity of Sypro Red protein gel stain has been extensively characterized on polyacrylamide slab gels.[13, 16] Sypro dye shows excellent chemical stability in aqueous solution and does not require special reaction conditions. Non-covalent labeling is essentially complete within 15 minutes of dye addition yet it is suggested that sampling not occur within this time frame to ensure equilibrium conditions prevail. Lower detection limits are obtained by using a 1000x dilution of stock dye solution rather than the 10 000x dilution typically used for a slab-gel format. In addition, a pH study concluded that no gain in detection limit could be obtained by using more acidic or basic conditions (data not shown). To our knowledge, this is the first time a non-covalent fluorophore has been used to enhance the detection limit of SDS-CGE.

Denaturing, Non-reducing Gel Electrophoresis. Denaturing SDS-CGE allows one to determine sample purity and molecular mass estimates. In slab gel SDS-PAGE, samples are typically prepared in a buffer containing 1 to 2% SDS to ensure proteins are extensively denatured. It has been shown that with such elevated SDS concentrations, Sypro Red will bind primarily to pure SDS micelles, labeling few of the SDS-protein complexes.[13] Sample preparation in the presence of 0.05% SDS ensured the absence of micelles. Our attempts to incorporate Sypro Red in the run buffer and label SDS-protein complexes on-column were

unsuccessful, presumably due to selective dye binding to SDS since a 10-fold increase in background was observed.

A common feature of most proteins complexed with SDS during electrophoresis is a constant binding ratio of 1.4 g SDS per gram of protein. Pre-column labeling of SDS-protein complexes could thus be performed by using submicellar concentrations of SDS while satisfying the above constant ratio since our protein concentrations were μM or less. The ratio of SDS to protein was fixed at 3 to 1 (w/w) in all experiments, and is sufficient to maintain proteins in their denatured state following boiling. Figure 4.2 shows the SDS-CGE separation of (in order of elution) carbonic anhydrase, ovalbumin, BSA, and conalbumin labeled with Sypro Red, all proteins commonly employed as molecular mass standards for SDS-CGE separations. Peak identification was achieved using individual protein samples. Analyte zone widths were on the order of 0.5 to 1 min, comparing favorably with zone widths obtained with covalent fluorogenic agents.[10, 12, 17]

Low efficiencies could be due in part to the non-covalent nature of the labeling. The larger widths of the ovalbumin and conalbumin peaks are expected from the potential heterogeneity of glycoproteins. Baseline resolution was not achieved at this polyacrylamide concentration yet separation was adequate for the purposes of molecular weight and sample purity determination. Attempts to achieve baseline resolution by increasing the effective length were unsuccessful due to increased dispersion. For improved resolution, a higher percentage of polyacrylamide or a step gradient[11] is suggested. Capillary thermostating at some optimal temperature has also been shown to significantly increase peak efficiency.[18]

Separation of standard proteins in the molecular weight range of 29 kDa - 78 kDa was complete within 18 min. It should be noted that a large peak was observed at about 8 minutes. This is thought to be analogous to the dye front

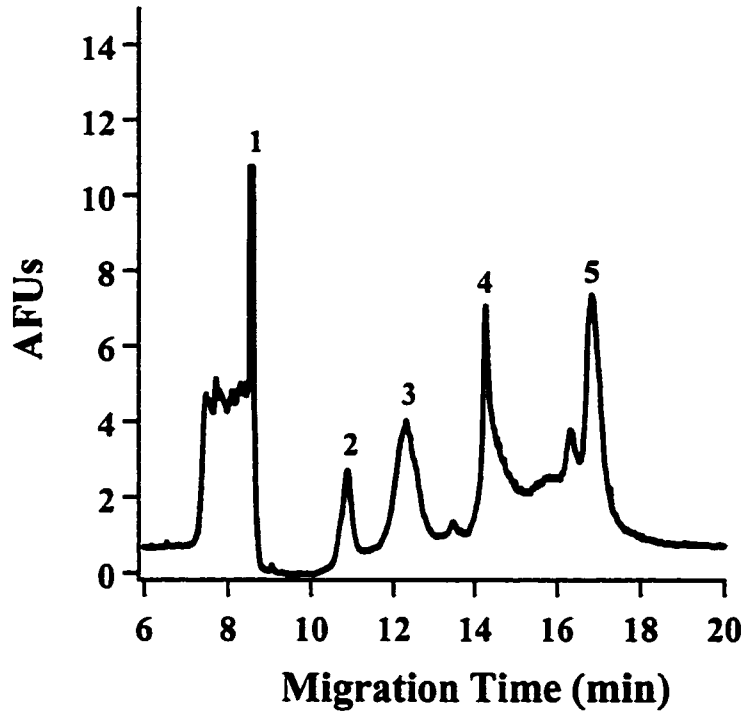

Figure 4.2 Electropherogram of Sypro Red labeled standard proteins using 8% linear polyacrylamide gel and LIF detection. Proteins at 50 μg/mL: (1) Dye front, (2) Carbonic Anhydrase, (3) Ovalbumin, (4) BSA, (5) Conalbumin. Conditions: uncoated 50 μm i.d. capillary, 12.5 cm effective length, 40.1 cm total length. 5 sec electrokinetic injection at cathodic end (62 V/cm), 249 V/cm separation voltage. Run buffer (all experiments): 0.1 M Tris-0.25 M Borate, pH 8.10 + 0.05% SDS + 8% PAA. Laser output: 1.5 mW at 543.5 nm, PMT @ -600 V.

observed in slab gel SDS-PAGE consisting of lower molecular weight dye-SDS complexes. The peaks at 13.4 and 16.3 minutes remain unidentified though these were also observed in previous work using ovalbumin and conalbumin as protein standards (from the same commercial source).[12]

Molecular Weight and Purity Assessment of Chorismate Mutase-Prephenate Dehydrogenase

CMPD purified from *Escherichia coli* was analyzed using the present SDS-CGE system. CMPD is a dimer of two 42 kDa subunits, and plays an important role in tyrosine biosynthesis in plants and microorganisms. Six alternating runs of protein molecular weight standards and CMPD were performed. In order to determine the molecular weight of CMPD by SDS-CGE, a linear plot of log(molecular weight) versus migration time was constructed from the average migration times of standard proteins (Figure 4.3). The equation obtained was $y=0.081x + 3.672$, with an $(R^2)=0.921$. The average migration time of CMPD was 10.95 min, corresponding to a molecular weight of 36 225 Da. This value is 13.8% lower than the accepted molecular weight of 42 kDa yet compares favorably with the 10% accuracy of SDS-PAGE slab gel determinations. The molecular weight of CMPD determined by slab gel SDS-PAGE was 46 507 Da, 10.7% greater than the accepted value.

A single band was observed for CMPD upon Coomassie-Blue staining of a slab gel, suggesting successful purification. In comparison, a peak corresponding to a molecular weight of 79 233 Da was observed in addition to the CMPD monomer peak in SDS-CGE (Figure 4.4). Whereas both peaks are of similar

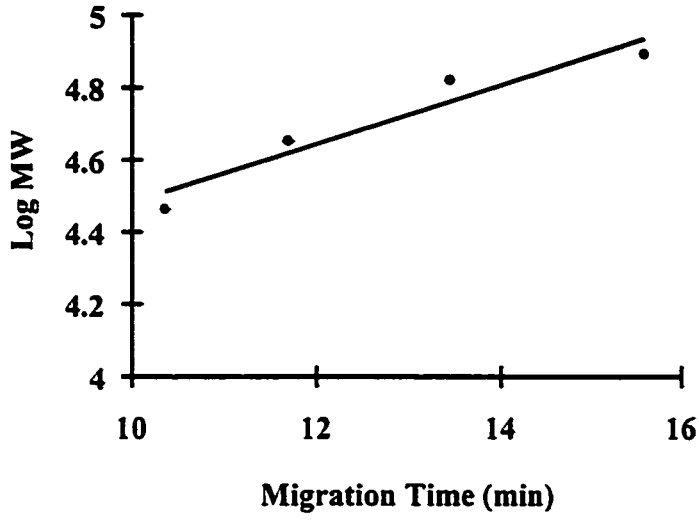

Figure 4.3 Plot of log (molecular mass) vs. average migration time of standards listed in Table 4.1, for molecular weight determination of CMPD.

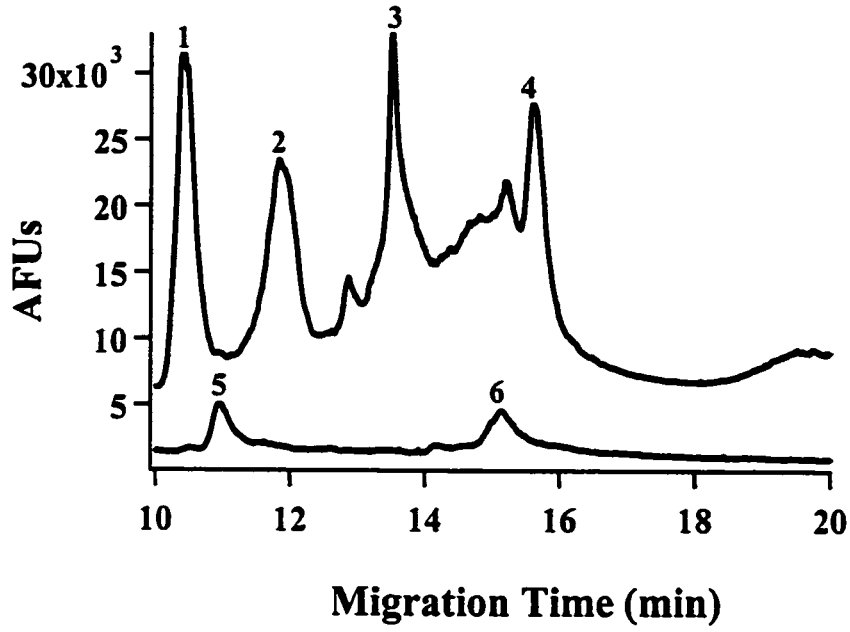

Figure 4.4 Electropherograms of Sypro Red labeled standard proteins and purified CMPD using 8% linear polyacrylamide gel and LIF detection. Proteins at 50 μg/mL: (1) Carbonic Anhydrase, (2) Ovalbumin, (3) BSA, (4) Conalbumin, (5) CMPD monomer, (6) CMPD dimer. Conditions: uncoated 50 μm i.d. capillary,14.4 cm effective length, 44.6 cm total length. 5 sec electrokinetic injection at cathodic end (112 V/cm), 224 V/cm separation voltage. Laser output same as Fig. 4.2, PMT @ -700 V. Electropherograms offset in fluorescence axis.

intensity, no corresponding band was observed on the slab gel. Contrary to the slab gel experiment, non-reducing conditions were utilized in SDS-CGE, thus disulfide bond formation between monomers through exposed Cys residues is possible. CMPD is composed of three Cys residues and thus at least one cysteine is available for such bond formation. Intra-monomer cystine bond formation would similarly lead to more compact Sypro Red-SDS-CMPD complexes of greater relative mobility. The molecular weight of this second peak is in good agreement with an expected dimer mass of 84 kDa.

Reproducibility of SDS-CGE Using Sypro Red. A migration time reproducibility study was conducted using six alternating runs of standard protein mixtures and purified CMPD (Table 4.1). Values for migration time % RSD of molecular weight standards ranged from 0.52 to 1.0. CMPD migration time reproducibility was also excellent with a % RSD of 0.51. To compare migration time reproducibility for runs performed on different days, a total of nine CMPD migration times were obtained over two consecutive days. Day-to-day CMPD migration time precision was 1.2 %. These values compare favorably with several commercial SDS-CGE kits. It has been shown that careful control of gel-filled capillary temperature can enhance migration time reproducibility.[19] The system described here was not subject to temperature control and thus may show enhanced reproducibility with the proper cooling apparatus. Peak area precision for protein standards was not possible due to inadequate baseline resolution. As a result, SDS-CGE using Sypro Red is presently qualitative in nature.

Run	C. Anh.	Ovalbumin	BSA	Conalbumin	CMPD
1	10.42	11.84	13.52	15.62	11.03
2	10.37	11.69	13.39	15.51	10.95
3	10.38	11.69	13.37	15.44	10.96
4	10.39	11.79	13.41	15.64	10.94
5	10.35	11.52	13.51	15.63	10.88
6	10.26	11.60	13.52	15.67	-
Average	10.36	11.69	13.45	15.59	10.95
% RSD	0.52	1.0	0.53	0.57	0.51

Table 4.1 Migration time reproducibility of Sypro Red SDS-CGE (8% Linear PAA).

Detection limit of Sypro Red Protein Stain in SDS-CGE. It is important to distinguish between instrumental and assay detection limits in SDS-CGE with laser-induced fluorescence (LIF). Instrumental detection limits refer to the detection of dilute labeled protein solutions whereby a fairly concentrated protein solution (typically mM to μM) is derivatized, followed by serial dilutions until the S/N ratio deteriorates to the limit of detection. The assay detection limit refers to the minimum amount of unlabeled protein that can be labeled and detected, and takes into account difficulties encountered in labeling dilute protein solutions. Thus, in comparing various SDS-CGE approaches for improving detection limits, assay detection limits are of paramount importance (Table 4.2). An approach which is unable to label proteins at submicromolar levels cannot be considered as sensitive as silver staining, even though completed derivatizations are serially diluted to subnanomolar levels. To our knowledge there have been no reported SDS-CGE LIF detection schemes capable of matching the detection limit of slab gel silver staining. Using Sypro Red it was possible to label and detect 1.5 nM of denatured BSA by SDS-CGE (Figure 4.5). This corresponds to 100 ng/mL of protein, comparing favorably to silver staining detection limits of 10 ng/mL.[20] An estimate for the BSA assay detection limit was computed by determining the standard deviation of the signal from 12 to 14 minutes and using this as the noise. Then using the peak height for 1.5 nM BSA, the assay detection limit at 3σ was determined to be 73 pM. It is apparent that we can achieve similar levels of detection to slab-gel silver staining. Further optimization of dye concentration during sample preparation, and improved peak efficiency through careful temperature selection and thermostating is expected to further lower assay detection limits.

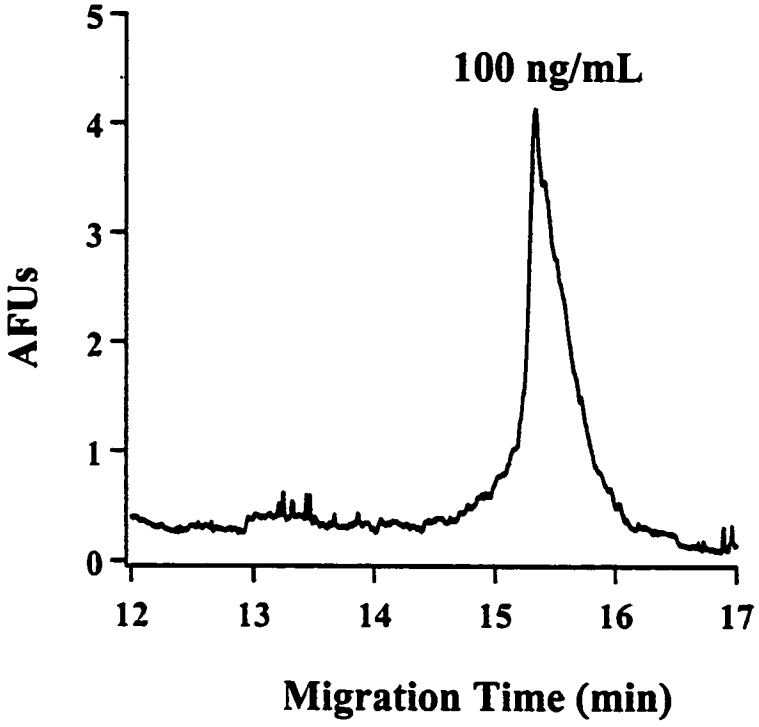

Figure 4.5 Electropherogram of 1.5 nM BSA labeled with Sypro Red using 8% linear polyacrylamide gel and LIF detection. Conditions: uncoated 50 μm i.d. capillary, 14.2 cm effective length, 44 cm total length. 5 sec electrokinetic injection at cathodic end (114 V/cm), 227 V/cm separation voltage. Laser output same as Fig. 4.2, PMT @ -800 V.

Reagent	Concentration of protein labeled (M)[a)]	Reference
FITC	Unreported	11
FQ	1.0×10^{-7}	6
NBD-Cl	1.5×10^{-5}	12
NBD-F	2.1×10^{-6}	12
NDA	1.1×10^{-5}	10
Fluorescamine	1.2×10^{-5}	10
OPA	1.2×10^{-5}	10
Sypro Red	1.5×10^{-9} [b)]	This study

a) Lowest derivatizable concentration reported

b) Calculated assay detection limit (3σ) = 73 pM

Table 4.2 A Comparison of SDS-CGE LIF labeling approaches: lowest derivatizable protein concentrations reported.

CONCLUDING REMARKS

We have described a method for the size separation of proteins by capillary electrophoresis using 8% linear PAA as the sieving matrix. The use of Sypro Red protein stain has been demonstrated in an SDS-CGE format with a detection limit which exceeds that of Coomassie Blue staining and compares favorably with silver staining. The companion dye to Sypro Red, Sypro Orange, is expected to produce similar results using 488 nm excitation with an Argon Ion Laser. The work reported here is the most sensitive SDS-CGE LIF assay method described thus far, capable of detecting protein labeled at silver staining levels, and demonstrates good reproducibility in the absence of temperature control. All previous SDS-CGE LIF studies have focused on the covalent attachment of amine reactive fluorescent probes whereby detection limit is greatly dependent on the number of protein amine groups accessible for derivatization. Sypro dyes provide a more universal detection scheme than multiple-label LIF in SDS-CGE and hold potential for protein quantitation. Our group is currently investigating the use of these non-covalent dyes with less viscous, replaceable sieving matrices such as dextran, and evaluating their use in protein quantitation. The use of replaceable polymer solutions is expected to enhance reproducibility, greatly increase capillary lifetime, and allow for system automation.

ACKNOWLEDGEMENTS

We gratefully acknowledge the donation of purified CMPD by Dinesh Christendat. This project was funded by the Natural Sciences and Engineering Research Council of Canada (NSERC), and the Fonds pour la Formation de Chercheurs et l'Aide à la Recherche (FCAR). M.D.H. acknowledges a Concordia University fellowship from David J. Azrieli. D. Bandilla acknowledges support from Bayerische Apothekerstiftung.

REFERENCES

(1) Cohen, A. S.; Karger, B. L. *J. Chromatogr.* **1987**, 397, 409.

(2) Widhalm, A.; Schwer, C.; Blaas, D.; Kenndler, E. *J. Chromatogr.* **1991**, 549, 446.

(3) Wu, D.; Regnier, F. E. *J. Chromatogr.* **1992**, 608, 349.

(4) Ganzler, K.; Greve, K. S.; Cohen, A. S.; Karger, B. L.; Guttman, A.; Cooke, N. C. *Anal. Chem.* **1992**, 64, 2665.

(5) Nickerson, B.; Jorgenson, J. W. *J. Chromatogr.* **1989**, 480, 157.

(6) Ueda, T.; Mitchell, R.; Kitamura, F.; Metcalf, T.; Kuwana, T.; Nakamoto, A. *J. Chromatogr.* **1992**, 593, 265.

(7) Shippy, S. A.; Jankowski, J. A.; Sweedler, J. V. *Anal. Chim. Acta* **1995**, 307, 163.

(8) Klonis, N.; Sawyer, W. H. *J. Fluorescence* **1996**, 6, 147.

(9) Banks, P. R.; Paquette, D. M. *J. Chromatogr. A* **1995**, 693, 145.

(10) Gump, E. L.; Monnig, C. A. *J. Chromatogr. A* **1995**, 715, 167.

(11) Wang, C. C.; Beale, S. C. *J. Chromatogr. A* **1996**, 756, 245.

(12) Wise, E. T.; Singh, N.; Hogan, B. L. *J. Chromatogr. A* **1996**, 746, 109.

(13) Steinberg, T. H.; Jones, L. J.; Haugland, R. P.; Singer, V. L. *Anal. Biochem.* **1996**, 239, 223.

(14) Little, M. J.; Paquette, D. M.; Harvey, M. D.; Banks, P. R. *Anal. Chim. Acta* **1997**, 339, 279.

(15) Figeys, D.; Renborg, A.; Dovichi, N. J. *Electrophoresis* **1994**, 15, 1512.

(16) Steinberg, T. H.; Haugland, R. P.; Singer, V. L. *Anal. Biochem.* **1996**, 239, 238.

(17) Pinto, D. M.; Arriaga, E. A.; Craig, D.; Angelova, J.; Sharma, N.; Ahmadzadeh, H.; Dovichi, N. J. *Anal. Chem.* **1997**, 69, 3015.

(18) Guttman, A.; Horváth, J.; Cooke, N. *Anal. Chem.* **1993**, 65, 199.

(19) Shieh, P. C. H.; Hoang, D.; Guttman, A.; Cooke, N. *J. Chromatogr. A* **1994**, 676, 219.

(20) Merril, C. R.; Switzer, R. C.; Van Keuren, M. L. *Proc. Natl. Acad. Sci. USA* **1979**, 76, 4335.

CHAPTER 5

Site Specific Fluorescent Derivatization and LC/MS Characterization of Long R^3 IGF-I for Bioanalytical Applications

(Harvey, M.D., Banks, P.R. Submitted *Bioconjugate Chemistry*)

ABSTRACT

Recombinant Long R^3 IGF-I was derivatized with fluorescein isothiocyanate (FITC) at a single location by careful selection of reaction conditions (i.e. pH, and FITC / protein amino group ratio). High-performance liquid chromatography (LC) and electrospray mass spectrometry (MS) were utilized to confirm the extent of fluorescein conjugation. The protein conjugate was isolated and subjected to cyanogen bromide (CNBr) cleavage, followed by LC/MS to determine the site of modification. The isolated species of Long R^3 IGF-I-FITC was labeled at the N-terminal Met residue. Recognition of this fluorescent analog by monoclonal anti-IGF-I was preserved, indicating its potential for immunodiagnostic applications.

INTRODUCTION

Human insulin-like growth factor I (IGF-I) is a basic polypeptide consisting of 70 amino acid residues and three disulfide bonds. IGF-I is a potent growth factor both *in vivo* and *in vitro*, with activity modulation by at least six specific binding proteins and a host of proteases.[1,2] The potent anti-apoptotic function of IGF-I is achieved via stimulation of a Type I IGF receptor which contains a tyrosine kinase domain and is linked to the ras-raf-MAPK signalling cascade.[3] Disruption of this complex regulatory system has been associated with various cancers, particularly cancers of the breast and prostate.[4,5] Development of a fluorescent IGF-I conjugate may thus be utilized in various bioanalytical

applications such as early disease detection, and the elucidation of disease mechanisms.

The use of fluorescent probes offers a number of advantages over radioisotopes: safety, longer shelf life, inexpensive disposal. In addition, fluorescence-based high-throughput screening instruments are commercially available. Microtitre plate-based fluorescence polarization and capillary electrophoresis instrumentation with laser induced fluorescence detection are well suited to the clinical laboratory.

Fluorescein has found widespread use in bioanalytical applications as a fluorescent probe due in part to its relatively high molar absorptivity and quantum yield, water solubility, and efficient excitation by relatively inexpensive argon ion lasers.[6] Use of the amine reactive dye, FITC, to produce fluorescein thiocarbamylated conjugates is a common labeling strategy. Targeting free amino functional groups may however result in a complex mixture of reaction products. It has been demonstrated that for a molecule with n primary amino groups, 2^n-1 reaction products can be formed.[7] Selectivity towards the N-terminus of an analyte can be achieved by careful selection of reaction pH and the ratio of probe to protein. Human insulin has been selectively labeled at its N-terminus at a pH of 7.0, and FITC/insulin ratio of 3:1.[6] Since insulin is structurally similar to IGF-I, and contains a comparable number of derivatizable sites, it was deemed possible to achieve similar labeling selectivity with IGF-I.

In developing a fluorescent IGF-I conjugate it was desirable to elucidate the most cost effective process. Recently, an efficient expression system which produces a potent, biologically active IGF-I fusion peptide analogue in *Escherichia coli* has been described.[8] The 9110 Da analogue is referred to as Long R^3 IGF-I and is composed of the entire IGF-I sequence (Glu-3 replaced by Arg), and an N-terminal 13 amino acid residue linker. This paper describes for the first time: (1) conjugation of Long R^3 IGF-I with FITC; (2) LC purification of the fluorescein-labeled analogue; (3) structural characterization of the labeled analogue by chemical cleavage and LC/MS; (4) demonstration of the binding of monoclonal anti-IGF-I to this fluorescein conjugate for use in immunodiagnostic applications.

EXPERIMENTAL SECTION

Chemicals. Nanopure water was obtained from a Sybron/Barnstead, 18 MΩ-cm water purification system (Sybron/Barnstead, Boston, MA). HPLC-grade acetonitrile was purchased from Fisher Scientific (Fair Lawn, NJ), trifluoroacetic acid (TFA) and anhydrous dimethylformamide were obtained from Aldrich (Milwaukee, WI). Boric acid, sodium tetraborate, monobasic and dibasic sodium phosphate, cyanogen bromide, ethylenediaminetetraacetic acid (EDTA), FITC (Isomer I), and Long R^3 IGF-I were obtained from Sigma (St. Louis, MO). Monoclonal anti-IGF-I (Clone 82-9A) was purchased from Oncogene Research Products (Cambridge, MA).

Instrumental Procedures. All HPLC separations were performed with Vydac C_{18} (5-μm d_p) columns: 250 x 4.6 mm and 250 x 1.0 mm for conjugate purification and CNBr digest analysis, respectively. A HP 1090 Series II/M HPLC system with binary DR5 solvent delivery and HP 1050 series multiple wavelength diode-array UV-visible absorbance detector (Hewlett Packard, Mississauga, ON, Canada) was used for all LC separations. The following gradient was utilized in all HPLC determinations: 0 –15 min (100% to 15% A), where A was 0.05% TFA in nanopure water and B was 100% acetonitrile / 0.05% TFA. Flow rates of 1.00 and 0.040 mL/min were used for conjugate purification and CNBr digest analysis, respectively.

Samples were injected manually using a Rheodyne 7125 manual valve injector (Hewlett Packard) and 100-μL glass, gastight syringe (Hamilton, Reno, Nevada). For Long R^3 IGF-I conjugate analysis and purification, a 100-μL stainless steel injection loop was used, and for CNBr digest analysis, a 20-μL injection loop was utilized. Peaks were monitored by UV absorbance at 215 nm.

Electrospray mass spectra were obtained using a Finnigan SSQ 7000 single-quadrupole mass spectrometer (Thermoquest, Mississauga, ON, Canada). Long R^3 IGF-I conjugate analysis was performed on-line by splitting the LC eluent into a 50-μm i.d. bare-fused silica capillary, reducing flow rates to approximately 40 μL / min. Analyses of CNBr digests were performed on-line

without flow splitting. Positive ion detection was employed in all cases, scanning over a m/z range of 300 – 2500 at a scan rate of 2 sec. The following conditions were used in all analyses: 4.5 kV spray voltage, 210 °C capillary temperature, 40 p.s.i sheath and 15 p.s.i auxillary gas pressures (prepurified N_2), electron multiplier set at 1200 V, centroid mode.

Monoclonal anti-IGF-I recognition was analyzed using an ATI-Unicam (Mississauga, ON, Canada) Model Crystal 310 capillary electrophoresis system with a 48-position peltier-cooled autosampler. Laser-induced fluorescence of the protein conjugate was achieved using a detection system described previously.[9] Briefly, the output beam of a Uniphase (San Jose, CA) air-cooled, light-controlled 4 mW Ar^+ laser (Model 2012-4SLL) was focused onto the window of a 50-μm i.d. / 186-μm o.d. 60 cm long (45 cm to detector) bare-fused silica capillary (Polymicro Technologies, Phoenix, AZ). Fluorescence was collected at 90 ° to the excitation beam, spatially filtered using a 800-μm pinhole, and spectrally filtered with two optical filters (515EFLP and 535DF35) (Omega Optical, Brattleboro, VT). Fluorescence was detected using a Hamamatsu (Bridgewater, NJ) Model R1477 photomultiplier tube set at -800 V.

Preparation of Long R^3 IGF-I – Fluorescein Conjugate. A 100 mM FITC stock solution was prepared by dissolving 1 mg FITC in 25.6 μL of anhydrous DMF. A 10 mM substock was made by performing a 10x dilution of

this stock, and was used for all derivatizations. Conjugations were initiated by adding 1.76 μL of 10 mM FITC to a solution containing 204.8 μL of 100 mM Phosphate (pH 7.00) / 400 μM EDTA and 40 μL of 1 g/L Long R^3 IGF-I. Upon addition of FITC, tubes were protected from light, gently vortexed for three hours, then allowed to react overnight at room temperature. Single-labeled Long R^3 IGF-I was purified by HPLC, lyophilized, and subjected to CNBr digestion.

CNBr Cleavage. CNBr cleavage reactions were performed on unlabeled and labeled Long R^3 IGF-I as previously described.[10] Briefly, a small crystal of CNBr was added to a solution containing 10 μL of 1 g/L unlabeled protein and 190 μL of 0.12 N HCl. In the case of labeled protein, the lyophilized product (ca. 10 μg) was resuspended in 200 μL of 0.12 N HCl, with the subsequent addition of a small crystal of CNBr. All cleavage reactions were performed in an oven at 38 °C, protected from light. Reactions were stopped after three hours by quenching with 500 μL of nanopure water. Samples were lyophilized and resuspended in 50 μL of nanopure water prior to LC/MS analysis.

Immunorecognition of Labeled Long R^3 IGF-I. Purified Long R^3 IGF-I conjugate (c.a. 10 μg) was resuspended in 100 μL of nanopure water. A 20 μL volume of this solution was transferred to a glass CE sample vial, 1 μL of 100 μg / mL monoclonal anti-IGF-I (prepared in sterile phosphate buffered saline, pH

7.4) added, mixed, and analyzed immediately on the Crystal CE system. Injections were performed at 50 mbar for 0.1 min, followed by a 20 kV separation using a 100 mM Borate (pH 8.50) run buffer.

RESULTS AND DISCUSSION

FITC Labeling of Long R^3 IGF-I. Derivatization of Long R^3 IGF-I with FITC can produce 15 different conjugate species. This is attributed to the presence of one N-terminal α-amino and three Lys ε-amino groups. In the development of a bioanalytical fluorescent conjugate, it is highly desirable to preserve immunorecognition and/or biological activity. Functional epitope mapping of IGF-I by anti-IGF-I monoclonal antibodies, and the production of novel recombinant fusion protein analogues of IGF-I has indicated that certain residues or regions of residues are important for binding of the IGF-I receptor.[8,11] These studies have shown that the N-terminus is not involved in receptor binding. The selective introduction of fluorescein on the α-amino group of Long R^3 IGF-I is thus expected to have minimal impact on bioactivity.

In order to target the N-terminus of Long R^3 IGF-I, a variety of FITC to protein amino group ratios and reaction pH values were employed. A 10-fold molar excess of dye at pH 7.0 resulted in the production of multiple labeled species which were poorly resolved by HPLC (data not shown). Performing the derivatization at pH values of 8.5 and above also proved undesirable, with the dual disadvantage of multiple conjugates and increased FITC hydrolysis (data not

shown). Production of single-labeled Long R^3 IGF-I appeared to be achieved by simultaneously lowering the FITC to protein amino group ratio and decreasing the reaction pH to 7.0. Performing the reaction at pH 7.0 seemed to best exploit pK_a differences between the α- and ε-amino groups, whereas lowering the FITC to amino group ratio served to limit the amount of available dye.

LC/MS Characterization of Single-Labeled Long R^3 IGF-I. The products of the 1:1 FITC / Long R^3 IGF-I conjugation reaction (pH 7.0) were analyzed by LC/MS. The total ion chromatogram (TIC) obtained from LC/MS analysis of the FITC labeling reaction indicated the presence of multiple peaks (see Figure 5.1). Unreacted FITC and its hydrolysis products, fluorescein amine and difluorescein thiourea, were identified from extracted ion mass spectra (see Figure 5.2). It is necessary to purify labeled Long R^3 IGF-I from these species since they are known bioassay interferents, binding non-specifically to various biofluid proteins. In producing a single-labeled Long R^3 IGF-I competitive immunoassay reagent, it is equally important to adequately remove any remaining unlabeled protein from its labeled counterpart. Failure to do so would result in an overestimation of the amount of IGF-I present in a particular biofluid. The peaks corresponding to unlabeled and single-labeled Long R^3 IGF-I were identified by LC/MS analysis (see Figure 5.3). The LC conditions established in this study thus provide for the rapid separation of labeled Long R^3 IGF-I from unreacted FITC,

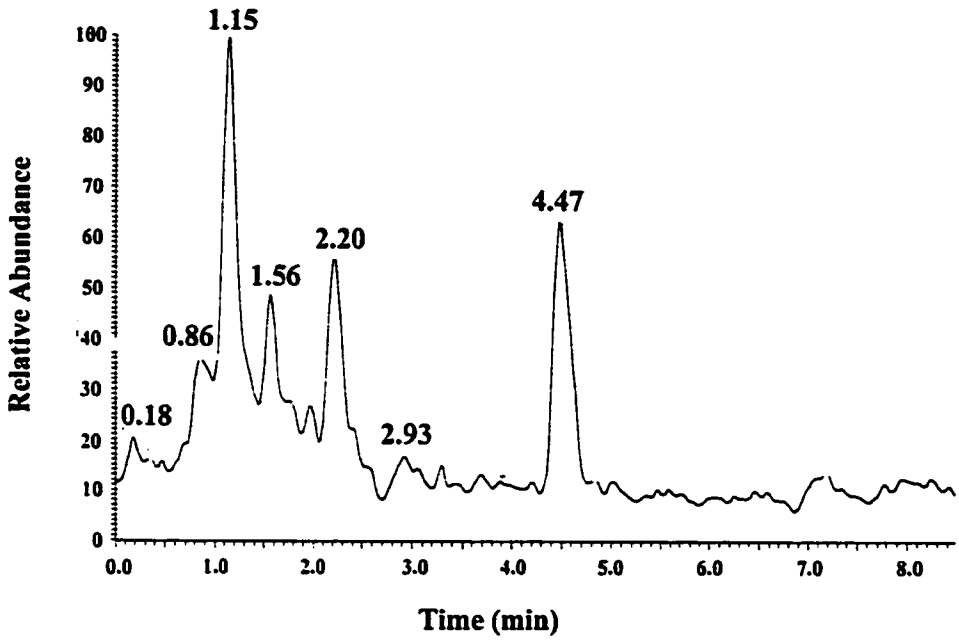

Figure 5.1 Total ion chromatogram (TIC) of LC separated Long R^3 IGF-I / FITC reaction products.

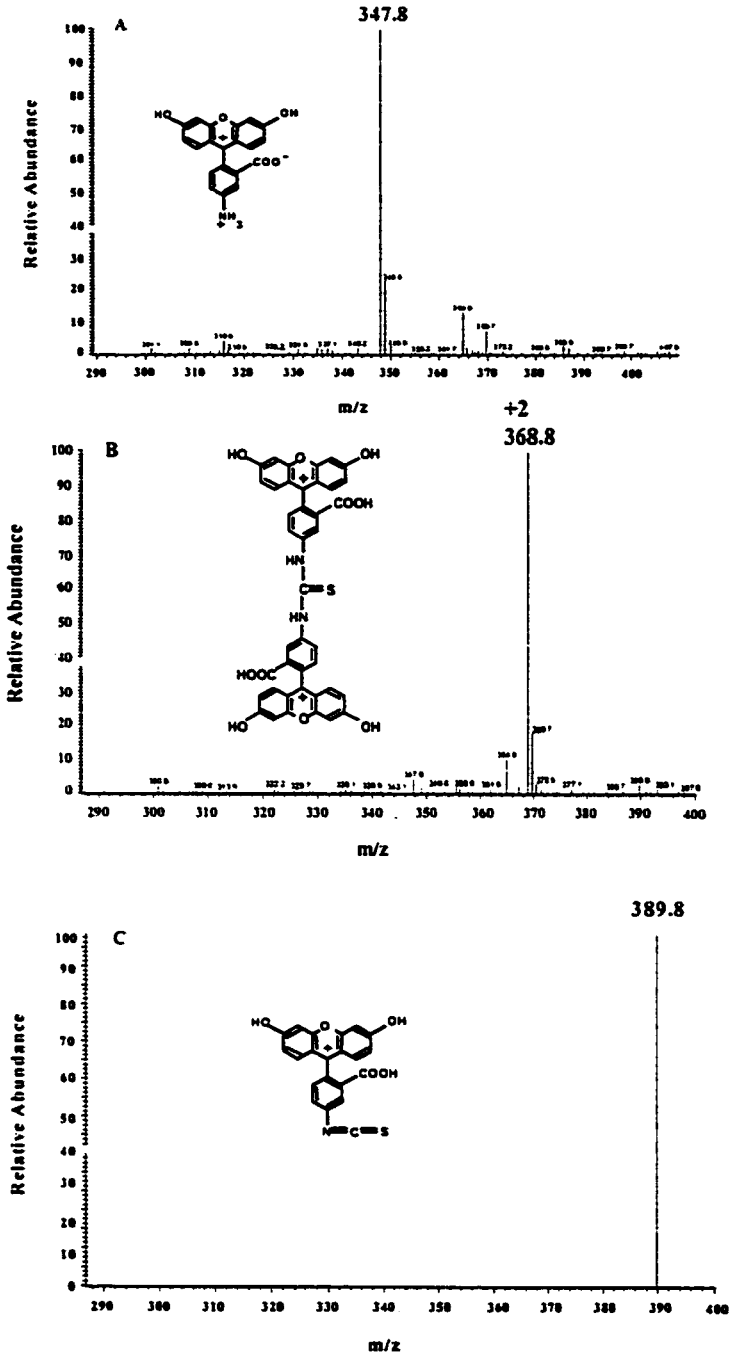

Figure 5.2 Extracted ion mass spectra for FITC and its hydrolysis products.

(A) 0.20-0.33 min of the TIC corresponding to fluorescein amine. (B) 2.82 – 3.03 min of the TIC corresponding to difluorescein thiourea. (C) 4.37 – 4.64 min of the TIC corresponding to unreacted FITC.

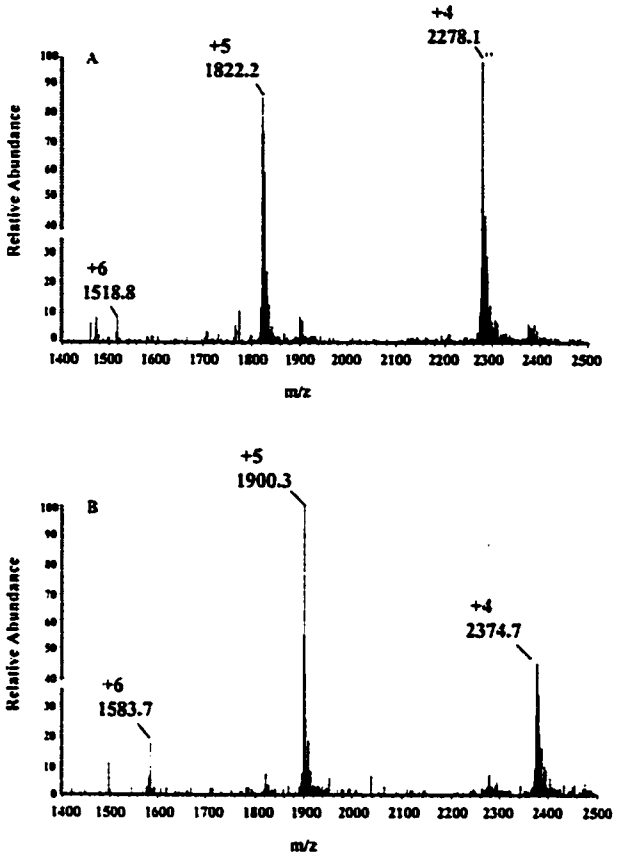

Figure 5.3 Convolved mass spectra of (A) Peak at 0.99-1.38 min of LC separated Long R^3 IGF-I / FITC reaction TIC. Calculated mass of 9107.7 +/- 0.4 mass units (mu). Corresponds to unreacted Long R^3 IGF-I. (B) Peak at 2.06 – 2.31 min of the TIC for the LC separated Long R^3 IGF-I / FITC reaction. Calculated mass of 9496.4 +/- 1.0 mu. Corresponds to single-labeled Long R^3 IGF-I.

various FITC hydrolysis products, as well as unlabeled protein. The peak at 0.86 min of the TIC (Figure 5.1) had a deconvolved mass of 9125 Da, and is believed to correspond to singly oxidized Long R^3 IGF-I. Further analysis of the LC/MS data indicated a 9132 Da species at 1.56 min of the TIC. This peak does not correspond to any possible oxidized Long R^3 IGF-I species and remains to be identified.

After initial LC/MS characterization of the Long R^3 IGF-I / FITC derivatization reaction, it was necessary to determine the modification site in LC purified single-labeled protein.

Structural Characterization of Single- Labeled Long R^3 IGF-I by Chemical Cleavage and LC/MS. Cyanogen bromide selectively reacts with the sulfur of the thioether side chain of methionine, resulting in cleavage of the methionyl peptide bond. The fragments produced by the action of CNBr contain C-terminal homoserine or its lactone except for the C-terminal peptide of the protein.[12] This chemical cleavage reagent is well-suited to LC/MS analysis of single-labeled Long R^3 IGF-I. Complete CNBr cleavage of Long R^3 IGF-I should produce only three fragments (see Figure 5.4).[13] Furthermore, since the first residue at the N-terminus is Met, conjugation of the α-amino group is expected to produce a fragment consisting of fluoresceinated homoserine lactone. Determining

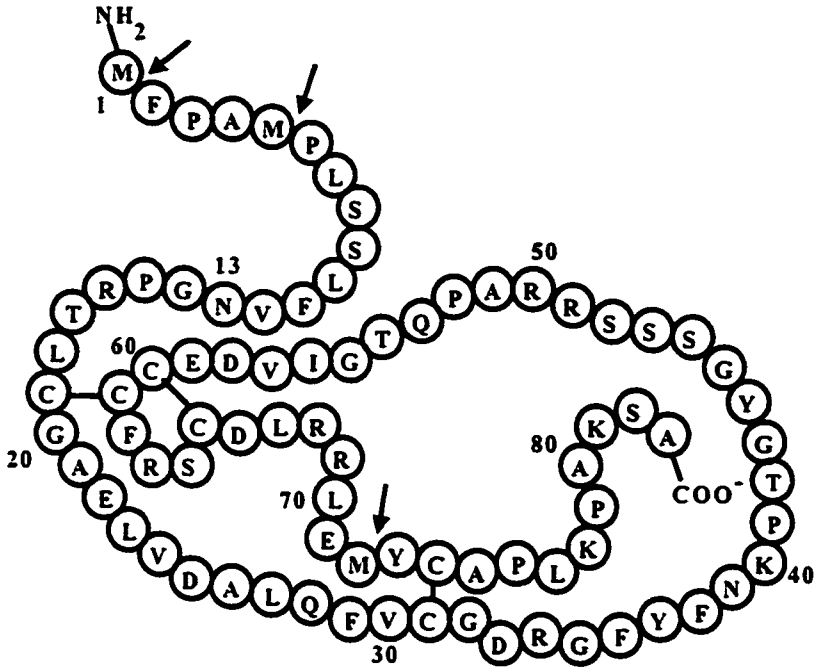

Figure 5.4 Amino acid sequence of Long R^3 IGF-I. Disulfide bonds for correctly folded Long R^3 IGF-I are shown (—). Arrows indicate CNBr cleavage sites.

the site of modification could thus be achieved by LC/MS using a single-quadrupole instrument.

In order to characterize the CNBr cleavage reaction, unlabeled protein was incubated in the presence and absence of CNBr and subsequently analyzed by LC/MS. As expected, Long R^3 IGF-I remained intact in the absence of CNBr (see Figure 5.5). In the presence of cleavage reagent, protein was digested into three fragments (Met^1, residues 2-5, and residues 6-83). Both of the larger fragments were detected with masses of 417 and 8533 Da, respectively (see Figure 5.6). It was thus determined that a three hour cleavage reaction at 38 °C was sufficient to completely cleave the protein.

Purified single-labeled Long R^3 IGF-I was incubated in the presence and absence of CNBr to determine the location of the fluorescein label. Contrary to the unlabeled protein control, in the absence of cleavage reagent, single-labeled protein was cleaved. A fragment of 8977 Da, corresponding to residues 2-83 of Long R^3 IGF-I was observed (see Figure 5.7). It is postulated that this was attained via an Edman reaction. In this instance, FITC rather than phenylisothiocyanate was previously coupled to the N-terminal Met. Subsequent cleavage (acidic conditions, 38 °C) to release the original N-terminal amino acid as fluoresceinated Met (loss of 520 Da) would produce a 8977 Da fragment. The 520 Da fragment was not detected. This may have been due to loss on the C_{18} column and/or poor ionization. These results suggest that CNBr is not necessary to determine the site

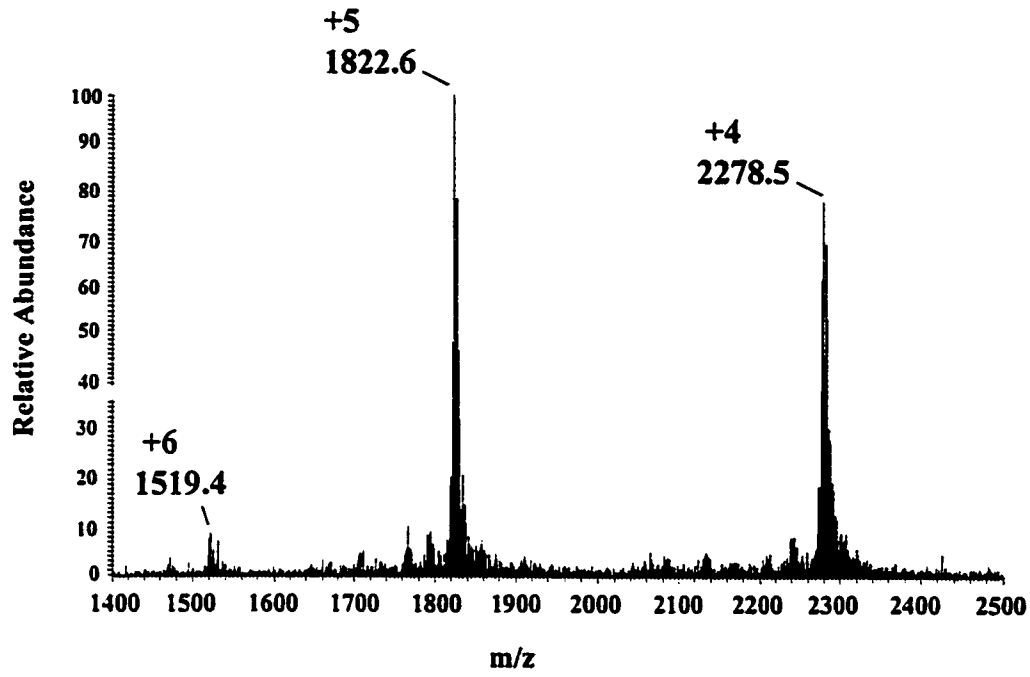

Figure 5.5 Unlabeled Long R^3 IGF-I (No CNBr). Convolved mass spectrum of peak at 5.00-6.09 min of the TIC. Calculated mass of 9110 +/- 0.9 mu.

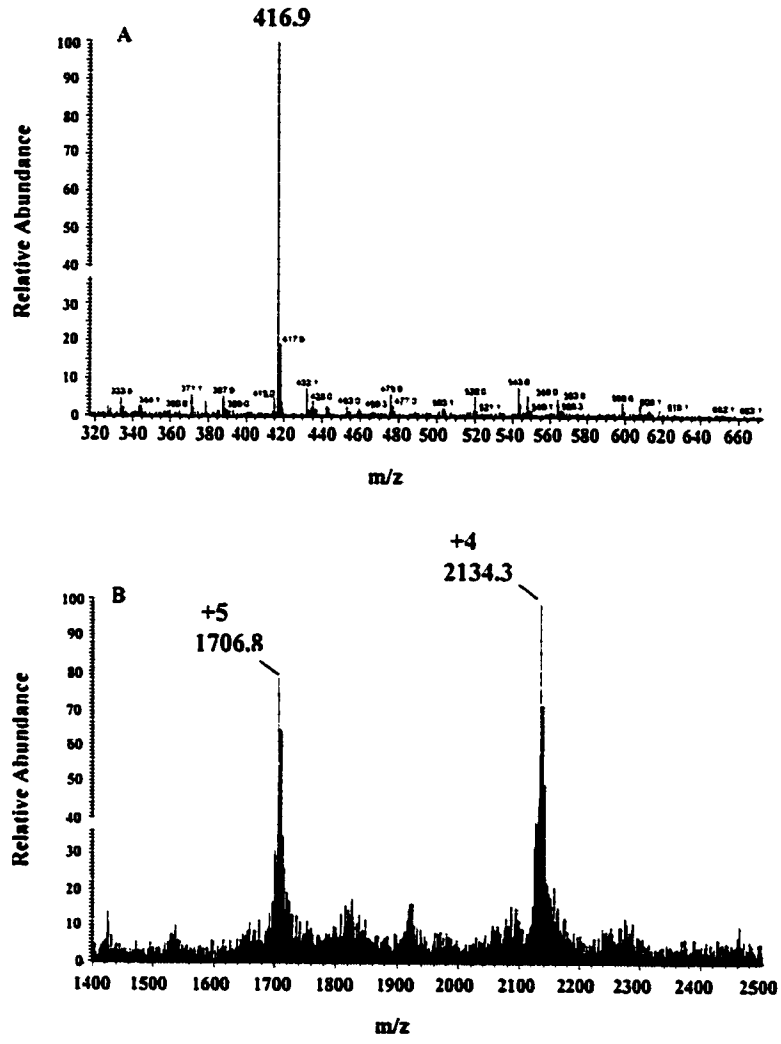

Figure 5.6 Unlabeled Long R^3 IGF-I CNBr digestion. (A) Peak at 2.81-3.73 min of the TIC. Fragment corresponding to residues 2-5. (B) Convolved mass spectrum of peak at 4.16-5.78 min of the TIC. Calculated mass of 8533 +/- 2.0 mu, corresponding to residues 6-83.

of modification. However, since the 520 Da fragment was not detected, a CNBr reaction was performed on the purified conjugate protein.

CNBr cleavage of single-labeled Long R^3 IGF-I resulted in the formation of three fragments. Two fragments corresponding to residues 2-5 and 6-83, were identified by LC/MS (see Figure 5.8). These fragments match those previously observed for cleavage of unlabeled protein and thus indicate that the fluorescein label does not reside on residues 2-83. Unequivocal proof that the modification site is the α-amino group of Met^1 requires detection of the 490 Da fluoresceinated homoserine lactone. This species was not observed by LC/MS analysis for the same possible reasons stated above. Nonetheless, there exists further proof that the N-terminal amino acid was labeled. The third fragment, with m/z of 474.8, can be attributed to the +2 charged state of fluoresceinated MFPAM (residues 1-5) whereby Met^1 has been oxidized to methionine S-oxide. It was apparent from the TIC that only a small amount of Met^1 exists as methionine S-oxide. It should be noted that previous studies have shown that CNBr will not cleave at oxidized Met residues, hence this fragment may be observed.

Monoclonal anti-IGF-I Binding to Single-Labeled Long R^3 IGF-I. Following LC/MS characterization of the site of modification, it was necessary to determine if this bioanalytical reagent could be used in a competitive immunoassay format. Purified single-labeled Long R^3 IGF-I was incubated with monoclonal anti-IGF-I and binding analyzed by capillary electrophoresis with laser-induced fluorescence (CE-LIF) (Figure 5.9). Addition of antibody resulted in

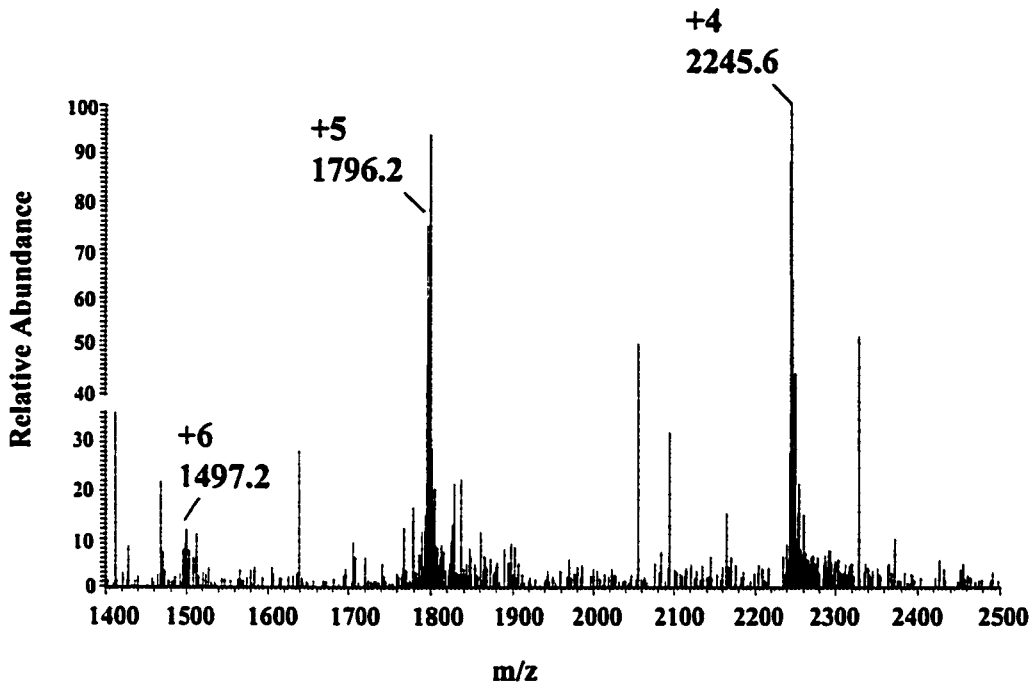

Figure 5.7 Labeled Long R^3 IGF-I (No CNBr). Convolved mass spectrum of peak at 5.79-6.72 min of the TIC. Calculated mass of 8977 +/- 0.7 mu, corresponding to residues 2-83.

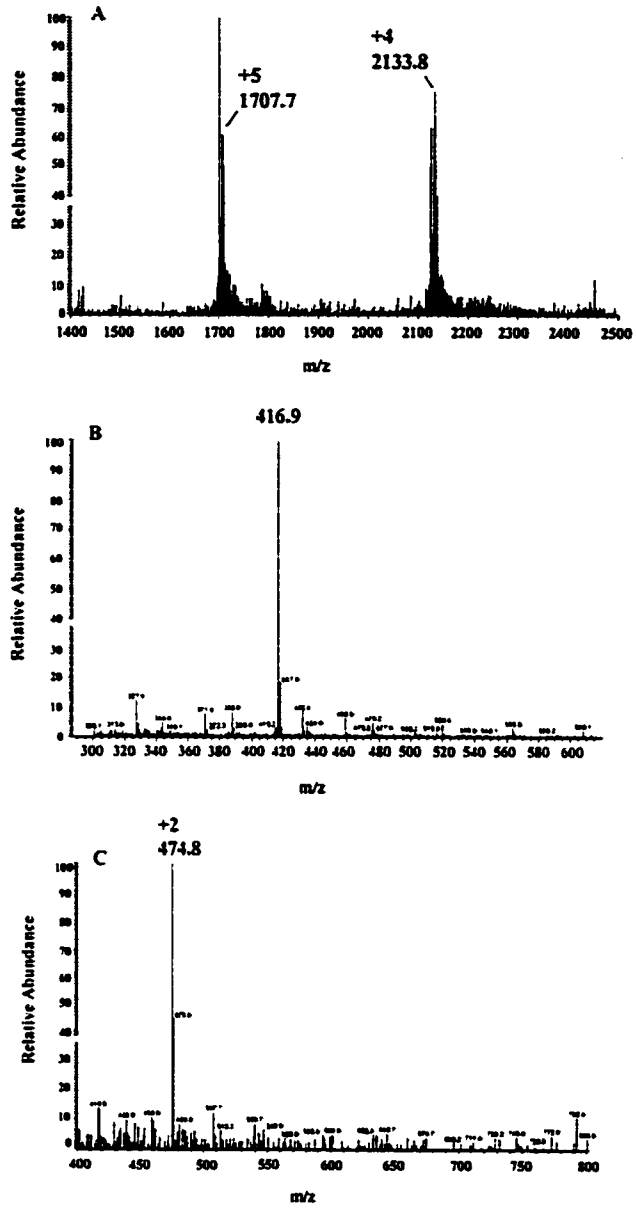

Figure 5.8 Single-labeled Long R^3 IGF-I CNBr digestion. (A) Convolved mass spectrum of peak at 5.33-6.42 min of the TIC. Calculated mass of 8532.5 +/- 1.0 mu corresponding to residues 6-83. (B) Peak at 3.6-4.7 min of the TIC, corresponding to residues 2-5. (C) Peak at 5.69-5.99 min of the TIC consisting of the +2 charged state of oxidized MFPAM fragment (residues 1-5).

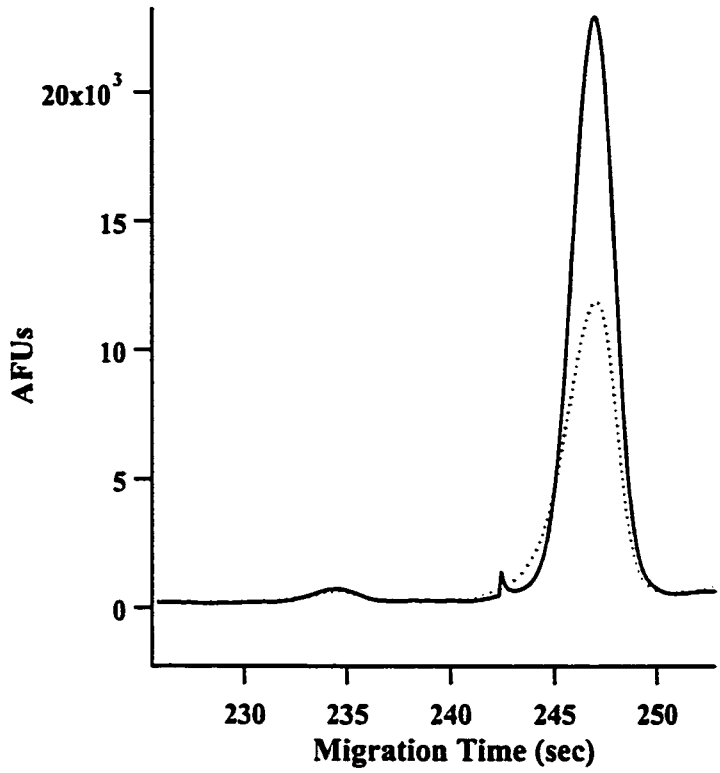

Figure 5.9 CE-LIF electropherogram for the titration of purified single-labeled Long R^3 IGF-I with monoclonal anti-IGF-I. Solid line denotes labeled protein in the absence of antibody. Dashed line represents labeled protein after the addition of antibody. Arbitrary fluorescence units (AFUs) are on the y-axis.

a substantial decrease in the fluorescence intensity of free, labeled Long R^3 IGF-I. Furthermore, control experiments in which labeled Long R^3 IGF-I was competed with the unlabeled ligand for monoclonal anti-IGF-I, indicated specific binding (data not shown). Immunorecognition of labeled analyte by monoclonal anti-IGF-I was thus preserved.

CONCLUSIONS

For the first time, a complete protocol for derivatization of Long R^3 IGF-I with FITC at a single site has been developed. This includes a specific derivatization procedure, LC purification conditions, and a LC/MS approach for the characterization of single-labeled protein. There is substantial LC/MS evidence that selective modification of the α-amino group of Met^1 can be achieved by performing the conjugation reaction at pH 7.0, with a 1:1 FITC to protein amino group ratio. Work is currently underway toward improving the reaction yield, and in the development of a CE-LIF IGF-I competitive immunoassay using single-labeled Long R^3 IGF-I. Future work includes testing this bioanalytical reagent for its ability to bind the Type I IGF-I receptor.

ACKNOWLEDGMENTS

We thank Dr. Ann English and Angelo Filosa for use of the HP 1090 LC system and Finnigan SSQ 7000, and helpful discussions. The authors gratefully acknowledge financial support from NSERC, FCAR and David J. Azrieli.

REFERENCES

(1) Butt, A.J.; Firth, S.M.; Baxter, R.C. *Immunol Cell Biol* **1999**, 77, 256.

(2) Ferry, R.J. Jr; Katz, L.E.; Grimberg, A.; Cohen, P.; Weinzimer, S.A. *Horm Metab Res* **1999**, 31, 192.

(3) Zumkeller, W; Schwab, M. *Horm Metab Res* **1999**, 31, 138.

(4) Pollak, M. *Recent Results Cancer Res* **1998**, 152, 63.

(5) Chan, J.M.; Stampfer, M.J.; Giovannucci, E.; Gann, P.H.; Ma, J.; Wilkinson, P.; Hennekens, C.H.; Pollak, M. *Science* **1998**, 279, 563.

(6) Hentz, N.G.; Richardson, J.M.; Sportsman, J.R.; Daijo, J.; Sittampalam, G.S. *Anal. Chem.* **1997**, 69, 4994.

(7) Banks, P.R.; Paquette, D.M. *J. Chrom. A* **1995**, 693, 145.

(8) Francis, G.L.; Ross, M.; Ballard, F.J.; Milner, S.J.; Senn, C.; McNeil, K.A.; Wallace, J.C.; King, R.; Wells, J.R.E. *Journal of Molecular Endocrinology* **1992**, 8, 213.

(9) Lau, S.K.; Zaccardo, F.; Little, M.; Banks, P.R. *J. Chrom A* **1998**, 809, 203.

(10) Chapman, J.R (ed.). *Methods in Molecular Biology* **1996**, 61, 171.

(11) Manes, S.; Kremer, L.; Albar, J.P.; Mark, C.; Llopis, R.; Martinez, C. *Endocrinology* **1997**, 138, 905.

(12) Darbre, A. (ed.). *Practical Protein Chemistry: A Handbook.* **1988**, pp. 83.

(13) Frosberg, G. et al. *Biochem. J.* **1990**, 271, 375.

CHAPTER 6

CONCLUSIONS AND FUTURE WORK

GENERAL CONCLUSIONS

The importance and originality of the studies presented in Chapters 2 thru 5 can be broken down into two categories: their individual contributions to the fields of clinical chemistry and biochemistry, and as a set of complimentary tools for nanoscale protein analysis. These studies were designed to either address areas that have received little or no attention in CE, facilitate nanoscale protein analysis, and/or overcome fundamental problems in CE protein analysis.

The objective of the research presented in Chapter 2 was to provide a comprehensive characterization of seminal plasma by capillary electrophoresis. To our knowledge, this is the first report on the extensive characterization of seminal plasma in terms of temperature stability, protease degradation, freeze-thaw cycling, and protein/non-protein zone identification. This lays the foundation for further studies aimed at obtaining seminal plasma profiles for various disease states. Similar to the use of CE in serum analysis, it is envisaged that seminal plasma profiling could occupy a similar niche in the clinical laboratory.

In line with the studies in Chapter 2, it is of interest to further characterize a particular complex matrix by quantitating various proteins in the nanomolar range. This is particularly important in the case of diseases such as microalbuminuria and prostate cancer, whereby early detection of particular proteins is advantageous. The work presented in Chapter 3 focused on the development of a CE-LIFD

method for this purpose. The advantage of this approach is primarily its simplicity, cost-effectiveness, and the preservation of sample material for subsequent complimentary analyses. Contrary to the numerous microplate methods available for bulk protein quantitation, CE offers the advantage of resolving the complex matrix into its various components. NanoOrange detection limits are competitive with other CE-LIFD approaches utilizing fluorescamine[1] and CBQCA[2], without the need to carefully control reaction pH and temperature. The approach described in Chapter 3 illustrates the ability to label nanomolar concentrations of protein. This is not typically true of many competing CE methods in which the labeling reaction is performed at micromolar protein concentrations followed by serial dilution. The research presented herein thus allows one to effectively utilize CE in protein analysis applications requiring detection in the nanomolar range (i.e. proteomics and clinical diagnostics).

A similar improvement in protein detection was achieved using capillary gel electrophoresis and LIFD. To our knowledge, the system described in Chapter 4 was the first to report on the ability to label and detect nanomolar concentrations of protein in a CGE format. In comparison to the methodology developed in Chapter 3, this approach was simple, cost-effective, and rapid. This has drawn particular interest in the field of proteomics due to the possibility of combining the method with CE tryptic protein digest analysis tools developed at the Université de Montreal.[3] The work presented in Chapter 4 thus has potential use in the

biochemical laboratory where a significant reduction in labour and analysis time associated with slab-gel SDS-PAGE is expected.

The significance of the work described in Chapter 5 is clearly related to the particular analyte studied. As described previously, IGF-I plays an important role in various disease states, including prostate cancer. Traditional IGF-I immunoassays have relied on enzymatic amplification[4], non-competitive time-resolved immunofluorometry[5], and radioactive ligands.[6] These assays provide detection limits in the ng/L range yet rely on several wash steps. In addition, standard radioimmunoassays are not accurate for IGF-I quantitation in the presence of IGF-I binding proteins. Analysis of IGF-I by CE has received little attention, primarily due to problems associated with detection. Typical serum IGF-I concentrations are in the 2 to 10 ng/mL range.[7] The use of dynamically coated capillaries and on-line solid-phase extraction (SPE) in IGF-I analysis by CE has been recently reported.[7] In addition to capillary coating reproducibility and stability issues, this approach was unable to provide detection limits below 195 ng/mL. It is also questionable whether the on-line SPE utilized in this study would maintain its effectiveness following injection of a complex sample. Absorbance detection also does not confer the same degree of component selectivity that can be achieved by LIFD.

Several factors drove the research reported in Chapter 5, including lack of a simple CE-based method capable of detecting IGF-I concentrations in the low ng/mL range, and the absence of a commercially available fluorescently labeled

IGF-I.[8] The aim was to produce a single-labeled fluorescent analog of IGF-I at a fraction of the cost of IGF-I, while demonstrating preservation of immunorecognition using CE-LIFD. The result was a well-characterized process for producing N-terminally labeled Long R^3 IGF-I for use in bioanalytical applications. This fluorescent ligand holds significant potential in receptor binding assays since careful control of reaction conditions selectively labels the N-terminus. The N-terminus has been shown not to participate directly in receptor binding.[9] CE-LIFD limits of approximately 8 ng/mL have been obtained for analysis of fluorescein isothiocyanate labeled Long R^3 IGF-I (data not shown).

Each of the above studies is connected by the common thread of capillary electrophoresis for protein analysis and for the most part LIFD approaches. In addition to their individual contributions, they may be viewed as a complimentary collection of protein analysis tools. For example, seminal plasma profiles may be screened for significant deviations from the "normal" profile. Subsequent quantitation of various proteins in the profile may be achieved in solution utilizing the NanoOrange CE-LIF approach, and/or molecular weight info obtained using the Sypro Red SDS-CGE system. Fluorescently-labeled ligands such as Long R^3 IGF-I could then be used in a competitive immunoassay format to selectively quantitate their native ligand counterpart.

Limitations of these CE protein analysis tools. It is equally important to realize the limitations of the methods described in this thesis. It is the hope of this researcher that others will continue to find creative solutions to these

limitations, and further improve these tools. Outlined below are a series of problems and some potential solutions.

It is clear that CE seminal plasma profiling (Chapter 2) will be most useful in rapid screening and cannot compete with the resolution obtained on two-dimensional gels. The hundreds of proteins typically found on such a gel are in essence still part of the seminal plasma profile observed in an electropherogram. Whereas major components such as TF, PSA, and HSA can be localized to certain zones, these no doubt mask the presence of minor components. The identification of specific components in a disease profile would thus require immunosubtraction. Furthermore, more efficient protease inhibition strategies must be employed in order to avoid interference by peptidic fragments. A suitable protease inhibitor cocktail appears to be appropriate.

The CE-LIFD NanoOrange methodology presented in Chapter 3 is expected to suffer somewhat from protein selectivity. In the absence of a dye structure, it is postulated that binding with protein targets involves a mixture of electrostatic and hydrophobic interactions. As such, as with any of the other traditional colorimetric approaches such as the Bradford[10] and bicinchoninic[11] assays, a certain degree of protein variability is expected. If this should be the case, it would be necessary to incorporate a heating / surfactant binding step in the CE-LIFD protocol. Heating would enable protein denaturation, facilitating the binding of surfactant. Similar to the case of SDS, the surfactant would serve to minimize dye binding variation. Addition of surfactant prior to the separation

would most likely abolish electrophoretic mobility differences between the various protein components. One possible solution is to inject unlabeled sample, allow sample components to separate electrophoretically, pass analytes through a heated zone, followed by post-column detection with NanoOrange. This heated zone approach has been successfully utilized in the analysis of N-methylcarbamates.[12]

A significant limitation of the approach that followed in Chapter 4 was the inability to easily replace the polymer solution between runs. The ability to flush polymer into and out of the capillary with standard commercial CE instrumentation is a prerequisite for use of this research in the clinical / biochemical laboratory. Though a variety of proprietary polymer formulations are commercially available, these typically require coated capillaries. In addition, the proprietary nature of these solutions makes it very difficult to perform the Sypro Red SDS-CGE assay, since SDS concentrations are believed to exceed those determined optimal for this approach. The quantity of SDS is unknown and attempts to dilute the polymer solutions to reduce the level of SDS have a negative impact on component resolution.

Future Work. The above limitations form the basis for future research. The use of commercial polymers in conjunction with Sypro Red SDS-CGE is currently being investigated by Pieter Roos through a potential collaboration with Bio-Rad which, to date, provides the only formulation which does not require a capillary coating. In continuation of the seminal plasma studies, future work involves analysis of seminal plasma samples representing various disease states.

As discussed below, the majority of future work involves NanoOrange and Fluo-Long R^3 IGF-I.

Perhaps the most exciting aspect of the CE-LIFD NanoOrange system involves its suitability to biofluid analysis. Whereas serum, urine, and cerebral spinal fluid have been extensively examined utilizing CE, there is relatively little research on other clinically relevant biofluids. Recent CE-LIFD analysis of human tear and amniotic fluid using on-column NanoOrange labeling has produced interesting profiles (Figures 6.1 & 6.2). These are the focus of on-going research, with potential applications in ocular and pre-natal disease diagnosis. Similarly, the use of NanoOrange in analyzing recombinant protein expression is an area of interest. Bacterial flagella have been recently labeled with NanoOrange in a non-CE based system.[13] It is envisioned that the NanoOrange system described in Chapter 3 can be utilized in the quantitation of a recombinant protein of interest. This would allow one to identify those bacterial strains producing the largest yields of a particular recombinant protein secreted into the growth medium.

The logical progression of the work presented in Chapters 2 & 3 is to transfer the methodologies to microfluidic devices. These devices are the focus of intense research due to the ability to perform multiple analyses on the order of milliseconds using a compact instrument design. NanoOrange method transfer to a chip format was indeed initiated during preparation of this manuscript.[14]

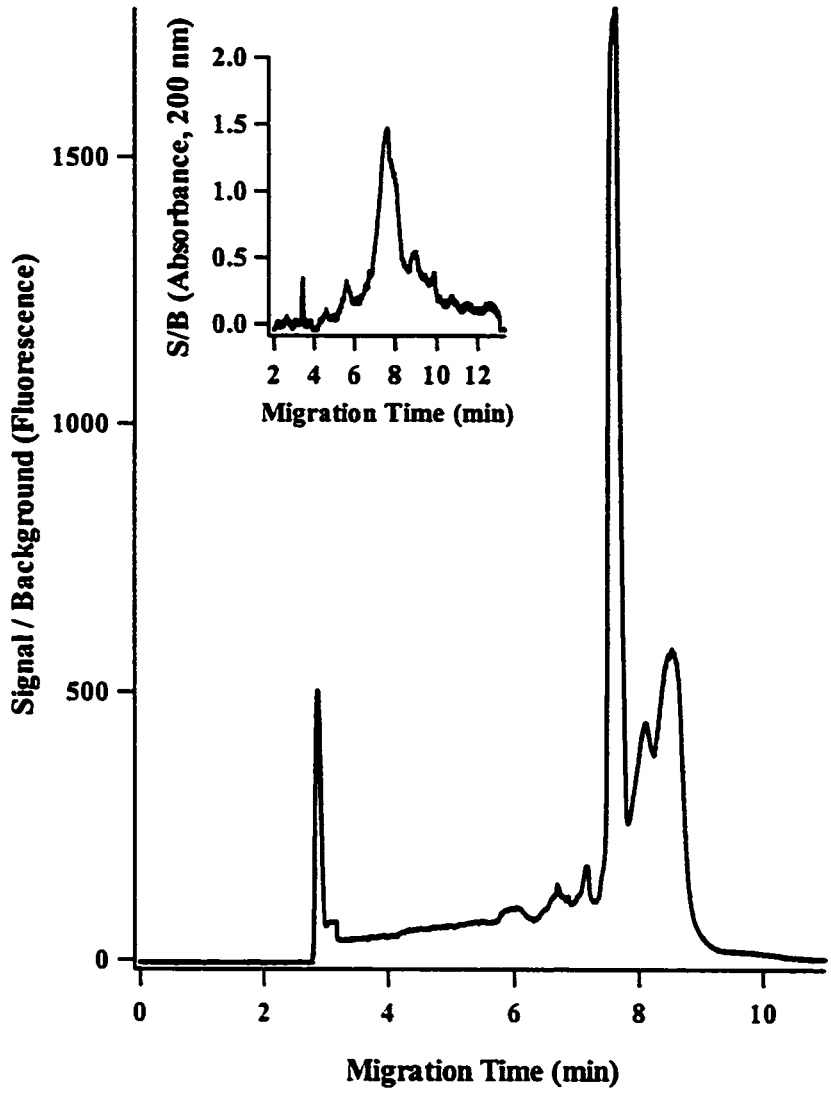

Figure 6.1 Undiluted human reflex tear fluid CE analysis using absorbance detection (no dye) and LIFD (NanoOrange in run buffer).

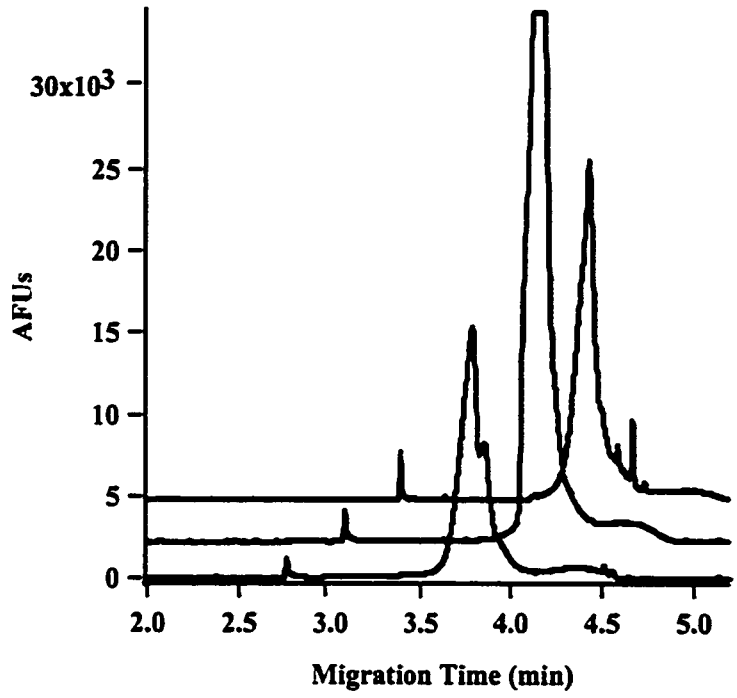

Figure 6.2 CE-LIFD analysis of on-column NanoOrange labeled human amniotic fluid. Each trace represents a different patient sample and is offset horizontally for clarity.

This work is particularly feasible here at Concordia University due to the recent acquisition of expertise and microfluidic instrumentation.

In terms of Fluo-Long R^3 IGF-I, there are several avenues of future research. Initial studies have shown that this analyte can be determined in a physiologically revelant concentration range, and that immunorecognition is preserved. As such, the development of a CE-LIFD competitive immunoassay for IGF-I is warranted. Key issues include sample matrix interferences and IGF-I / binding protein interactions. Subsequent method transfer to a chip format is anticipated. The receptor binding ability of this new conjugate could be determined by confocal microscopy experiments and/or fluorescence polarization (FP).[15] The development of FP assays could facilitate the screening of compounds designed to bind the IGF-I receptor.

REFERENCES

(1) Zhu R., Kok W.T. *J. Chromatogr. A.* **1998**, 814, 213.

(2) Asermely K.E., Broomfield C.A., Nowakowski J., Courtney B.C., Adler M. *J. Chromatogr. B Biomed. Sci. Appl.* **1997**, 695, 67.

(3) Bonneil, E. Doctoral Thesis, University of Montreal, February 2000.

(4) De León, D.D., Asmerom, Y. *Endocrinology* **1997**, 138, 2199.\

(5) Frystyk, J., Dinesen, B., Orskov, H. *Growth Regul.* **1995**, 5, 169.

(6) Francis, G.L., Ross, M., Ballard, F.J., Milner, S.J., Senn, C., McNeil, K.A., Wallace, J.C., King, R., Wells, J.R.E. *Journal of Molecular Endocrinology* **1992**, 8, 213.

(7) Roche, M.E., Anderson, M.A., Oda, R.P., Riggs, B.L., Strausbauch, M.A., Okazaki, R., Wettstein, P.J., Landers, J.P. *Anal. Biochem.* **1998**, 258, 87.

(8) Cowley, E.A., Pratten, M.K. *Placenta* **1996**, 17, 321.

(9) Manes, S.; Kremer, L.; Albar, J.P.; Mark, C.; Llopis, R.; Martinez, C. *Endocrinology* **1997**, 138, 905.

(10) Bradford M.M. *Anal. Biochem.* **1976**, 72, 248.

(11) Smith P.K., Krohn R.I., Hermanson G.T., Mallia A.K., Gartner F.H., Provenzano M.D., Fujimoto E.K., Goeke N.M., Olson B.J., Klenk D.C. *Anal. Biochem.* **1985**, 150, 76.

(12) Wu Y.S., Lee H.K., Li S.F. *Anal Chem* **2000**, 72, 1441.

(13) Grossart H.P., Steward G.F., Martinez J., Azam F. *Appl. Environ. Microbiol.* **2000**, 66, 3632.

(14) Liu Y., Foote R.S., Jacobson S.C., Ramsey R.S., Ramsey J.M. *Anal. Chem.* **2000**, 72, 4608.

(15) Hentz, N.G.; Richardson, J.M.; Sportsman, J.R.; Daijo, J.; Sittampalam, G.S. *Anal. Chem.* **1997**, 69, 4994.

Concordia
UNIVERSITY

Montreal, April 10th, 2001

Michael D. Harvey
255 Acres, Kirkland
Quebec, Canada
H9H 4M1

Dear Michael,

We hereby authorize you to reproduce, in your doctoral thesis, the manuscript(s) for which we appeared as co-authors.

Dr. Peter R. Banks

Dr. Cameron D. Skinner

Dirk Bandilla

Vicky Bablekis

1455, de Maisonneuve Blvd. W.
Montreal, Quebec H3G 1M8